N73-25969

HANDBOOK ON PASSIVE THERMAL CONTROL COATINGS - FINAL REPORT

T. K. Mookherji, et al

Teledyne Brown Engineering
Huntsville, Alabama

April 1973

SE-SSL-1717

Final Report

HANDBOOK ON PASSIVE THERMAL CONTROL COATINGS

April 1973

TELEDYNE BROWN ENGINEERING

Research Park • Huntsville, Alabama 35807

FINAL REPORT
SE-SSL-1717

HANDBOOK ON PASSIVE THERMAL CONTROL COATINGS

By

T. K. Mookherji

J. D. Hayes

April 1973

Prepared For

SPACE THERMOPHYSICS DIVISION
SPACE SCIENCES LABORATORY
GEORGE C. MARSHALL SPACE FLIGHT CENTER

Contract No. NAS8-25900

Prepared By

SCIENCE AND ENGINEERING
TELEDYNE BROWN ENGINEERING
HUNTSVILLE, ALABAMA

TABLE OF CONTENTS

LIST OF ILLUSTRATIONS

LIST OF TABLES

LIST OF SYMBOLS

A	Area
A_o	Area of heat absorber
A_1	Area of heat source
$A_{\lambda\theta}$	Absorbed radiation at a wavelength λ which is incident at an angle of θ
C	Constant
d	Particle diameter
F_a	View factor
F_e	Emittance factor
H_λ	Spectral distribution of Sun
I	Transmitted intensity
I_o	Incident intensity
J_n	Normal intensity
$J(X)$	Radiation distribution function
k	Extinction coefficient
K	Thermal conductivity
N	Complex refractive index
N_b	Equivalent black plate
n	Refractive index, real part
n_o	Refractive index of binder
n_1	Ratio of refractive index of the pigment to n_o

LIST OF SYMBOLS (Concluded)

q_λ	Quantity of heat radiated at wavelength λ
$R_{\lambda, T}$	Spectral reflectance at wavelength λ and a temperature T°K
$R_{\lambda_\perp}$	Reflected intensity for perpendicular polarization at wavelength λ
$R_{\lambda_\parallel}$	Reflected intensity for parallel polarization at wavelength λ
T	Absolute temperature, °K
T_0	Heat absorber's temperature
T_1	Heat source temperature
W	Total hemispherical emitted flux
W_λ	Spectral power radiated into a hemisphere by a unit area Planckian radiator
X	Absorption coefficient
α_S	Solar absorptance
α_θ	Total angular absorptance
$\alpha_{\lambda, T}$	Spectral absorptance at wavelength λ and a temperature T °K
ϵ_o	Emittance of absorber
ϵ_T	Total hemispherical emittance
$\epsilon_{\lambda, T}$	Spectral emittance at wavelength λ and a temperature T °K
θ	Angle of viewing
θ_i	Angle of incidence
θ_r	Angle of refraction
σ	Stefan-Boltzmann constant

INTRODUCTION

Maintenance of a narrow temperature range within a space vehicle is very essential in both unmanned and manned space programs. Control of temperature on a space vehicle is based on the exchange of radiant energy with the vehicle's environment and, hence, on the thermal-radiation properties of the exterior surfaces. Thermal control coatings with the desired radiative properties are being used to maintain a predetermined heat balance on spacecraft. Solar absorptance, α_S, and hemispherical emittance, ϵ_T, of the coating are the prime characteristics for controlling the heat balance. Design requirements often require the use of a low α_S-to-ϵ_T ratio surface. These surfaces are generally susceptible to damage by solar radiation, resulting in an increase in α_S.

Considerable effort during the past 12 years has been made in developing coatings which would be stable in a space environment, be relatively easy to apply and to maintain, and have the desired radiative properties. The result of all work performed in developing stable thermal control coatings has been documented in various scientific and engineering journals and reported at various conferences. The scatter of this essential data over such a large publication media has hindered the efficient use of coating materials by thermal design engineers.

To alleviate the problem of data collection and comparison for the thermal design engineer and to provide a basic treatise on the use of such data, the present handbook of passive thermal control surfaces data has been compiled.

The handbook is divided into two parts. Part I consists of two chapters. Chapter 1 is a discussion of passive temperature control techniques and selection of control surfaces. Chapter 2 is a discussion

of the space environmental damage mechanisms in passive thermal control surfaces. Part II presents pertinent data on the coatings for which data are available, followed by a tabular summary of the available data on passive thermal control coatings.

In selecting the data for the different thermal control coatings, emphasis was placed on consulting only those references where the experimental simulation of the space environment appeared to be more appropriate. All laboratory data which were not taken in situ or in which space environment was not properly simulated were discarded. Flight data where the samples were not returned to Earth under vacuum were also discarded. Reliance was given to the data obtained by the research groups who are more familiar with the thermal control coating and space environment problems.

Appendix A is a compilation of data that was used in making the tabular summary and that was subsequently used to describe the thermophysical properties of the individual coatings.

PART I
PHYSICS OF THERMAL CONTROL

CHAPTER 1
PASSIVE TEMPERATURE CONTROL TECHNIQUES AND SELECTION OF CONTROL SURFACES

This chapter reviews the basic fundamental and engineering considerations in heat transfer that are related to passive temperature control.

Also discussed in this chapter are the sources of radiant energy, the methods used in obtaining thermophysical design data, and the criteria used in selecting passive thermal control surfaces.

FUNDAMENTAL AND ENGINEERING CONSIDERATIONS IN HEAT TRANSFER

The solar absorptance and thermal emittance characteristics of surfaces ultimately control the temperature of objects in space, and satellite instrumentation must generally be maintained within a specified temperature range. Temperature control is established through radiation balancing, i.e., by arranging for the power absorbed from sunlight to be balanced by the power radiated from the surface at a temperature level compatible with the payload requirements. When the internal power dissipation is low or is zero, this absorptance-emittance balance establishes the mean temperature of the payload. The addition of high internal power dissipation requires readjustment of surface characteristics to achieve a new balance, but, in all cases, an important parameter for temperature control is the ratio of solar absorptance to thermal emittance for the external surface. If the external surface is composed of more than one material, the effective absorptance-emittance ratio will be determined from a properly weighted average of the absorptance and emittance of each material.

This type of temperature control system is called a passive system, and the most critical factor in such a system is the ability to prepare surfaces with reproducible and accurately known values of absorptance and emittance.

This section reviews the interrelationship between material properties, optical properties, and thermal properties. This review is designed to give a practical working knowledge of the basic laws of optics and thermodynamics as they apply to the use of coatings to control heat transfer.

Kirchhoff's Law

This law states that at a given temperature and wavelength the ratio of the emittance and absorptance of all surfaces is the same, and the ratio is equal to that of a blackbody. This means that there can be no net heat transfer in a closed isothermal system and that a surface that has low absorption must have low emission and good reflection within the isothermal environment. To satisfy this condition:

$$\alpha_{\lambda, T} = \epsilon_{\lambda, T} = 1 - R_{\lambda, T} \quad . \tag{1}$$

The significance of this expression in heat transfer is best indicated by illustrations of its limitations:

$$\alpha_{\lambda_1 T_1} \neq \epsilon_{\lambda_2 T_1} \quad (\lambda_1 \neq \lambda_2)$$

and

$$\alpha_{\lambda_1 T_1} \neq \alpha_{\lambda_1 T_2} \quad (T_1 \neq T_2)$$

Lambert's Law

This cosine law forms the basis for the view factor. The direction of radiation from a surface is very important in calculating the view factors for complex satellite shapes. The law holds exactly

for blackbody radiation and almost exactly for diffusely reflecting surfaces. This law states that the intensity of a radiating surface is independent of the angle of viewing. Since the apparent area

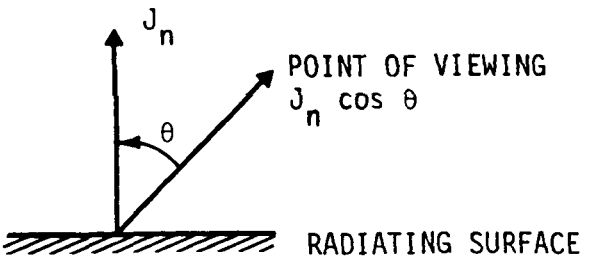

decreases with the cosine of the angle of incidence θ, the radiant flux is the normal intensity J_n times cos θ. The total hemispherical emitted flux W is π times the normal flux, i.e.,

$$W = \pi J_n \quad . \tag{2}$$

In general, Lambert's law is a fair approximation of the radiation pattern from a surface. If it were obeyed exactly, the radiant flux measured at any angle to a surface could be used to calculate total hemispherical radiation, and could also be used to measure hemispherical emittance when compared to a blackbody cavity at the same temperature and viewed from the same angle.

The surface condition of material has a great influence on the emittance. As the surface roughness is increased, the emittance approaches Lambert's law in flux distribution. Considering an infinitely thick section of a dielectric which has a light transmission of zero, the emittance is the internal radiation that is not reflected by the surface, i.e.,

$$\epsilon = 1 - R \quad . \tag{3}$$

The surface reflection in the normal direction is given by

$$R = 1 - \epsilon = \left(\frac{n - 1}{n + 1}\right)^2 \quad . \tag{4}$$

Similarly for metals,

$$R = 1 - \epsilon = 1 - \frac{2}{n} \quad . \tag{5}$$

Thus, the index of refraction may be considered a basic parameter controlling heat radiation. Since the index of refraction varies directly with the density, porous, low-density surfaces are more emissive, particularly if the pores are small compared to the wavelength of light radiated.

Wein's Displacement Law

Planck's law, in its simplest form, can be written as

$$q_\lambda = T^5 f(\lambda T) \tag{6}$$

It has been shown that if q_λ/T^5 is plotted against λT (Ref. 1) the same curve is obtained for all values of the temperature T. From this fact, Wein's law can be derived directly as

$$\lambda T = C \tag{7}$$

where C is a constant. The values of C in micron °K have been plotted for fractions of thermal energy (at shorter wavelengths) varying from 1 to 99 percent, and are shown in Figure 1. This plot can be used to obtain the relative radiation intensity or the fraction of the total energy radiated between any two wavelengths.

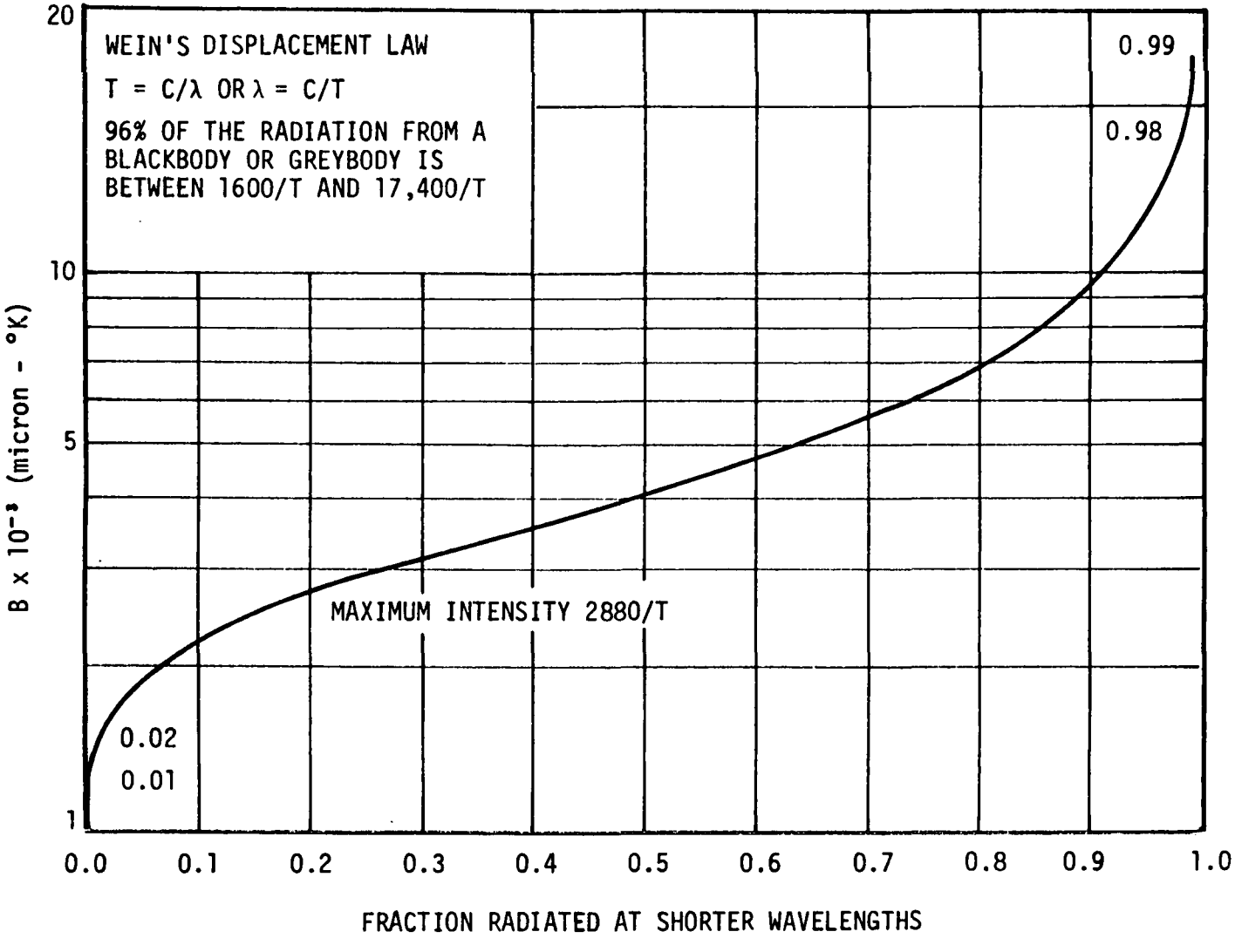

FIGURE 1. THE USE OF WEIN'S DISPLACEMENT LAW TO DETERMINE THE SPECTRAL DISTRIBUTION OF RADIATION FROM A SURFACE

The Physics of Absorption and Emission

The absorption or emission of electromagnetic radiation is the result of physical changes within the radiating atoms or molecules. Absorption results in excitation of the aborbing species to some higher energy level, whereas emission is the reverse process. At the lower end of the energy scale are the molecular rotational transitions. In solids, these are associated with the bending of bands and absorb most strongly in materials having a high dipole moment. Pure rotational absorption occurs in the far infrared and microwave frequencies. The rotational spectra are overlapped by the lattice vibrational spectra which measure intermolecular interactions or vibrations involving a lattice or molecules or ions. These transitions control heat absorption and emission at very low temperatures.

At wavelengths between 2 to 50 microns, the molecular vibrations associated with band stretching become the most important. These transitions control heat transfer at moderate temperatures. The infrared absorption or emittance spectra are a measure of the "allowedness" of a vibration transition which is resonant with the respective wavelength of light. As the temperature is increased, vibrational levels with larger energy gaps are excited and short-wavelength light is emitted. This causes the shift of the emission spectra toward the visible in accordance with Wein's law.

When light at a wavelength between 0.15 and 2.0 microns is absorbed, it generally excites an outer-shell electron to a higher energy level. In most cases, this electron returns to the ground state by giving up its energy through vibrational excitation of its own molecule or molecules which collide with the excited atom. The energy is then dissipated as thermal energy at longer wavelengths.

When the X-ray region is reached below 0.01 micron, inter-shell electrons are ejected from the absorbing atom. When this vacancy is filled by outer-shell electrons, the energy is radiated to excite many electronic transitions in neighboring molecules. The ejected electron may cause electronic excitation in other molecules.

At even shorter wavelengths, a gamma photon excites a cascade of electrons when it is captured in a dense material. The bulk of the electrons and vacancies quickly give up their electronic excitation to vibrational modes, causing a localized overheating called a thermal spike. A similar thermal spike is caused by the penetration of cosmic radiation (energetic protons) into a surface.

Surface Reflection

The surface reflection of materials is related to the absorption coefficient and the real and complex indices of refraction. The complex index of refraction is defined as

$$N = n - ik \tag{8}$$

where N is used in Fresnel's equation and Snell's law to determine the surface reflection and refraction in absorbing materials, respectively. The extinction coefficient k is related to the absorption coefficient α in Lambert's law ($I = I_o e^{-\alpha t}$) by the equation

$$\alpha = 4\pi k/\lambda \quad . \tag{9}$$

The absorption coefficients of good metallic conductors are generally very high in both the visible and infrared. However, the reflection of smooth metal surfaces is so high that the actual absorption remains relatively low. On the other hand, when a metal such as gold

is deposited in colloidal form at low density, the real index of refraction is so reduced that the absorption approaches that of a blackbody.

The absorption coefficient of dielectrics is determined by the vibrational and electronic transitions, as discussed previously. Generally, dielectrics vary between transparency and moderate to high absorption as the wavelength changes. Therefore, the complex index of refraction will change erratically with wavelength for many dielectrics.

The absorption coefficient has a strong effect on the change in reflection with the angle of incidence of the light. From Snell's law, the angle of refraction is given by

$$\sin \theta_i = N \sin \theta_r \tag{10}$$

where θ_i and θ_r are the angles of incidence and refraction, respectively. The reflection of light is then given by the relationships

$$R_{\lambda_\perp} = \frac{\sin^2 (\theta_i - \theta_r)}{\sin^2 (\theta_i + \theta_r)} \tag{11}$$

$$R_{\lambda_\parallel} = \frac{\tan^2 (\theta_i - \theta_r)}{\tan^2 (\theta_i + \theta_r)} \tag{12}$$

for perpendicular and parallel polarized light. For unpolarized light, these combine to give

$$R_\lambda = 1/2(R_{\lambda_\perp} + R_{\lambda_\parallel}) \ . \tag{13}$$

This explains why the light is polarized by reflection and why the degree of polarization varies with the absorption. Surface reflection is a very important property of pigments used in white coatings.

Reststrahlen Reflection

Reststrahlen reflection (or radiation) occurs at wavelengths associated with a fundamental resonant vibration of the lattice in a glassy material and of the polymer backbone in a resinous material. At the resonant frequency, the bonding electrons are free to oscillate in harmony with the electromagnetic radiation and act the same as conductive electrons in a metal. This causes a strong metallic reflection for a narrow band of wavelengths near the resonant frequency. The reflection considerably reduces the spectral emittance of the dielectric material. Therefore, one of the requirements for maximum emittance is to avoid materials with strong Reststrahlen reflection in the wavelengths of interest or to reduce the strong resonant lattice vibrations by diluting the material.

Light Scattering by White Coatings

Within limited spectral ranges, white coatings can reflect light with equal or higher efficiencies than polished metals. The high reflectivity is achieved by a scattering process. This reflection is of the Fresnel type, i.e., it occurs because the index of refraction of the pigment is greater than the binder. When the pigment has a diameter of less than one-tenth the wavelength of the incident light, the light is dispersed in accordance with the Rayleigh scattering law. Rayleigh scattering varies rapidly with the particle size and wavelength of incident light. It is evident that the thermal control technique using Rayleigh criteria should be very inefficient. For larger particles, these criteria break down and the light reflection goes through a peak at a certain particle size and then decreases again to a constant value for a larger size. The particle diameter for maximum reflection is given by (Ref. 2)

$$d = \frac{0.90\,\lambda}{\pi\, n_o} \left(\frac{n_1^2 + 2}{n_1^2 - 1} \right). \qquad (14)$$

Equation 14 is quite satisfactory for calculating the optimum particle size of pigment where a low concentration of spherical, or nearly spherical, particles are used. However, in an actual coating, the pigment particles are packed tightly together, and smaller particle sizes have been found to be more effective (Ref. 3).

Surfaces in Close Proximity

When two surfaces are brought into close proximity, there are two new phenomena that affect the rate of heat transfer. These are optical interference and "tunneling" radiation, the latter begin the interaction of the internal radiation within a body, with the second body in close proximity.

The interference effect is maximum at about 0.05 λ_{max}, which is the peak of the blackbody distribution (Ref. 4). The tunneling effect is the transfer of energy that is normally internally reflected by the metal. The range of radiation tunneling extends to about 0.25 λ_{max}. These distances are affected by the complex index of refraction and require separation in the range of λ_{max} to ensure freedom from these effects.

Heat Transfer Between Parallel Plates

A number of mathematical relationships have been developed for calculating heat transfer between parallel plates. One of the earliest equations is

$$q = A\,\sigma\,\epsilon(T_1^4 - T_0^4) \quad . \qquad (15)$$

Equation 15 is accurate only when ϵ is approximately 1; therefore, there is little or no reflected radiation. An improved relationship which also considers the reflection is (Ref. 5)

$$q = \left[A_1 \sigma (T_1^4 - T_0^4)\right] \left[\frac{1}{\epsilon_1} + \frac{A_1}{A_o} \left(\frac{1}{\epsilon_o} - 1\right)\right]^{-1} \qquad (16)$$

where the subscripts "1" and "0" apply to the hot and cold surfaces, respectively. This relation was described in Reference 6 as an emittance factor F_e, defined as follows:

$$F_e = \frac{1}{\left[\frac{1}{\epsilon_1} + \frac{A_1}{A_o} \left(\frac{1}{\epsilon_o} - 1\right)\right]} \quad . \qquad (17)$$

This formula is valid for concentric spheres, a coaxial cylinder, or an equatorial plane within a sphere (Ref. 7). It is also accurate for two parallel plates, where the separation distance is much smaller than the dimensions of the plate.

Where one of the surfaces is discontinuous or the separation distance is not small as compared to the surface area, a view factor F_a is combined into Equation 17, as follows:

$$q = \sigma F_a F_e (T_1^4 - T_0^4) \quad . \qquad (18)$$

The view factor also depends on conformance to Lambert's law, and the existence of an exposed edge or interface makes it improbable that either surface is isothermal. Thus, any calculation using Equation 18 must be considered as being approximate.

On the other hand, it should be remembered that when the parallel plates are packed too closely (in the order of the wavelength of radiation) the rate of heat transfer increases markedly because of the interference and tunneling effects, as discussed previously.

The simplest heat transfer is between plates with equal emittance and involves a cryogenic surface at temperature T_0 receiving heat q from high-temerature surface T_1. Assuming $F_a = 1$, the rate of heat flow is

$$q = \sigma F_e (T_1^4 - T_0^4) \quad . \tag{19}$$

If $T_1 > 3\ T_0$, then

$$q = \sigma F_e T_1^4 \quad . \tag{20}$$

Now, if the surface at temperature T_1 receives heat from another parallel plate with the same F_e at temperature T_2, the heat transfer will be

$$q = \sigma F_e (T_2^4 - T_1^4) \quad . \tag{21}$$

Under steady-state conditions, the heat lost is only to the cryogenic surface, eliminating T_1:

$$2q = \sigma F_e T_2^4 \quad . \tag{22}$$

Therefore, generalizing for n parallel plates:

$$q = \frac{\sigma F_e T_n^4}{n} \quad . \tag{23}$$

When $T_1 < 3\ T_0$, the same relationship holds, and

$$q = \frac{\sigma F_e (T_n^4 - T_0^4)}{n} \quad . \tag{24}$$

These two equations neglect the temperature drop through each plate and alternate methods of heat transfer such as conduction or convection.

The "Equivalent Black-Plate" Concept

Since the rate of heat transfer varies inversely with the number of plates, a single plate with an emittance factor of 0.1 is equivalent to 10 plates, with each of them having an emittance of 1.0. Thus, any coating combination can be represented by a number of "equivalent black plates", defined as the sum of the reciprocal emittance factors F_e, as follows:

$$N_b = \sum \frac{1}{F_e} = \sum n_b \tag{25}$$

where

$$n_b = \frac{1}{F_e}$$

$$N_b q = \sigma (T_n^4 - T_0^4) \quad . \tag{26}$$

This equation permits the calculation of heat transfer where the parallel plates have a multiplicity of different coatings.

Insulators and Parallel Plates in Series

The temperature drop across an insulator is given by

$$\Delta T = qx/k \tag{27}$$

where x is the thickness of the insulator.

When the insulator is part of, or in series with, the parallel plates, the heat flux must be the same across each interface. However, the effect of the insulator on the heat-transfer rate varies with the location of the insulator relative to the heat source.

SOURCES OF RADIANT ENERGY

An Earth satellite is heated by three external energy sources, i.e., sunlight, albedo, and Earth radiation. Figure 2 shows the spectral distribution of energy from the above heat sources, neglecting the reduction in intensity caused by the distance from the Earth (Refs. 8 and 9).

Albedo is sunlight reflected from terrain, water, and clouds. Also, some light in the blue end of the spectrum is backscattered from the atmosphere by dust and haze. Reflection varies from about 80 to 90 percent from clouds and snow and 10 percent or less from water and certain types of terrain. The average albedo of the Earth is reported as 39 to 40 percent (Ref. 10); however, large variations should be expected.

When a satellite is placed in an orbit just above the atmosphere reflecting layers, the Earth is a good approximation of an infinite flat plane blocking out one hemisphere of view. The albedo would be isotropically radiated from this plane, and the intercepted flux would vary only with the intensity of solar energy incident on the plane.

As the orbital distance of the satellite increases, the Earth occupies less of the satellite's view and appears to be a circular plane extending to the horizon. This would decrease the intensity of the albedo in proportion to the view factor (Ref. 11) and the inverse square law. Also, since the magnitude of the solar flux varies inversely as the square of the distance from the Sun, it is approximately constant

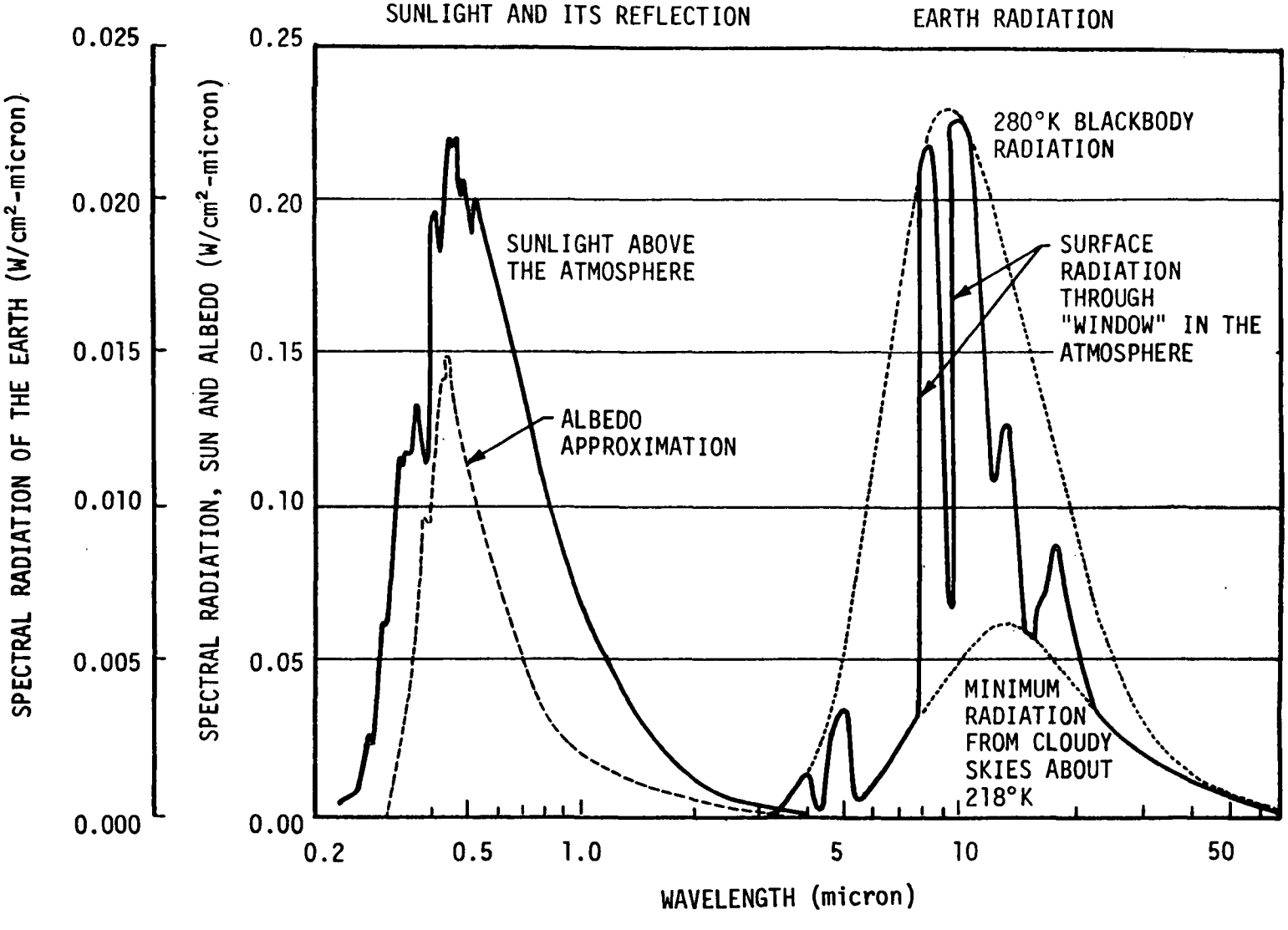

FIGURE 2. THE SPECTRAL DISTRIBUTION OF SOLAR RADIATION AS COMPARED TO ALBEDO AND EARTH RADIATION

for Earth satellites. Thus, the satellite has one large and two small external sources of heat, each source having a different spectral distribution of energy.

In addition to the albedo, the Earth radiates heat in the infrared because of its own temperature. Earth radiation comes partly from the atmosphere, a stable component, and partly from the Earth's surface in clear weather. Clouds, haze, and dust reduce the ground radiation and make the Earth appear colder from space. The cloudy sky radiates at about 140 W/m^2, and the intensity increases to about 320 W/m^2 when weather permits strong radiation from the Earth's surface. An average flux W_E of 250 W/m^2 is frequently used. The view factor and area relationship is the same for Earth radiation and albedo. The Earth radiation flux is relatively constant through a circular orbit, even during the periods of darkness. For this reason, only one calculation of Earth radiation is necessary for a stable elliptical orbit.

METHODS OF OBTAINING THERMOPHYSICAL DESIGN DATA

The optical surface parameters of interest are absorptance, reflectance, and emittance. From these general terms, more specialized quantities, such as solar absorptance and thermal emittance, can be derived, which are of great importance to spacecraft. These three fundamental parameters are linked for opaque materials by means of Kirchhoff's law, as mentioned previously.

The thermal emittance or solar absorptance of a surface may be determined either directly or indirectly. In particular, the reflectance of a surface can be determined and used as an indirect method of arriving at the desired parameter. It should be noted that the pertinent spectral region for solar absorptance is significantly different from the

region pertinent for emittance at close to room temperature. About 97 percent of the solar flux is contained in the spectral region from 0.3 to 3.0 microns; however, the corresponding bracket for a 27° C souce is from 4.8 to 60 microns.

Reflectance Measurements

The determination of spectral reflectance data in the visible and/or near infrared is a straightforward procedure in principle, and is facilitated by the existence of commercially available spectrophotometers. Spectrophotometer measurements are usually made with normal, or near normal, radiation incidence; frequently, in solar absorptance problems, the values for normal, or near normal, incidence are adequate, so that such a measurement technique is not unduly restrictive. The determination of a standard of reflectance required by most instruments is a reason of caution in this area. Magnesium oxide is a frequently used standard, but its spectral reflectance is subject to variation (Ref. 12). Other standards are defined by the National Bureau of Standards (Ref. 13).

A number of approaches avoid the requirement for a standard of reflectance. Use of a varying number of multiple reflections from identical specular surfaces (Ref. 14), use of an integrating sphere reflectometer (Ref. 15), and use of a strong-type reflectometer (Refs. 16 and 17) are some of the methods.

In principle, most of the above techniques can be used into the far infrared wavelengths with appropriate dispersing and detecting elements and careful attention to the necessity of rejecting short wavelength radiation. In the infrared, however, there are other frequently used approaches concerned with the evaluation of emittance from reflectance data.

Although the determination of diffuse reflectance is not significant for specular surfaces, diffuse reflection geometries are being used with specular surfaces. The simplest type is the Coblentz reflectometer, in which the radiation strikes the sample at a fixed angle of incidence and the reflected radiation is focused by the hemisphere on a detector conjugate to the sample. This system has many disadvantages (Ref. 18).

The standard integrating sphere reflectometer is unsatisfactory at wavelengths beyond about 2.0 microns because of the lack of an adequate diffuse reflectance coating for the longer wavelengths. However, the inverted approach, which uses diffuse illumination and observation at a particular angle to the normal, is a popular one.

When the angular spectral reflectance R_λ of a surface is available, the corresponding values of α_θ or ϵ_T, for $\theta \approx 0$, may be computed from

$$\alpha_\theta = \frac{\int_0^\alpha A_{\lambda\theta} H_\lambda \, d\lambda}{\int_0^\alpha H_\lambda \, d\lambda} \tag{28}$$

and

$$\epsilon_T = \frac{\int_0^\alpha \epsilon_\lambda W_\lambda \, d\lambda}{\int_0^\alpha W_\lambda \, d\lambda} \tag{29}$$

and the Kirchhoff's relation. The fundamental integrals to be evaluated, thus, have the general form

$$F = \frac{\int_0^{\alpha} f(\lambda)\, J_\lambda\, d\lambda}{\int_0^{\alpha} J(\lambda)\, d\lambda} = \frac{1}{J} \int_0^{\alpha} f(\lambda)\, J(\lambda)\, d\lambda \quad . \tag{30}$$

This integral may be conveniently evaluated in terms of another function $P(\lambda)$, which is the fraction of radiation contained in wavelengths shorter than λ. Since by definition

$$P(\lambda) = \frac{\int_0^{\lambda} J(\lambda)\, d\lambda}{J} \tag{31}$$

then

$$dP = \frac{1}{J}\, J(\lambda)\, d\lambda$$

and

$$F = \int_0^1 f(\lambda)\, dP = \int_0^1 g(P)\, dP \quad . \tag{32}$$

Figure 3 illustrates a type of graph (Ref. 19) for this computation. Here, $J(\lambda)$ is the extraterrestrial solar distribution $H(\lambda)$, which is shown in Table 1. These tabulated values are essentially correct down to 0.24 micron; however, below 0.24 micron, the values are low compared to recent measurements (Ref. 20).

TABLE 1. EXTRATERRESTRIAL SOLAR SPECTRAL IRRADIANCE DATA*

λ	H_λ	P_λ	λ	H_λ	P_λ	λ	H_λ	P_λ	λ	H_λ	P_λ	λ	H_λ	P_λ
0.22	0.0030	0.02	0.36	0.116	5.47	0.50	0.198	23.5	0.68	0.151	46.7	2.6	0.00445	96.90
0.225	0.0042	0.03	0.365	0.129	5.89	0.505	0.197	24.2	0.69	0.148	47.8	2.7	0.00390	97.21
0.23	0.0052	0.05	0.37	0.133	6.36	0,51	0.196	24.9	0.70	0.144	48.8	2.8	0.00343	97.47
0.235	0.0054	0.07	0.375	0.132	6.84	0.515	0.189	25.6	0.71	0.141	49.8	2.9	0.00303	97.72
0.24	0.0058	0.09	0.38	0.123	7.29	0.52	0.187	26.3	0.72	0.137	50.8	3.0	0.00268	97.90
0.245	0.0064	0.11	0.385	0.115	7.72	0.525	0.192	26.9	0.73	0.134	51.8	3.1	0.00230	98.08
0.25	0.0064	0.13	0.39	0.112	8.13	0.53	0.195	27.6	0.74	0.130	52.7	3.2	0.00214	98.24
0.255	0.010	0.16	0.395	0.120	8.54	0.535	0.197	28.3	0.75	0.127	53.7	3.3	0.00191	98.39
0.26	0.013	0.20	0.40	0.154	9.03	0.54	0.198	29.0	0.80	0.1127	57.9	3.4	0.00171	98.52
0.265	0.020	0.27	0.405	0.188	9.65	0.545	0.198	29.8	0.85	0.1003	61.7	3.5	0.00153	98.63
0.27	0.025	0.34	0.41	0.194	10.3	0.55	0.195	30.5	0.90	0.895	65.1	3.6	0.00139	98.74
0.275	0.022	0.43	0.415	0.192	11.0	0.555	0.192	31.2	0.95	0.0803	68.1	3.7	0.00125	98.83
0.28	0.024	0.51	0.42	0.192	11.7	0.56	0.190	31.8	1.0	0.0725	70.9	3.8	0.00114	98.91
0.285	0.034	0.62	0.425	0.189	12.4	0.565	0.189	32.5	1.1	0.0606	75.7	3.9	0.00103	98.99
0.29	0.052	0.77	0.43	0.178	13.0	0.57	0.187	33.2	1.2	0.0501	79.6	4.0	0.00095	99.05
0.295	0.063	0.98	0.435	0.182	13.7	0.575	0.187	33.9	1.3	0.0406	82.9	4.1	0.00087	99.13
0.30	0.061	1.23	0.44	0.203	14.4	0.58	0.187	34.5	1.4	0.1328	85.5	4.2	0.00080	99.18
0.305	0.067	1.43	0.445	0.215	15.1	0.585	0.185	35.2	1.5	0.0267	87.6	4.3	0.00073	99.23
0.31	0.076	1.69	0.45	0.220	15.9	0.59	0.184	35.9	1.6	0.0220	89.4	4.4	0.00067	99.29
0.315	0.082	1.97	0.455	0.219	16.7	0.595	0.183	36.5	1.7	0.0182	90.83	4.5	0.00061	99.33
0.32	0.085	2.26	0.46	0.216	17.5	0.60	0.181	37.2	1.8	0.0152	82.03	4.6	0.00056	99.38
0.325	0.102	2.60	0.465	0.215	18.2	0.61	0.177	38.4	1.9	0.01274	93.02	4.7	0.00051	99.41
0.33	0.115	3.02	0.47	0.217	19.0	0.62	0.174	39.7	2.0	0.01079	93.87	4.8	0.00048	99.45
0.335	0.111	3.40	0.475	0.220	19.8	0.63	0.170	40.9	2.1	0.00917	94.58	4.9	0.00044	99.48
0.34	0.111	3.80	0.48	0.216	20.6	0.64	0.166	42.1	2.2	0.00785	95.20	5.0	0.00042	99.51
0.345	0.117	4.21	0.485	0.203	21.3	0.65	0.162	43.3	2.3	0.00676	95.71	6.0	0.00021	99.74
0.35	0.118	4.63	0.49	0.199	22.0	0.66	0.159	44.5	2.4	0.00585	96.18	7.0	0.00012	99.86
0.355	0.116	4.05	0.495	0.204	22.8	0.67	0.155	45.6	2.5	0.00509	96.57			

*Wavelength λ is in microns; the mean zero air mass spectral-irradiance, H_λ, is in $W/cm^{-2}/\mu^{-2}$, and P_λ is the percentage of the solar constant associated with wavelengths shorter than wavelength λ.

The abscissa of Figure 3 is linear in terms of $P(\lambda)$ and is, thus, nonlinear in λ. The corresponding λ values (Table 1) are listed on the bottom scale, and the abscissa is graduated in terms of the λ scale. The values of $f(\lambda)$ (which is chosen to be the reflectance) are plotted on the chart at the appropriate λ positions. The chart essentially establishes the transform $f(\lambda) \rightarrow g(P)$, and the area under the plotted curve is the integral F.

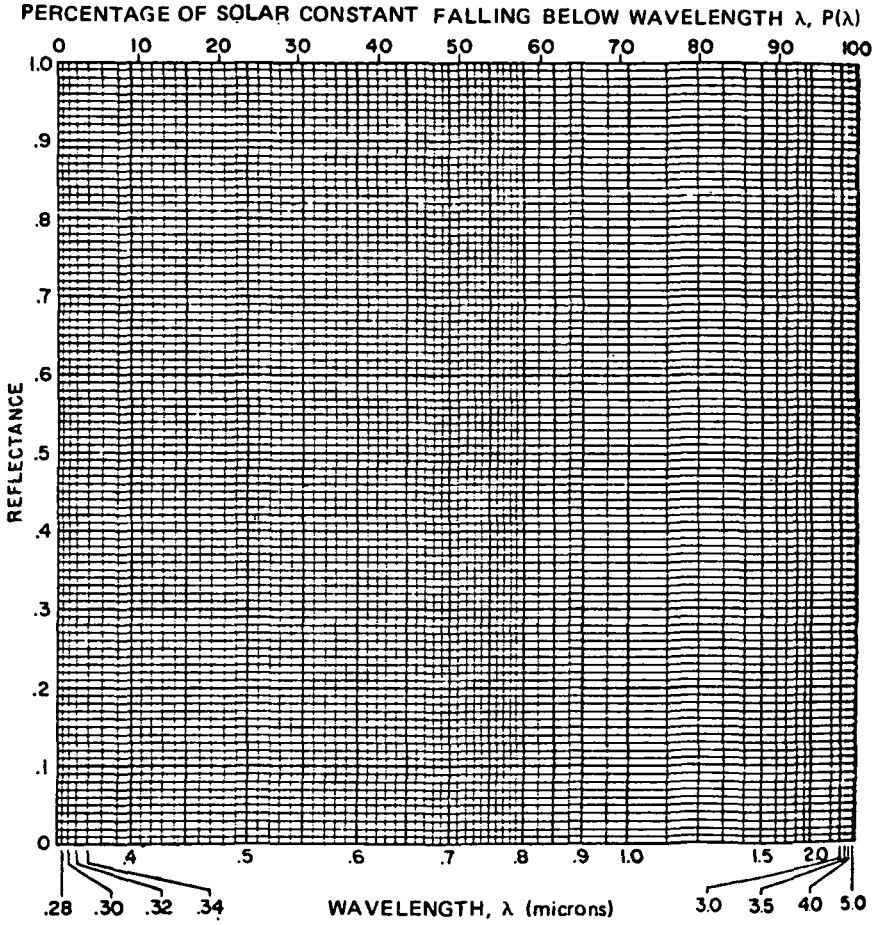

FIGURE 3. DISTORTED λ CHART FOR THE DETERMINATION OF EXTRATERRESTRIAL SOLAR REFLECTANCE OR ABSORPTANCE

A similar graph is easily constructed for a blackbody distribution at a lower temperature, and it is useful for the computation of the normal emittance of a material at a specified temperature. Table 2 gives $P(\lambda)$ data for several low-temperature distributions (Ref. 21).

Calculation of hemispherical emittance (ϵ_T), solar absorptance (α_S), and Earth infrared absorptance (α_{IR}) of coatings can be computed using a numerical integration scheme programmed on a computer (Ref. 22). In this numerical method, the equation used is

$$X_i = \frac{1}{100} \sum_{m=1}^{100} \alpha_m \qquad (33)$$

where $X_i = \epsilon_T$, α_S, or α_{IR}, with the α_m and $\Delta\lambda$ chosen in a special way.

Direct Determination

In addition to the determination of emittance and solar absorptance values from reflectance data, there are more direct methods for determining these parameters and their ratios. It is possible to determine, with some limitations, the angular spectral emittance, angular total emittance, and hemispherical emittance of samples by radiometric or calorimetric methods; and to determine solar absorptance and α/ϵ ratios with the aid of solar simulators and calorimetric techniques.

Measurement of Emittance - Although the determination of normal or angular emittance of a surface by the radiometric technique is a common practice, the measurements at temperatures below several hundred degrees centigrade are severely limited by the available radiated power (Refs. 23 and 24).

TABLE 2. FRACTION (Pλ) IN PERCENT OF TOTAL RADIATION CONTAINED IN WAVELENGTHS BELOW THE WAVELENGTH λ IN MICRONS

λ(μ)	0°C	Pλ(%) 27°C	50°C	100°C	λ(μ)	0°C	Pλ(%) 27°C	50°C	100°C
3.5	0.02	0.06	0.12	0.45	22.0	73.83	78.31	81.41	86.42
4.0	0.08	0.21	0.41	1.24	23.0	76.02	80.22	83.09	87.72
4.5	0.26	0.59	1.03	2.65	24.0	77.99	81.92	84.59	88.86
5.0	0.64	1.29	2.09	4.74	25.0	79.76	83.44	85.92	80.87
5.5	1.29	2.39	3.66	7.49	26.0	81.36	84.80	87.11	90.76
6.0	2.28	3.93	5.75	10.80	27.0	82.80	86.02	88.17	91.56
6.5	3.64	5.92	8.30	14.53	28.0	84.11	87.11	89.12	92.27
7.0	5.36	8.31	11.24	18.55	29.0	85.29	88.10	89.98	92.90
7.5	7.43	11.03	14.49	22.73	30.0	86.36	89.00	90.75	93.46
8.0	9.79	14.02	17.96	29.96	32.0	88.22	90.54	92.07	94.43
8.5	12.41	17.22	21.56	31.15	34.0	89.76	91.81	93.16	95.22
9.0	15.22	20.53	25.21	35.25	36.0	91.05	92.87	94.06	95.86
9.5	18.17	23.92	28.87	39.19	38.0	92.14	93.76	94.81	96.40
10.0	21.21	27.32	32.47	42.97	40.0	93.06	94.50	95.44	96.85
11.0	27.39	34.01	39.39	49.92	42.0	93.85	95.14	95.97	97.23
12.0	33.48	40.36	45.79	56.06	44.0	94.52	95.68	96.43	97.55
13.0	39.31	46.24	51.58	61.41	46.0	95.10	96.14	96.82	97.82
14.0	44.76	51.60	56.76	66.05	48.0	95.60	96.55	97.15	98.05
15.0	49.78	56.43	61.36	70.05	50.0	96.03	96.89	97.44	98.26
16.0	54.37	60.75	65.42	73.50	55.0	96.90	97.58	98.01	98.65
17.0	58.52	64.60	68.99	76.49	60.0	97.53	98.08	98.43	98.94
18.0	62.27	68.03	72.14	79.06	65.0	98.01	98.45	98.73	99.15
19.0	65.64	71.07	74.91	81.30	70.0	98.37	98.73	98.97	99.31
20.0	68.87	73.78	77.35	83.24	75.0	98.64	98.95	99.15	99.43
21.0	71.39	76.18	79.50	84.94	--	--	--	--	--

The most direct approach of measuring hemispherical emittance is the calorimetric method. In this technique, a sample is thermally isolated so as to lose heat primarily by radiation, and the hemispherical emittance is obtained either by measuring the power input required to maintain the sample at a fixed temperature or by determining the time-temperature response of the sample.

The sample is suspended in a relatively large isothermal evacuated encloser and is provided with an internal electric heater. The sample temperature is sensed with a thermocouple. The thermal equation for the system is

$$\frac{dT}{dt} = C\left(P + P_1 - P_2 - \sigma \epsilon_T A T^4\right) . \qquad (34)$$

P_1 is the power contributed to the sample by radiation from the enclosure and by sample radiation reflected back to the sample by the enclosure, and P_2 is the power lost by conduction and convection. T is the sample temperature, and C is the heat capacity of the sample. P is the heater power.

The quantity P_1 may be readily reduced in magnitude by cooling the enclosure to a temperature to well below T. In addition, the enclosure walls may be treated to provide high infrared emittance and consequent low reflectance for sample radiation. In the common spherical geometry, the quantity P_1 can then be evaluated from the expression

$$P_1 = A\alpha\sigma T_0^4 + A\sigma T^4 R \epsilon_T \left[\frac{1}{1 - (1 - \epsilon_T) R}\right] \qquad (35)$$

where the sample is considered to have an absorptance α_S for the wall radiation, and the walls to have a reflectance R for the sample radiation.

It is possible to consider $\alpha_S = \epsilon_T$, but the adequacy of this assumption must be verified; and to neglect the second term in the above equation, depending on the ultimate accuracy desired, as well as the values of α_S, ϵ_T, and R. For example, if $\alpha_S = \epsilon_T = 0.5$ and $R = 0.1$, then the error in P_1 will be 5 percent if the second term is neglected.

The part of P_2 which is the conduction loss via the suspension and heater leads may be minimized by the use of small leads and evaluated by auxiliary measurement using an extra set of dummy leads (Ref. 25). The gas conduction loss, which is also a part of P_2, is minimized by evacuating the chamber to about 10^{-5} Torr. The exact loss in a system usually cannot be predicted, but the upper limit may be estimated through the approximate expression

$$2.5 \times 10^{-4} \quad \frac{T - T_0}{\sqrt{T_0}} \quad p \text{ W/cm}^2 \tag{36}$$

which represents the power lost from the sample, where p is the residual air pressure. At a pressure of 10^{-5} millimeters, Equation 36 predicts a loss of about 6×10^{-5} W/cm^2 for $T = 273°K$ and $T_0 = 70°K$. Radiation from a sample of 0.02 emittance is equivalent to 9×10^{-4} W/cm^2, so that the overestimated gas loss is predicted to be 15 percent of the radiative loss.

The emittance ϵ_T of the sample can now be determined from Equation 34, either by waiting for the establishment of thermal equilibrium ($dT/dt = 0$) or by reducing the electrical power P to zero and determining, from the cooling curve, the derivative dT/dt. The latter dynamic technique has the advantage of reducing the measurement time. A detailed discussion of the magnitude of different types of errors involved in calorimetric methods is given in Reference 26.

Measurement of Solar Absorptance and α_S/ϵ_T - It is also possible to use a calorimetric technique to determine solar absorptance. One approach is to employ essentially the same type of vacuum geometry and techniques as that used for the calorimetric determination of emittance. The only difference is that the input power P in this case is the power absorbed by the surface from a light beam of known irradiance whose spectral distribution is that of solar radiation.

If the emittance of the sample is known, an equilibrium or dynamic technique may be used to determine the absorptance.

If the emittance is not known, the emittance can be referred to some standard (Ref. 27). In this technique, the surface of interest is applied to one flat side of a disk-shaped holder, and the other flat side of it is coated with a surface of known absorptance. The sides are then alternately exposed to the solar-equivalent radiation, and, between exposures, the source is blocked to allow alternate heating and cooling cycles. If an appropriate temperature cycle is established, the heat losses may be expected to cancel each other, and the ratio of unknown to known absorptance can be determined (Ref. 28). This technique does not require the incident irradiance to be known, nor, in principle, does it require a vacuum, because both radiative and air losses cancel each other. The technique does require a surface of known absorptance and a holder of good thermal conductivity. The technique is not restricted to flat surfaces.

Because of the similar requirements for the calorimetric determination of α_S or ϵ_T, the two can be simultaneously evaluated with the aid of some appropriate solar simulation. The cooling curve can be used to derive the sample emittance if the heat capacity is known. Equation 34 and an equilibrium measurement with a known solar irradiance will permit the determination of α_S/ϵ_T.

CRITERIA FOR SELECTING COATINGS

The basic method of controlling spacecraft temperature is by using materials that exhibit the necessary thermal radiation characteristics (α_S/ϵ_T). These materials cause the various surface areas of the vehicle to emit and aborb the correct amount of energy to ensure the maintenance of proper temperature. The four basic thermal-control surfaces are shown in Figure 4.

The parameters that must be considered for thermal design of a spacecraft are

- Temperature requirements
- Energy sources.

The portion of the energy which the vehicle will absorb depends on vehicle geometry and surface thermal radiation characteristics (α_S, ϵ_T). From this information and a knowledge of the internal power dissipation, a gross energy balance for the vehicle can be determined which will yield a bulk temperature as a function of α_S and ϵ_T.

The important point in equilibrium temperature control is that any technique of insulating the vehicle from external heat fluxes will also make internal heat rejection more difficult. The internal heat must also be rejected to lower temperature surfaces in a multiwall structure. Therefore, the average exterior surface temperature of a multiwall structure must be lower than that of a single-wall structure to permit the rejection of the same amount of internal heat. This places increased emphasis on coatings with the lowest possible α_S/ϵ_T. The ideal coating should have an $\alpha_S/\epsilon_T = 0$.

Temperature cycling is caused by the interruption in solar energy during passage through the shadow (Earth's or another planet's) and by the variable albedo and infrared radiation caused by orbit

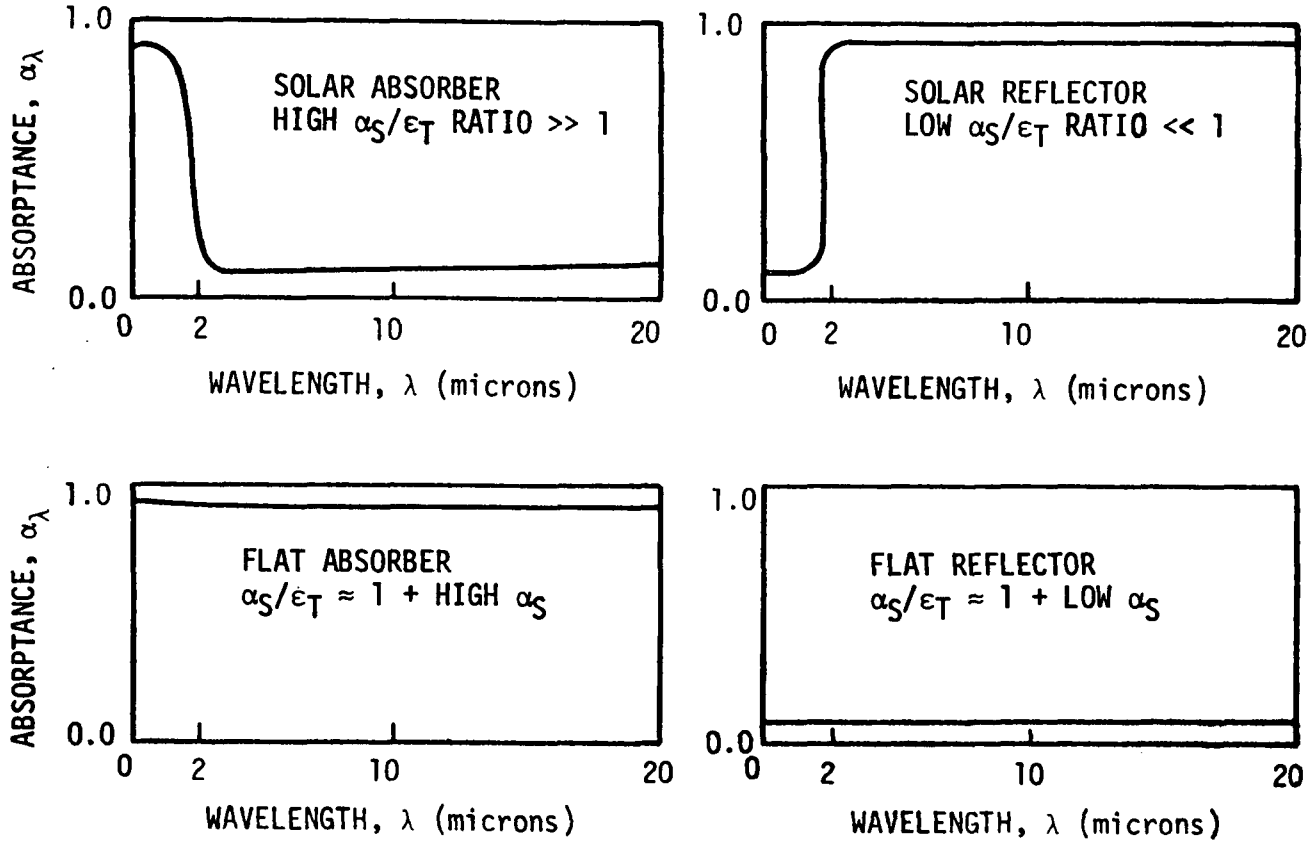

FIGURE 4. IDEAL REPRESENTATION OF FOUR BASIC SURFACES

orientation and eccentricity. The intensity of the solar flux also vaires on interplanetary missions. To reduce this temperature cycling, the effective heat capacity of the vehicle has to be increased. This can be achieved when a multiwall structure is used. When the vehicle is oriented toward the Sun, the heating can be reduced to zero or less by reducing the α_S/ϵ_T of the exterior coating to 0.33 or less, respectively. Where the satellite is oriented toward the Earth, the best thermal control is achieved by using a white coating on the outer surface of the multiwall structure.

Thermal control coatings have five principal functions:

- Balance energy absorption and emittance
- Increase the heat capacity of a vehicle
- Selectively transmit certain radiation
- Reflect or absorb heat
- Radiate heat.

There are numerous variations and combinations of these functions on each new spacecraft design.

Table 3 illustrates some of the criteria and control techniques that are being used.

The various types of windows necessary in a spacecraft designed for normal viewing or viewing through electronic instruments frequently transmit harmful ultraviolet radiation, in addition to useful ultraviolet radiation, and upset the thermal balance of the vehicle by the "greenhouse effect". If the window can be made with a small amount of iron oxide, it will not transmit ultraviolet light. To prevent sunburn, wavelengths shorter than 0.32 micron must be absorbed. A very thin film of gold over the outside of the window glass will prevent the heating of the interior and will prevent the temperature gradient. An interference or antireflection coating may be used to increase the transmittance of the glass in narrow wavelength bands. Magnesium fluoride is used for

TABLE 3. THERMAL COATING APPLICATIONS

COATING FUNCTION	CONTROL FACTORS	CONTROL TECHNIQUES
Equilibrium temperature control (without attitude control)	Low α_S/ε_T controlled-reflection shields	Low α_S/ε_T coating on outside of multiwall structure
Moderation of temperature cycling with attitude control	Heat capacity, low α_S/ε_T heat shields	Match heat shield and radiators with orientation to control the direction of heat flow
Temperature variation within vehicle	Thermal compartmentation	Various types of heat shields; frost
Windows	Ultraviolet and infrared absorption, transmission and reflection	Interference coatings; transparent metal coatings
High-temperature and cryogenic insulation	Reflective versus nonconductive insulation; deterioration	Mixed insulation: diffusion barriers and topcoats for reflectors
Heat radiators	α_S, ε_T thermal conductivity	Dense high ε above 1000°K; low α_S/ε_T at lower temperatures
Atmospheric reentry	Design concept; ε_T conductivity and oxidation of exterior	Low conductivity heat shield; radiation through leading edge
Solar-energy conversion	Type of conversion system and its thermodynamic efficiency versus temperature	Optimize collection efficiency to the thermodynamic efficiency; minimize heat losses; special window for photocells
Special-purpose coatings	Thermal, physical, and electrical properties	Use chemical and physical structure to predict the the most likely coatings

this purpose on telescope and camera optics. Where infrared windows are needed, it is desirable to reflect the visible light. This can be done by an interference reflector, or by absorbing the visible light with a low-energy-gap semiconductive coating. Radar and microwave windows permit a wide selection of coating materials, but the metallic materials in the coatings must be avoided. Table 4 summarizes some of the window coating materials.

In the manned space vehicle, the ideal passive temperature-control system would maintain a temperature of 20 to 25° C at times when the minimum internal heat is generated and the minimum external heat is absorbed. Then an active temperature-control system would dissipate any excess heat by use of radiators and heat exchangers. The heat shields that are used between space vehicles and radiators generally have a low-emittance coating on the inside and a white, high-emittance coating on the outside. Radiators that are used below about 500° to 700° C will generally require white coatings (low α_S/ϵ_T) of high emittance. Some of the common radiator coatings are listed in Table 5.

TABLE 4. WINDOW COATINGS

TYPE OF WINDOW	UNDESIRABLE RADIATION	POTENTIAL COATINGS
Visible light	Ultraviolet	Fe_2O_3, organic absorbers semiconductors
Visible light	Bremsstrahlung (X-rays)	Low-Z coatings-e.g., Al_2O_3
Visible light	Thermal (infrared)	Thin transparent SnO_2 or gold coating
Visible light	Surface reflection	MgF_2
Infrared light	Visible light	Interference reflector or semiconductor
Microwave	Ultraviolet, visible, or infrared	Low-dielectric constant insulators; thin films for antennas

TABLE 5. RADIATOR COATINGS

TYPE	α_S/ϵ_T	ϵ_T	MAXIMUM TEMPERATURE °C
White organic	0.2 to 0.3	0.9	200 to 300
Black organic	0.9	0.9	300 to 400
Anodized aluminum*	0.12 to 0.30	0.9	350
Waterglass enamel	0.2 to 0.3	0.8	500 (depends on metal substrate)
Porcelain enamel	0.25 to 0.35	0.8	600 to 700
Oxidized stainless steel	0.8	0.85	600 to 650 in vacuum
Alumina	0.22 to 0.4	0.6 to 0.8	Depends on metal
Refractory enamels	0.5 to 0.8	0.6	1,000
$MoSi_2 + Cr_2O_3$	0.8	0.6	1,200

*The 0.12 value is for anodized, high-purity aluminum prior to sealing.

CHAPTER 2
DAMAGE MECHANISMS IN PASSIVE THERMAL CONTROL SURFACES

This chapter discusses the presently understood mechanisms by which thermal control surfaces are degraded by the space environment. A short description is given of the space environment to which the thermal control surfaces are exposed, followed by descriptions of the observed effects of the individual environments.

THE SPACE ENVIRONMENT

The space environment is the combined effect of the vacuum, radiation, meteoroid impacts, and thermal factors related to space travel. In the planning of a space mission, all of these factors must be considered in their proper perspective.

The lower atmosphere or troposphere has been characterized quite well. The composition of this layer is relatively constant, but temperature and pressure decline with increasing altitude. The troposphere is bounded by the tropopause which contains the jet streams of high winds (Ref. 29). The tropopause varies in height from 6 to 18 kilometers and is higher and colder at the equator. The next atmosphere layer, the stratosphere, is a region of constant temperature of about -56°C (Ref. 30). At this altitude, there is a significant increase in solar ultraviolet light and an accompanying increase in ozone concentration. The stratosphere is thick over the poles and thin or nonexisting in equatorial regions. The mesopause forms the atmospheric temperature minimum near 200°K and corresponds approximately to the level of the D layer of the ionosphere. The region above the mesopause increases rapidly in temperature up to about 200 kilometers and

then increases more slowly in temperature until it reaches the extreme temperatures of the inner Van Allen radiation belt. This region is called the ionosphere or exosphere.

Most of the energy encountered above the atmosphere is electromagnetic radiation. This radiation controls the temperature of the spacecraft. Almost 10 percent of the solar electromagnetic radiation is near ultraviolet light (0.20 to 0.40 micron). This ultraviolet light can cause chemical and physical changes to many materials, and it is 5 to 1,000 times more intense than all the other ionizing radiations combined. Typical Van Allen radiation-belt intensities are about 0.03 percent of the near ultraviolet, whereas the normal solar wind is 0.0004 percent of the ultraviolet flux. However, the intensity of the solar wind and the outer Van Allen radiation belts is greatly enhanced by the solar flares and their concomitant magnetic storms.

The base of the exosphere is the maximum altitude at which satellites can operate without encountering significant quantities of hard radiation trapped in the Earth's magnetic field. At high altitude in the auroral zones, both solar corpuscular and Van Allen radiations penetrate to the ionosphere to deny a safe zone for polar orbital operation (Refs. 31 and 32). The inner belt and the outer ring current of the Van Allen belt system (Ref. 33) are composed of high- and low-energy protons, respectively. The crescent-shaped belt in between contains a high density of energetic electrons, but varies a great deal in intensity and size with its outer layers. The motion of the geomagnetically trapped particles makes the radiation somewhat anisotropic, with maximum flux parallel to the magnetic equator. The measured proton and electron fluxes are >40 MeV and >20 keV, respectively (Refs. 34 and 35). Analysis of the loss mechanism indicates a

substantial proton flux down to 1 MeV or less at large distances from the Earth. It is difficult to predict the electron energy flux below 20 keV. This data is important because the lower energy corpuscular radiation causes the most severe damage to the temperature control surfaces of the spacecraft.

It is known that virtually all gases are ionized out to Jupiter or beyond and, therefore, come under the influence of the solar magnetic field. Micrometeoroids might also be controlled by the Sun's magnetic field resulting from a radiation-induced surface charge. The surface charge might also cause interaction with the Earth's magnetic field, which might cause the ring of micrometeoroids near the geomagnetic equator. The radial and extended dipole models of the solar magnetic field point to higher radiation fluxes at higher heliomagnetic latitudes above or below the plane of the ecliptic (Refs. 33, 36, and 37). The energy and flux of the solar wind would increase slowly approaching the Sun. The solar flares appear to be contained in a "magnetic bottle" and are one of the greatest hazards to manned space travel.

Cosmic radiation from outside the solar system constitutes some hazard because of the low flux level. Elliot (Ref. 38) proposed a concept which would indicate a considerable increase in low-energy cosmic rays near the periphery of the solar magnetic field. There is no evidence of trapped radiation around other planets except for Jupiter. The Jovian Van Allen type belts are apparently much more intense than the Earth's, possibly a million times more. Jupiter has such a strong magnetic field that is may capture a considerable amount of corpuscular radiation from the Sun.

DAMAGE CAUSED BY THE SPACE ENVIRONMENT

With the exception of neutrons, most of the electromagnetic and corpuscular radiation is absorbed by interaction with the electron shells around the atomic nucleus of a material. Very low-energy radiation changes the rotational states of the molecules of the material, and the energy in the near infrared will change the lattice vibrational states to increase the temperature. This type of radiation will not damage coating materials directly, other than thermal degradation caused by overheating. However, high-energy radiation of ultraviolet light will cause transition of electrons to higher energy states and may weaken the bonds between atoms to affect the chemical reactivity of the molecule. This will cause the formation of radicals and ions, whereby the physical property of the material will be changed. Radiation of higher energy causes emission of electrons from the parent nucleus and could also result in the ionization of the molecule. The initial absorption or decay process that occurs when electromagnetic radiation interacts with matter is shown diagrammatically in Figure 5. The principal modes of energy decay for high-energy radiation are

- Pair production
- Compton scattering
- Photoelectric effect
- Electronic excitation
- Vibrational, or thermal, excitation.

Pair production is the formation of an electron-positron pair from a high-energy photon. The minimum photon energy required for this process is 1.02 MeV, or about 0.0122 Å.

Effect of Gamma and X Radiation

High-energy gamma (γ) and X radiation is lowered in energy and eventually absorbed in a stepwise manner when it interacts with matter. Virtually all the energy of the gamma- or X-ray photons ultimately become

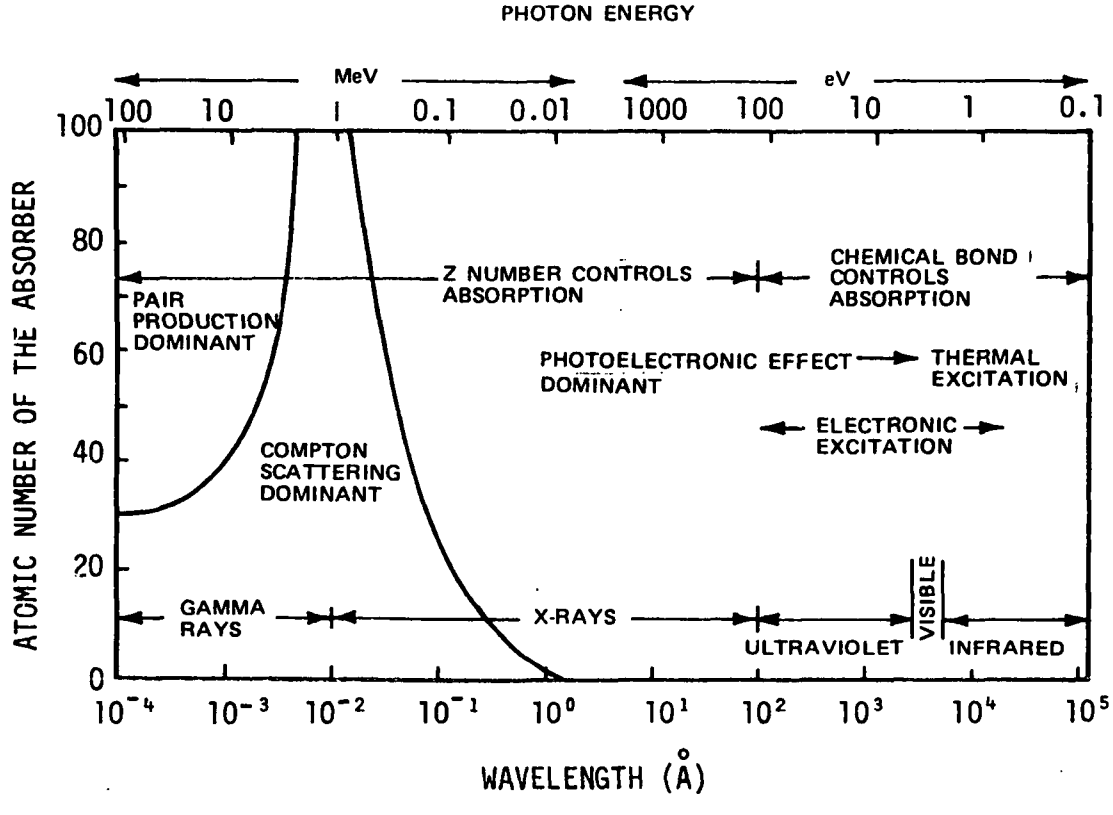

FIGURE 5. THE INITIAL ABSORPTION OR DECAY PROCESS THAT OCCURS WHEN ELECTROMAGNETIC RADIATION INTERACTS WITH MATTER

thermal energy or chemical energy. The cross section of an atom for electron-positron pair production varies approximately as the square of the nuclear charge Z. The electron formed in pair production decays in energy by excitation of neighboring molecules. The position diffuses through the material and is annihilated after a short time by collision with an electron. This results in emission of two photons with an energy of 0.51 eV, if the electron is not bound (Ref. 39).

Pair production is not very important for most environmental conditions encountered by spacecraft. However, when a nuclear power source is used, its gamma-radiation energy can be lowered to below 1.02 MeV by proper shields.

Compton scattering is the decay and scattering process of a photon by collision with electrons. For a free-recoilable electron, part of the photon momentum is transferred to the electron as kinetic energy, and the photon may be backscattered or absorbed by the photoelectric process. This scattering is the predominant form of photon-energy decay for a broad spectrum of high-energy radiation from nuclear reactors. This phenomenon is also important for the high-energy Bremsstrahlung generated by Van Allen radiation. The interaction is an electronic process and is, therefore, proportional to the electron density of the absorbing material. This electron density is roughly the same ($\sim 3 \times 10^{23}$ g) for equal masses of materials except for hydrogen.

In the low-energy range, when the collision is with bound electrons, the scattering is coherent and the photon is scattered with no, or little, energy change. High-Z materials have more tightly bound electrons, show coherent scattering over broader energy ranges, and cause increased backscattering of short X-rays, particularly for high-Z dielectric coatings.

The photoelectric effect dominates the absorption of X-rays and far ultraviolet light. The photoelectric cross section varies as the fourth power of nuclear charge (Z^4) and decreases rapidly with increasing photon energy, E, approximately as E^{-3}. The high-Z materials have a higher nuclear charge and more tightly bound electrons with higher resonant frequency; hence, more energetic radiation can be absorbed.

Effect of Ultraviolet Light

The absorption of short wavelength ultraviolet is actually an extension of the photoelectric effect to the outer electron shells of a molecule. These ultraviolet photons can also arise through the decay of high-energy radiation through fluorescence or Bremsstrahlung from secondary electrons. The distinction between photoelectric ultraviolet excitation is less prominent when low-Z materials are irradiated.

From a chemical point of view, the emission of an electron by ultraviolet light leaves a positively charged ion without necessarily exciting other electrons. This is a highly unstable condition, especially for covalent materials, and molecular rearrangement may occur. Ejection of protons from the positively charged molecule is the more probable reaction in organic materials.

When the vacuum or far ultraviolet light is incident on a coating surface, it is generally absorbed within only a few angstroms of the coating layer. This is true for most organic coatings and many inorganic materials, particularly those containing oxygen. Oxides absorb strongly at wavelengths of 0.16 micron or less. Thus, far ultraviolet light from the Sun affects only the surface of a coating, whereas gamma-rays and Bremsstrahlung interact more uniformly throughout the coating.

The near ultraviolet light accounts for 99.97 percent of the solar ultraviolet flux and 9.02 percent of the total solar constant. Therefore,

this radiation is important and has a significant effect on the thermal balance of the spacecraft.

The difference between the absorption of near ultraviolet and far ultraviolet is that the excited electron is generally not ejected from the material in the former case, except for some semiconductors and conductors. In most cases, the energy of the excited electron is transferred to the thermal or vibrational states of the molecule. In some materials, the energy can also be fluoresced or stored for later phosphorescence. In case of conductors and semiconductors, the energy transferred to the conduction electrons is converted to thermal energy when the electron is recaptured by the parent nucleus. Ultraviolet-excited organic materials may undergo a chemical rearrangement or reaction before the energy can be dissipated thermally or radiatively. For most materials, the absorption increases monotonically above the resonant frequency. The extinction coefficient measures the probability of an electronic transition and is governed by the nature of the chemical bond and the degree of overlap between the excited- and ground-state orbital. The excited electron may be transferred to another molecule by mutual interchange with a ground-state electron. Furthermore, the formation of F and V vacancy centers by the action of high-energy radiation can cause strong absorption of ultraviolet at some other wavelength.

These chemical changes invariably result in higher absorption of solar energy for organic and many other nonmetallic materials, with generally little or no effect on the emittance. This causes an increase in spacecraft temperature.

Effect of Electron Radiation

The electrons and protons in the Van Allen radiation belt is a more serious corpuscular radiation source than the solar wind. As

with high-energy gamma-rays, the energy of the corpuscular radiation is dissipated by a series of events. This radiation differs from electromagnetic radiation, in that it contains atomic and subatomic particles.

The electron environment encountered in orbital and interplanetary space flights includes a wide range of energies and densities. This radiation is also partially reflected at the material surface, as with any other type of radiation. Metals with high free-electron density show maximum reflection, whereas dielectric materials have very little reflection except for very low electron energies. Metallic materials are very reflective to electrons below 1 volt, but the reflection drops very rapidly to a constant value at higher energies (Ref. 40). Where $Z < 30$, the reflection remains constant into the keV range, but there is a slow increase in reflection for higher Z materials (Refs. 41 and 42). Since the number of electrons per unit mass is relatively constant, the penetration thickness of the electrons is approximately proportional to the mass of shielding material. Therefore, the thickness of the shielding coating required varies with the density of the coating material. A thickness of 6 mils (0.015 centimeter) of a coating with density near 1.0 is required to absorb the bulk of Van Allen radiation below 100 keV. It would require 3 centimeters of plastic to stop the 5-MeV electrons.

Effect of Proton Radiation

The interaction of protons and other positive ions with surfaces is somewhat more complex than the electron interaction. Low-energy secondary electrons are sometimes backscattered with fairly high yields, or the proton may be reflected as a negative ion. These interactions increase the positive charge on the bombarded surface. Another surface reaction is sputtering, which is the ejection of atoms or groups of atoms from a metallic surface by positive-ion-bombardment. Sputtering is the

most serious radiation effect on reflective metals. The penetration of protons into a material is controlled primarily by electrons. Coatings with high atomic numbers are more effective on a thickness basis than on a weight basis (Ref. 43). Although the main interaction of protons is with electrons, elastic and inelastic collisions with atomic nuclei are also possible. Inelastic collisions increase with proton energy and can cause excitation and fragmentation of the bombarded nuclei, leading to the radiation of neutrons. These neutrons are very penetrating and may cause other nuclear reactions and atomic displacements, or they may decay into a proton and an electron.

The estimated magnitude of the charge on the surface of the spacecraft from low-energy corpuscular radiation bombardment varies from tenths of a volt to thousands of volts. This kind of surface charge can make rendezvous hazardous, if the charges on the two spacecraft are different. This surface charge can be controlled through proper selection and blending of coatings.

Effect of Neutron Radiation

The density of neutrons which are generated by cosmic radiation is quite low and decreases with increasing distance from the Earth. A collision rate in the order of 1 n/cm^2-sec has been estimated. The penetration of neutrons is measured in centimeters or tenths of centimeters, so it is not a coating problem. However, the nuclear reactions of neutrons must be considered in selecting coating materials for use near nuclear reactors.

Effect of Space Vacuum

The Earth's atmosphere at an altitude of 200 miles above the Earth contains about 10^9 particles/cm^3 at solar maximum. The particles consist of approximately 75 percent atomic oxygen, 18 percent molecular

nitrogen, and the remainder, molecular oxygen, helium, and atomic nitrogen. This corresponds to a pressure of about 10^{-7} millimeters of mercury. The mean free path at this pressure is large; therefore, the particles leaving a surface have no chance of returning. Therefore, volatilization can be a potential problem.

Volatilization of metals at modest temperatures, other than zinc, cadmium, and tin, is not an expected thermal design problem. Dielectric materials have some history of degradation in vacuum. Organic materials are generally less stable in vacuum than are inorganic materials. Organic resins are oxidized by ultraviolet light to low-molecular-weight aldehydes, acids, etc., through "free radical" formation. In vacuum, these free radicals cannot oxidize because of the lack of oxygen, so they generally "cross-link". As the polymer becomes more lightly cross-linked, hydrogen may diffuse and escape, leading to unsaturation and conjugation. Inorganic oxides, such as zinc oxide and titanium dioxide, may reduce because of ultraviolet radiation under vacuum. Under atmospheric pressure, the oxygen ion vacancy that is created in zinc oxide because of ultraviolet becomes somewhat neutralized and the effect is reversible. However, under vacuum this reaction is severe and the reaction is mostly irreversible.

For thermal control surfaces operating at elevated temperature, e.g., nuclear reactor radiators operating between 600 to 1400°F, the volatilization may be a problem of great concern.

REFERENCES - PART I

1. Introduction to Modern Physics, McGraw-Hill Book Company, New York, p. 131, 1955

2. Z. Elektrochem, 60, 163, 1960

3. Organic Protective Coatings, Reinhold, New York, 1953

4. NASA Report 63270-04-02, May 1961

5. Ann. Phys. Chem., 19, 267, 1883

6. Introduction to Heat Transfer, 2nd Ed., Ch. 4, McGraw-Hill Book Company, New York, 1951

7. Proc. Phys. Soc., 41, 569, 1929

8. J. Meterol, 11, 431, 1954

9. "Satellite Environment Handbook", Ch. 7, Stanford University Press, 1961

10. Physical Meterology, John Wiley and Sons, Inc., New York, 1954

11. Am. Rocket Soc. J., 32, 1033, 1962

12. Surface Effects on Spacecraft Materials, John Wiley and Sons, Inc., New York, p. 123, 1960

13. Radiative Transfer from Solid Materials, The MacMillan Company, New York, p. 142, 1962

14. J. Opt. Soc. Am., 48, 88, 1958

15. J. Opt. Soc. Am., 51, 1279, 1961

16. J. Opt. Soc. Am., 50, 1, 1960

17. Procedures in Experimental Physics, Prentice-Hall Publishing Company, New Jersey, p. 376, 1938

REFERENCES (Continued)

18. Surface Effects on Spacecraft Materials, John Wiley and Sons, Inc., New York, p. 117, 1960

19. J. Opt. Soc. Am., 53, 1096, 1963

20. Space Sci. Rev. II, 1, 1963

21. Tables of Blackbody Radiation Functions, The MacMillan Company, New York, 1961

22. MSFC IN-SSL-T-68-10, October 1968

23. Radiative Transfer from Solid Materials, The MacMillan Company, New York, p. 157, 1960

24. J. Opt. Soc. Am., 49, 815, 1959

25. J. Opt. Soc. Am., 39, 1009, 1949

26. "Measurement of Thermal Radiation Properties of Solids", National Aeronautical Space Administration, Washington, D. C., NASA SP-31, p. 55, 1963

27. J. Sci. Inst., 33, 356, 1956

28. Proc. Roy. Soc., A161, 1, 1937

29. Handbook of Geophysics, 2nd Ed., The MacMillan Company, 1959

30. The Physics of Stratosphere, Cambridge, London, 1954

31. J. Geophys. Res., 65, 3163, 1960

32. Airglow and Aurora, Pergamon Press, New York, 1955

33. The Exploration of Space, The MacMillan Company, New York, 1960

34. J. Geophys. Res., 65, 1361, 1960

REFERENCES (Concluded)

35. J. Geophys. Res., 67, 397, 1962

36. Electromagnetic Phenomena in Cosmical Physics, Cambridge, London, 1958

37. J. Geophys. Res., 65, 1143, 1960

38. Nature, 186, 299, 1960

39. Radiation Shielding, Ch. 2, Pergamon Press, New York, 1957

40. Proc. Roy. Soc., A182, 17, 1943

41. Advances in Electronics and Electron Physics, Vol. 1, Academic Press, New York, p. 65, 1948

42. Solid State Physics, Vol. 6, Academic Press, New York, p. 251, 1958

43. Experimental Nuclear Physics, Part II, John Wiley and Sons, Inc., New York, 1953

PART II
THERMOPHYSICAL PROPERTIES

The purpose of a thermal control coating, as is evident, is to provide a surface with known and desirable properties. Coatings are used to obtain favorable values of solar absorptance (α_S) and hemispherical emittance (ε_T) for a system to maintain thermal balance.

Coatings used on different spacecraft have ranged from very simple (as - received metallic surface) to very complex (e.g., optical solar reflector). Many paints, chemically furnished surfaces, front and second surface mirrors, etc., have been used.

Table 6 indicates methods of obtaining specific α_S and ε_T values in a general sense and only indicates different ranges of values obtainable.

It is advantageous to group certain properties of the coatings to gain a general idea about them. This is done in Table 7 which shows the temperature limit for various coating groups. Cost and weight data are shown in the same manner in Table 8. It should be noted that these figures are not exact.

Series emittance tapes can exhibit a wide α_S/ε_T range depending on overcoat thickness.

The degradation of coatings with low initial values of α_S/ε_T is of prime interest to thermal design engineers. These coatings are generally used on space radiators which reject vehicle heat. Increases in α_S with time, caused by space radiation, raises the temperature of the vehicle and can lead to equipment failure. Figures 6 and 7 show the range of some available thermal-control surfaces for missions in space not exceeding 1 year and 5 years, respectively. These figures are adapted from the paper entitled "Recent Advances in Spacecraft Thermal-Control Materials Research", presented at the 20th IAF

Congress, Mar del Plata, Argentina, October 10, 1969, by D.W. Gates, G.A. Zerlaut, and W.F. Carroll.

TABLE 6. OBTAINABLE α_S AND ε_T FOR VARIOUS COATING TECHNIQUES

TYPE OF SURFACE	α_S	ε_T	POLISHED METALS	AS-RECEIVED METALS	SAND-BLASTED METALS	VACUUM METALLICS	VACUUM NON-METALLICS	CONVERSION COATINGS	PLATED COATINGS	METALLIC PAINTS	NON-METALLIC PAINTS	VITREOUS ENAMEL	INORGANIC BONDED	TRANSPARENT CONVERSION	TRANSPARENT NON-PIGMENTED PAINTS
Flat absorber	0.9	0.9	--	--	--	--	--	X	--	--	X	X	X	X	X
Median IR absorber	0.9	0.5	--	--	--	--	X	X	--	--	--	--	--	X	X
Solar absorber	0.9	0.1	--	--	--	X	X	--	X	--	--	--	--	--	--
Median solar absorber	0.5	0.9	--	--	--	--	--	X	--	--	X	X	X	X	X
Medium	0.5	0.5	--	--	X	--	X	X	--	X	--	--	X	X	X
Median solar absorber	0.5	0.1	X	X	X	X	X	--	X	--	--	--	--	--	--
Solar reflector	0.1	0.9	--	--	--	--	--	X	--	--	X	X	X	X	X
Median IR reflector	0.1	0.5	--	--	--	--	X	X	--	X	--	--	--	X	X
Flat reflector	0.1	0.1	X	X	--	X	X	--	X	--	--	--	--	--	--

TABLE 7. MAXIMUM TEMPERATURES FOR COATING GROUPS

DESCRIPTION	T Max. (°F)
Bare metal	N/A
Paint	
Urethane vehicle	150
Epoxy vehicle	300
Silicone-alkyd vehicle	650
Silicone vehicle	800
Chemical surface finish	
Alodine (conversion coating)	400
Anodize	1,000
Flame, plasma spray	1,000
Tapes	
Aluminized mylar	200
Series emittance	800
Optical solar reflector (OSR)	600

TABLE 8. RELATIVE COST AND WEIGHT FOR COATINGS

DESCRIPTION	WEIGHT (lb/ft^2)	COST ($dollars/ft^2$)
Bare metal	0	0
Paints	0.04	1 to 3
Chemical surface finishes	0.03 to 0.06	1 to 3
Tapes		
Aluminized teflon	0.06	4
Series emittance	0.06	4 to 5
Optical solar reflector (OSR)	0.09	500

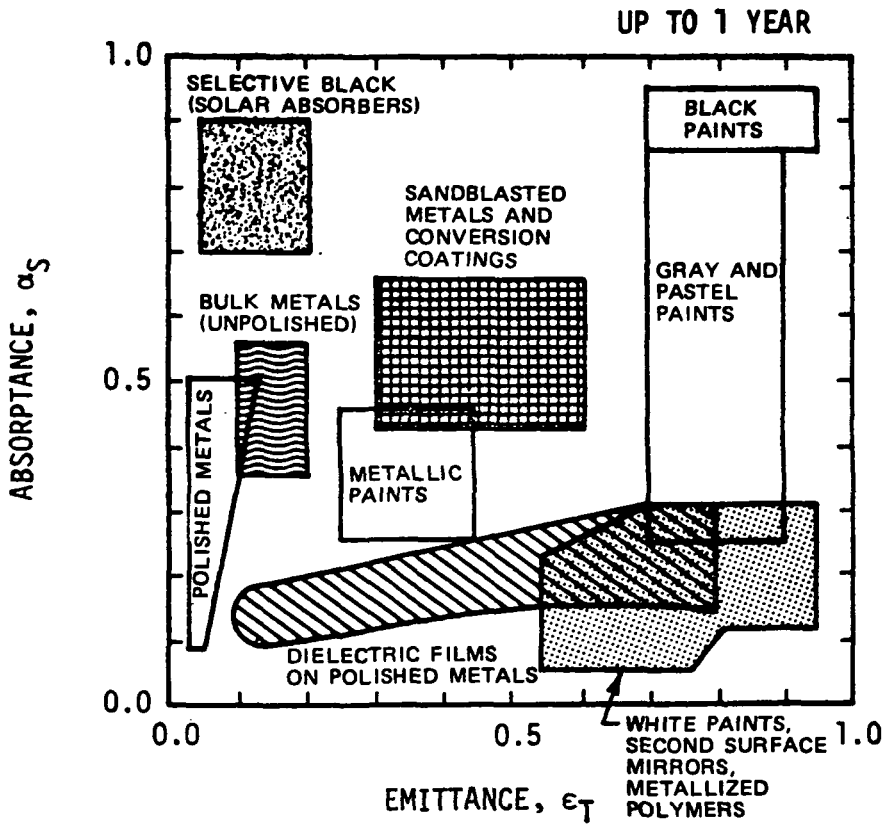

FIGURE 6. AVAILABLE COATINGS AND SURFACES BASED ON THE STATE OF THE ART

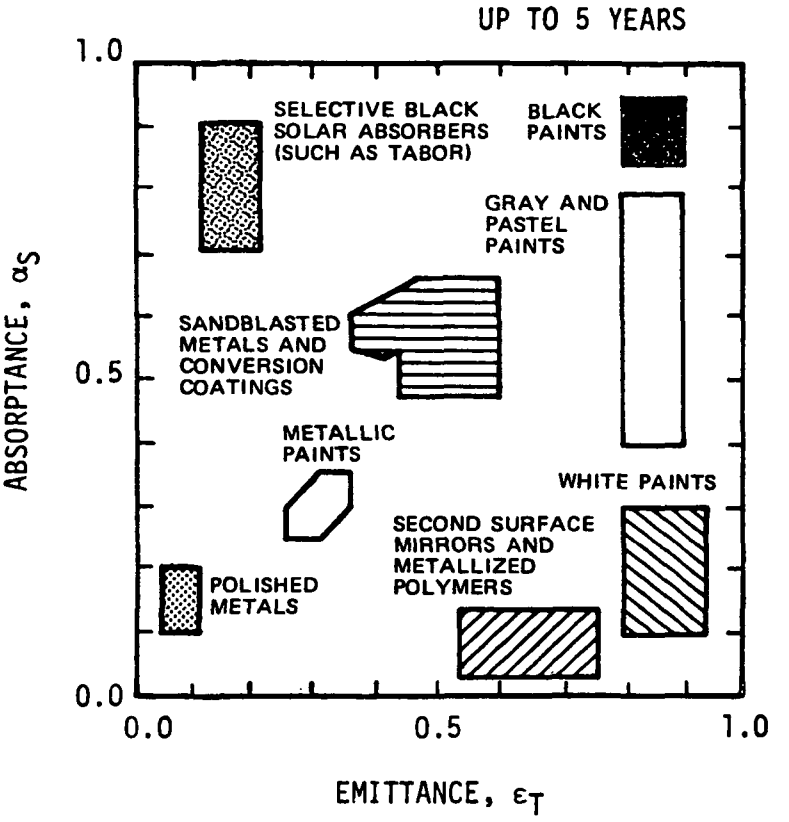

FIGURE 7. AVAILABLE COATINGS AND SURFACES BASED ON THE STATE OF THE ART

DATA SHEETS ON THERMAL CONTROL SURFACES

SILVER-COATED OPTICAL SOLAR REFLECTOR (OSR)

Composition: Vapor-deposited silver on Corning 7940 fused silica with an overcoating of vapor-deposited inconel.

Density: 2.2 gm/cm^3

Recommended Thickness: Recommended standard size is approximately 1 by 1 by 0.008 inches thick. No variation in α_S after the metal film is opaque. No variation in ϵ_T for fused silica thicker than 0.008 inch. Thickness less than this is very fragile. 1000 Å of silver overcoated with 500 Å inconel.

Maximum Temperature: 260°C

Substrate: Aluminum alloys

Adhesion: Has passed the sinusoidal and random vibration tests using GE-SS 4120 primer and RTV-615 adhesive. Another excellent adhesive is DC 92-024.

Thermophysical Properties:

Initial Solar Absorptance, $\alpha_S = 0.050$
Initial Hemispherical Emittance, $\epsilon_T = 0.810$
Initial $\alpha_S/\epsilon_T = 0.062$
Solar Absorptance after 1000 ESH of UV = 0.050
Solar Absorptance after 1000 EWH of protons = 0.050
Solar Absorptance after 6×10^{14} e/cm^2 = 0.050

Contamination Susceptibility: Surface contamination, including finger prints, oil, dust, and atmospheric weathering, does not cause permanent degradation after application and can be removed by sample cleaning.

Outgassing Characteristics: The RTV-615 silicone adhesive, used to apply the mirrors to the substrate, requires a minimum cure of 14 days at room temperature to minimize outgassing during ascent. The steady-state weight loss is 0.041%/cm^2/hr at 100°C. The constituents of the outgassing product are now known.

SILVER-COATED OPTICAL SOLAR REFLECTOR (OSR) - Concluded

Refurbishment Capability: OSRs are fragile. Temporary contamination must be removed prior to launch. Damaged parts may be removed and new ones applied. Difficult to apply on curved surfaces.

Source and Cost: The present source is Optical Coatings Laboratory, Inc., (707) 545-6440. Large quantity price is approximately $\$2.00/in^2$. Lockheed contact: Mr. L. Haslim, (415) 493-4411.

State of Development: Seems to be complete. Lockheed work on this coating was mostly performed under Contract Nos. AF 04(647)-787, AF 33 (615)-5066, and NAS2-3063.

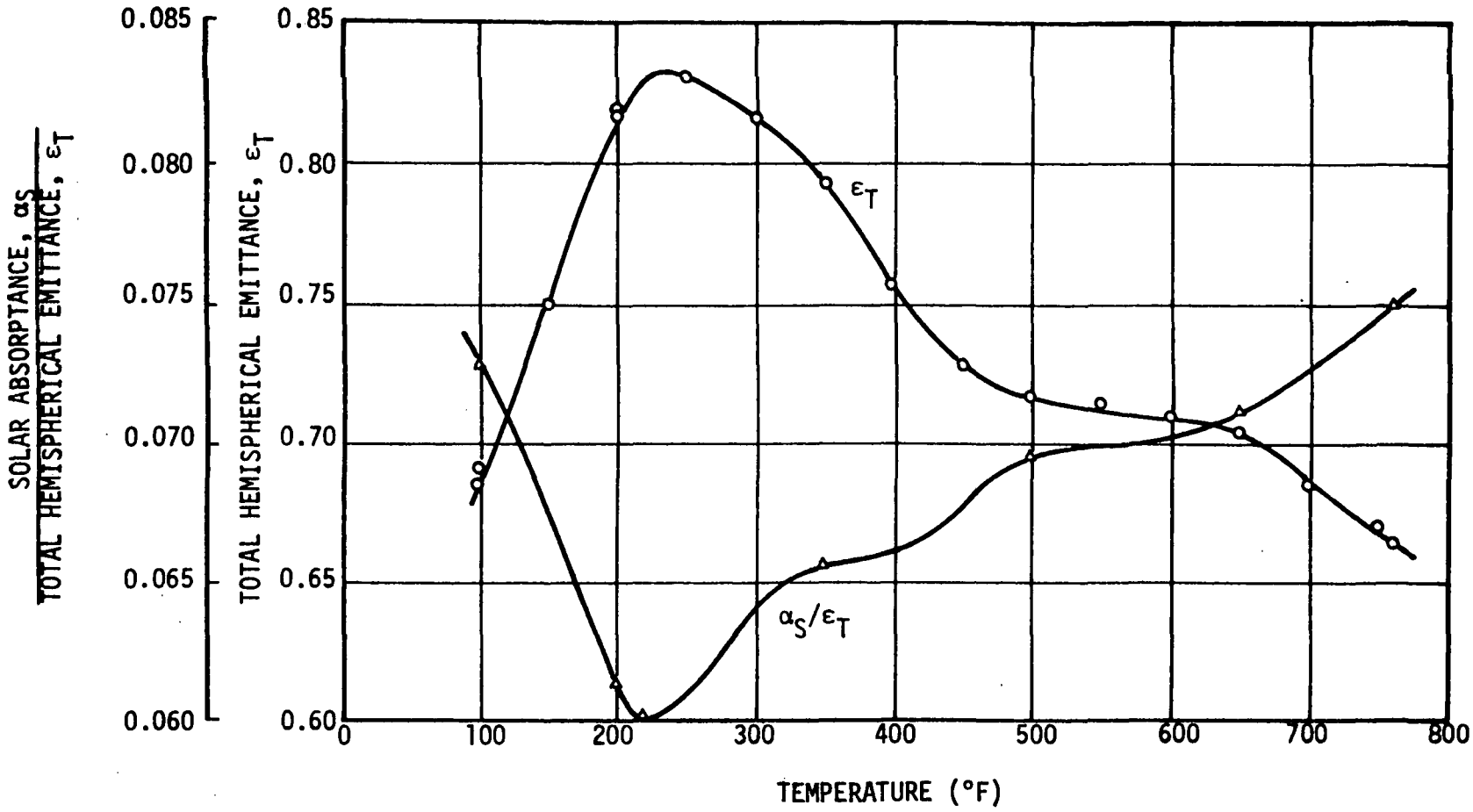

0.008-INCH FUSED SILICA SECOND-SURFACE MIRROR

ALUMINUM-COATED OPTICAL SOLAR REFLECTOR (OSR)

Composition: Vapor-deposited aluminum on Corning 7940 fused silica with an overcoating of vapor-deposited silicon monoxide.

Density: Approximately 2.2 gm/cm^3

Recommended Thickness: 1000 Å of aluminum overcoated with 500 Å of silicon monoxide. Recommended standard size is 1 by 1 by 0.008 inches thick. No variation in ϵ_T for silica thicker than this. Thickness less than this is very fragile. No variation in α_S for opaque metal film.

Maximum Temperature: 260°C

Substrate: Aluminum alloy

Adhesion: Has passed the sinusoidal and random vibration tests using GE-SS 4120 primer and RTV-615 adhesive. Another excellent adhesive is DC 92-024.

Thermophysical Properties:

Initial Solar Absorptance, α_S = 0.100
Initial Hemispherical Emittance, ϵ_T = 0.810
Initial α_S/ϵ_T = 0.123
Solar Absorptance after 1000 ESH of UV = 0.100
Solar Absorptance after 1000 EWH of protons = 0.100

Contamination Susceptibility: Surface contamination including fingerprints, oil, dust, and atmospheric weathering does not cause permanent damage after application and can be removed by sample cleaning.

Outgassing Characteristics: The RTV-615 adhesive used to apply the OSR to the substrate requires a minimum cure of 14 days at room temperature to minimize outgassing during ascent. The steady-state weight loss is 0.04%/cm^2/hr at 100°C. The constituent of the outgassing product is not known.

ALUMINUM-COATED OPTICAL SOLAR REFLECTOR (OSR) - Concluded

Refurbishment Capability: Temporary contamination must be removed prior to launch. Damaged parts can be removed and new ones applied. Difficult to apply on curved surfaces.

Source and Cost: The present source is Optical Coatings Laboratory, Inc., (707) 545-6440. Large quantity price is approximately $\$2.00/in^2$. Lockheed contact: Mr. L. Haslim, (415) 493-4411.

State of Development: Seems to be complete.

SILVER-COATED FEP TEFLON

Composition: Vapor-deposited silver on FEP Teflon sheet with an overcoating of vapor-deposited inconel.

Density: No data available.

Recommended Thickness: Emissivity depends on the thickness of Teflon. 2-mil, 5-mil, and 10-mil thick Teflon has been used.

Maximum Temperature: Approximately 250°F. Limited by the difference in expansion of Teflon and silver.

Substrate: Grit blasted. Aluminum alloy or other rigid surfaces depending on adhesive used. Adhesive promoters are used.

Adhesion: Good, depends on temperature and the adhesive used. Different adhesives are used for different range of temperatures.

Thermophysical Properties:

Initial Solar Absorptance, α_S = 0.059 to 0.090
Initial Hemispherical Emittance, ϵ_T = 0.680 to 0.820
Initial α_S/ϵ_T = 0.086 to 0.109
Solar Absorptance after 4600 ESH = 0.109
Solar Absorptance after 10,000 EWH of protons = 0.720

Contamination Susceptibility: At present, unknown.

Outgassing Characteristics: The steady-state weight loss of Teflon at 100°C is less than or equal to 0.04%/cm^2/hr. The outgassing of adhesive is dependent on the adhesive used.

Refurbishment Capability: Can be cleaned if no scrubbing is used. Best to use cotton soaked in organic solvent if care is taken not to run the solvent to the adhesive through the edges.

Source and Cost: G. T. Schjeldahl Corporation, (507) 645-5635. $65.00/ft^2. Langley Research Center contact: Mr. W. S. Slemp, (703) 827-3041.

SILVER-COATED FEP TEFLON - Concluded

State of Development: Development is continuing to find better adhesive and other polymers. Aeromatic heterocycling type polymers may be a replacement for FEP Teflon.

ALUMINUM-COATED FEP TEFLON

Composition: Vapor-deposited aluminum on FEP Teflon sheet with an overcoating of vapor-deposited inconel.

Density: No data available.

Recommended Thickness: Emissivity depends on the thickness of Teflon. 1-mil, 2-mil, 5-mil, and 10-mil thick Teflon has been used.

Maximum Temperature: Approximately 250°F. Limited by the difference in thermal expansion of the two materials.

Substrate: Grit blasted. Aluminum alloy or other substrates depending on adhesive used. Adhesive promoters are employed.

Adhesion: Good, depends on adhesive used and temperature. Different adhesives are needed for different temperature ranges of use.

Thermophysical Properties:

Initial Solar Absorptance, α_S = 0.130 to 0.210
Initial Hemispherical Emittance, ϵ_T = 0.550 to 0.890
Initial α_S/ϵ_T = 0.236 to 0.194
Solar Absorptance after 4000 ESH = 0.170
Solar Absorptance after 1.0 EWH of protons = 0.149

Contamination Susceptibility: No data available.

Outgassing Characteristics: The steady-state weight loss of Teflon at 100°C is less than or equal to 0.06%/cm^2 /hr. The outgassing of the adhesive depends on the kind used.

Refurbishment Capability: Can be cleaned. No scrubbing permitted. Best to use organic-solvent-soaked cotton. Solvent should not run through the edges.

Source and Cost: G. T. Schjeldahl Corporation, (507) 645-5635. Approximately $60.00/ft^2. Langley Research Center contact: Mr. W. S. Slemp, (703) 827-3041.

State of Development: Development in progress to find better adhesive for wide temperature range application, and better polymer to replace FEP Teflon.

SiO_2-COATED VAPOR-DEPOSITED ALUMINUM

Composition: Vapor-deposited aluminum with a dielectric coating of silicon dioxide.

Density: No data available.

Recommended Thickness: Solar absorptance controlled by choice of metal film; emittance determined by thickness of dielectric layer.

Maximum Temperature: Approximately 260°C

Substrate: Any clean rigid substrate. Lowest solar absorptance requires polished metal or glass substrate.

Adhesion: Good

Thermophysical Properties:

Initial Solar Absorptance, α_S = 0.140
Initial Hemispherical Emittance, ϵ_T = 0.420
Initial α_S/ϵ_T = 0.334
Solar Absorptance after 1000 ESH of UV = 0.170

Contamination Susceptibility: The surface is hard and abrasion-resistant. May be cleaned by conventional techniques without deterioration of optical properties.

Outgassing Characteristics: The steady-state weight loss at 100°C is less than or equal to 0.04%/cm^2/hr.

Refurbishment Capability: Cleanable

Source and Cost: The source appears to be G. T. Schjeldahl Corporation, (507) 645-5635.

State of Development: No further development is reported.

Al_2O_3-COATED VAPOR-DEPOSITED ALUMINUM

Composition: Vapor-deposited aluminum with a dielectric coating of aluminum.

Density: No data available.

Recommended Thickness: Solar absorptance controlled by choice of metal film; emittance determined by thickness of dielectric layer.

Maximum Temperature: Approximately 260°C

Substrate: Any clean rigid substrate. Lowest solar absorptance requires polished metal or glass substrate.

Adhesion: Good

Thermophysical Properties:

Initial Solar Absorptance, α_S = 0.140
Initial Hemispherical Emittance, ϵ_T = 0.450
Initial α_S/ϵ_T = 0.311
Solar Absorptance after 2000 ESH = 0.21

Contamination Susceptibility: The surface is hard and abrasion-resistant. May be cleaned by conventional techniques without deterioration of optical properties.

Outgassing Characteristics: No data available.

Refurbishment Capability: Cleanable

Source and Cost: Goddard Space Flight Center, (301) 982-5115.

State of Development: No further development reported.

ZINC OXIDE IN METHYL SILICONE (S-13)

Composition: New Jersey Zinc Company SP-500 zinc oxide, General Electric RTV-602 and USP toluene, each parts by weight of 240, 100, and 170, respectively. Ball milled. One part of catalyst SRC-05 is added in 20 parts of toluene per 670 parts of S-13 just before painting.

Density: No data available.

Recommended Thickness: 3.5 to 5.5 mils

Maximum Temperature: 250°F

Substrate: Any surface to which GE SS-4044 primer can be applied.

Adhesion: Adhesive failed at butt pressure of 9 psi at 70°F.

Thermophysical Properties:

Initial Solar Absorptance, α_S = 0.210
Initial Hemispherical Emittance, ϵ_T = 0.880
Initial α_S/ϵ_T = 0.238
Solar Absorptance after 2000 ESH of UV = 0.350
Solar Absorptance after 2×10^6 EWH of protons = 0.28

Contamination Susceptibility: No data available. Susceptible to contamination.

Outgassing Characteristics: The steady-state weight loss is 2.8×10^{-8} g/cm^2, and the time to reach the steady state is 44 hours.

Refurbishment Capability: Soiled or damaged areas can be recoated. Soiled areas must be cleaned thoroughly with detergent and water and dried. Damaged or gouged areas can be recoated with a paste of the paint.

Source and Cost: The source is IITRI and was developed in collaboration with NASA, MSFC under Contract No. NAS8-5379, (312) 225-9630, Ext. 5074.

State of Development: This coating is no longer available and is replaced by S-13G.

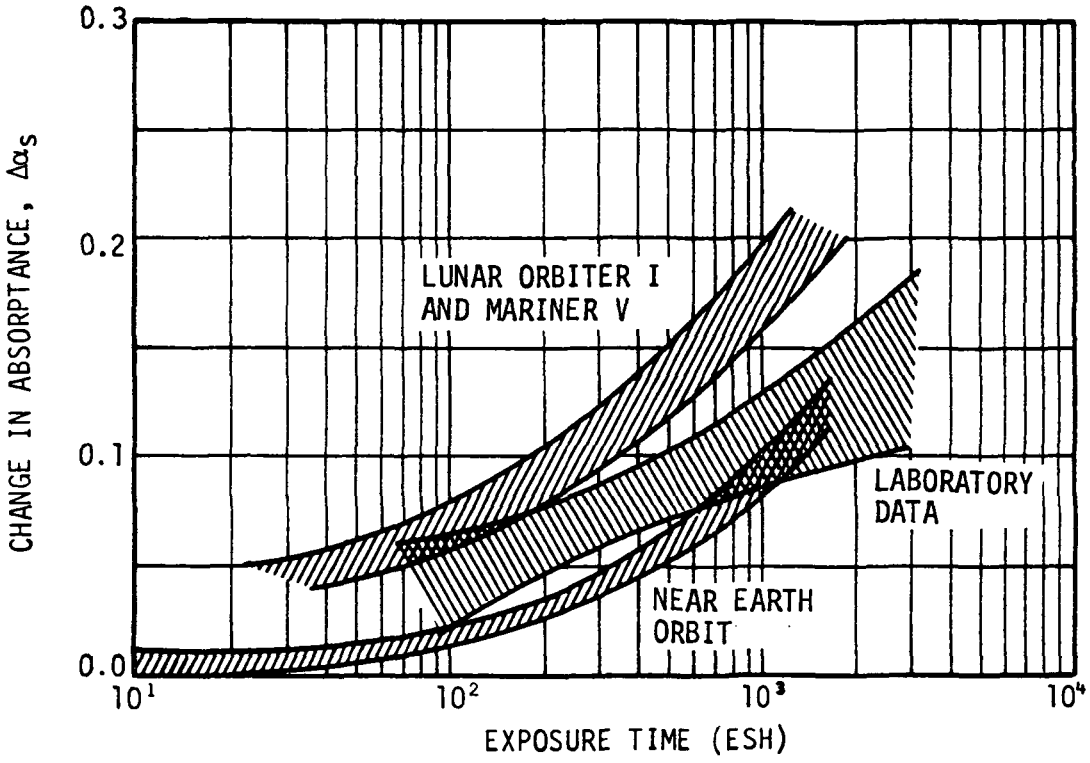

COMPARISON OF LABORATORY AND FLIGHT DATA FOR S-13

ZINC OXIDE IN METHYL SILICONE (S-13G)

Composition: PS7-treated New Jersey Zinc Company SP-500 zinc oxide, General Electric RTV-602, and USP toluene, each parts by weight of 240, 100, and 175, respectively. Ball milled. One part of SRC-05 catalyst is added in 10 parts of toluene to 1030 parts of S-13G just before painting. A catalyst concentration of 0.4% based upon RTV-602 provides optimum stability without greatly sacrificing thermal-cure properties.

Density: Coating weight is 0.006 lb/ft^2.

Recommended Thickness: 5.0 to 8.0 mil

Maximum Temperature: 250°F

Substrate: Any surface to which GE SS-4044 primer can be applied.

Adhesion: Thermal shock-resistant if primer is not too thick.

Thermophysical Properties:

Initial Solar Absorptance, α_S = 0.190
Initial Hemispherical Emittance, ϵ_T = 0.880
Initial α_S/ϵ_T = 0.216
Solar Absorptance after 1000 ESH of UV = 0.230
Solar Absorptance after 10,000 EWH of protons = Severe

Contamination Susceptibility: The change in α due to engine plume is between 10 to 250 % depending on the position and time of exposure.

Outgassing Characteristics: The steady-state weight loss at 100°C is equal to or less than 0.04 $\%/cm^2/hr$.

Refurbishment Capability: Soiled areas must be cleaned thoroughly with detergent and water and dried before application of additional S-13G. Damaged or gouged areas can be recoated with a paste of the paint.

ZINC OXIDE IN METHYL SILICONE (S-13G) - Concluded

Source and Cost: The source is IITRI and was developed in collaboration with NASA, MSFC under Contract No. NAS8-5379, (312) 225-9630, Ext. 5074. The cost is $75/pint (8 or more pints).

State of Development: This coating is in the process of being replaced by A-429M. This new paint is essentially S-13G pigment in Owing, Illinois 650 binder.

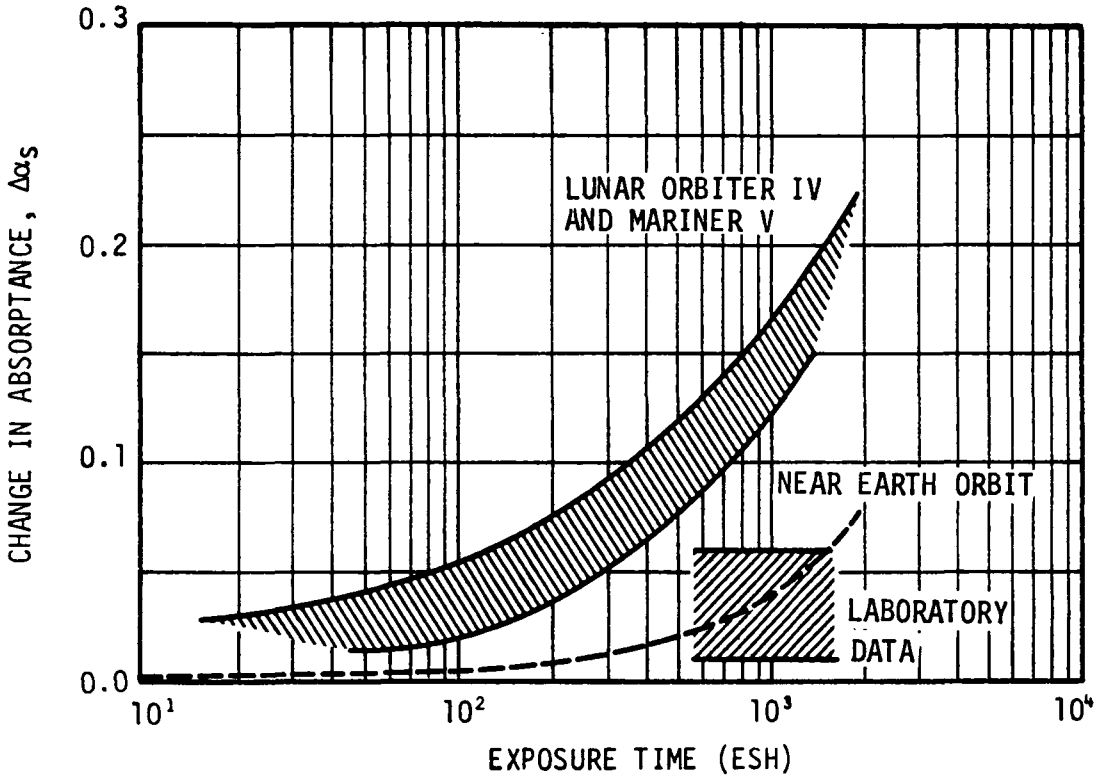

COMPARISON OF LABORATORY AND FLIGHT DATA FOR S-13G

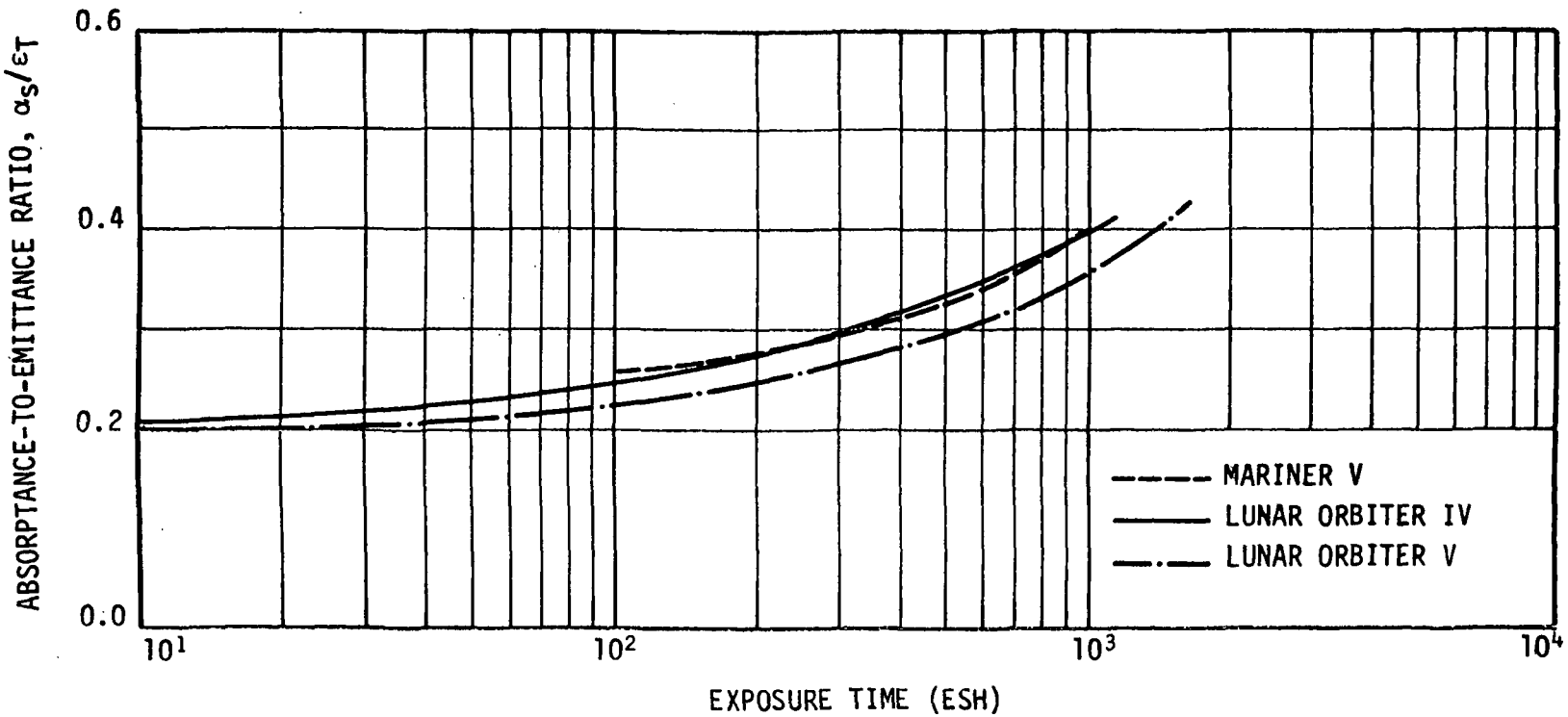

ANALYZED ABSORPTANCE-TO-EMITTANCE RATIO OF S-13G

ZINC OXIDE IN POTASSIUM SILICATE (Z-93)

Composition: The pigment is New Jersey Zinc Company SP-500 zinc oxide plasma calcined at 600 to 700°C for 16 hours. Balled milled with Sylvania's PS7 potassium silicate and distilled water. Pigment-to-binder ratio is 4.3:1 by weight. Should be prepared just before use. The shelf life is less than 24 hours.

Density: No data available.

Recommended Thickness: 4.5 to 6.0 mils

Maximum Temperature: 495°F

Substrate: Most metals except noble, aluminum preferred. Aluminum or plastic substrates should be abraded and thoroughly washed with detergent and water.

Adhesion: The butt tensile adhesion test shows that approximately 50 percent of paint structure failed at butt pressures of 1220 psi and 590 psi at temperatures of -270°F and 70°F, respectively.

Thermophysical Properties:

Initial Solar Absorptance, α_S = 0.184
Initial Hemispherical Emittance, ϵ_T = 0.880
Initial α_S/ϵ_T = 0.209
Solar Absorptance after 2000 ESH of UV = 0.184
Solar Absorptance after 10,000 EWH of protons = 0.324

Contamination Susceptibility: The change in α due to engine plume is between 5 to 80 percent depending on the position and time of exposure.

Outgassing Characteristics: The steady-state weight loss is 5×10^{-11} g/cm^2 and the time to reach steady state is 20 hours.

Refurbishment Capability: Contaminated areas should be scrupulously cleaned with detergent and water before repainting. Cleaning of the paint itself is extremely difficult; repainting needed in general.

ZINC OXIDE IN POTASSIUM SILICATE (Z-93) - Concluded

Source and Cost: The source is IITRI, (312) 225-9630, Ext. 5074. The coating was developed in collaboration with JPL. The cost is $320/gallon ($150 minimum order).

State of Development: No further development of this particular coating is anticipated.

General Information: Shelf life of this paint is less than 24 hours and preparation of the paint just before use is recommended. The formulation is applied by spraying from a distance of 6 to 12 inches until a reflection due to the liquid is apparent. This is followed by air-drying, at which time the spraying-drying cycle is repeated. The carrier gas for spraying should be clean. Prepurified nitrogen is a good source.

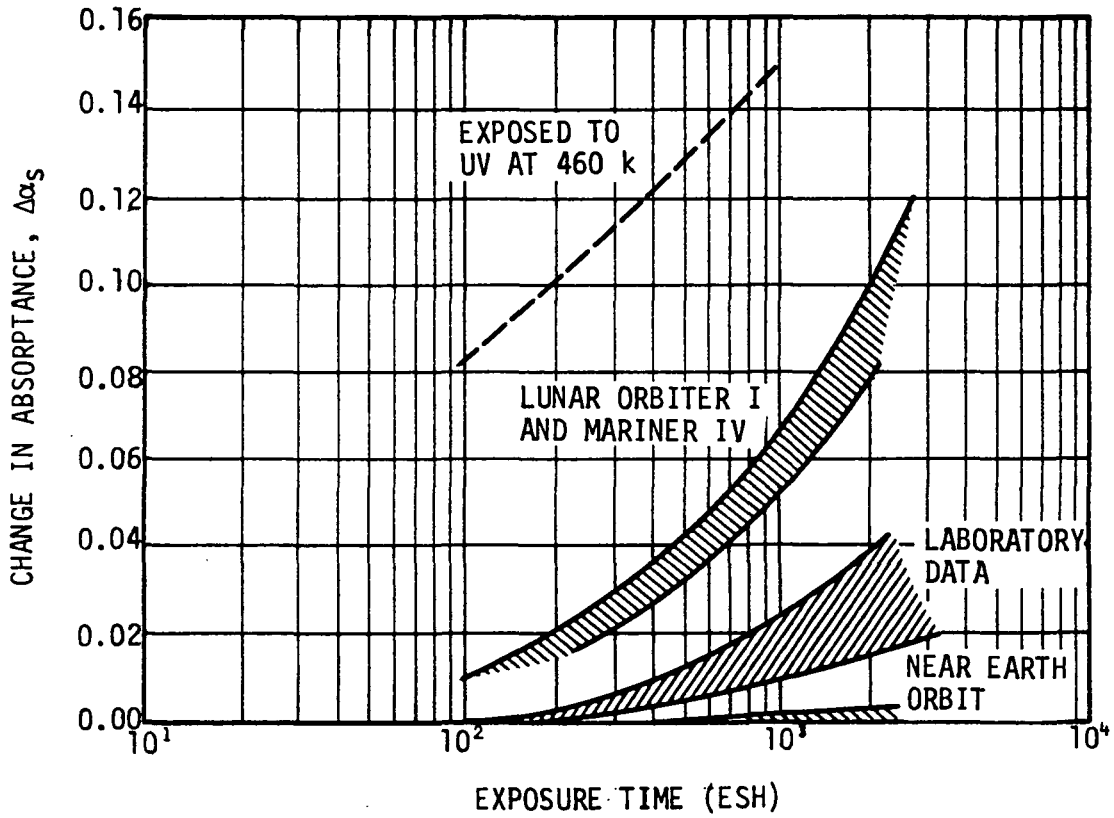

COMPARISON OF LABORATORY AND FLIGHT DATA FOR Z-93

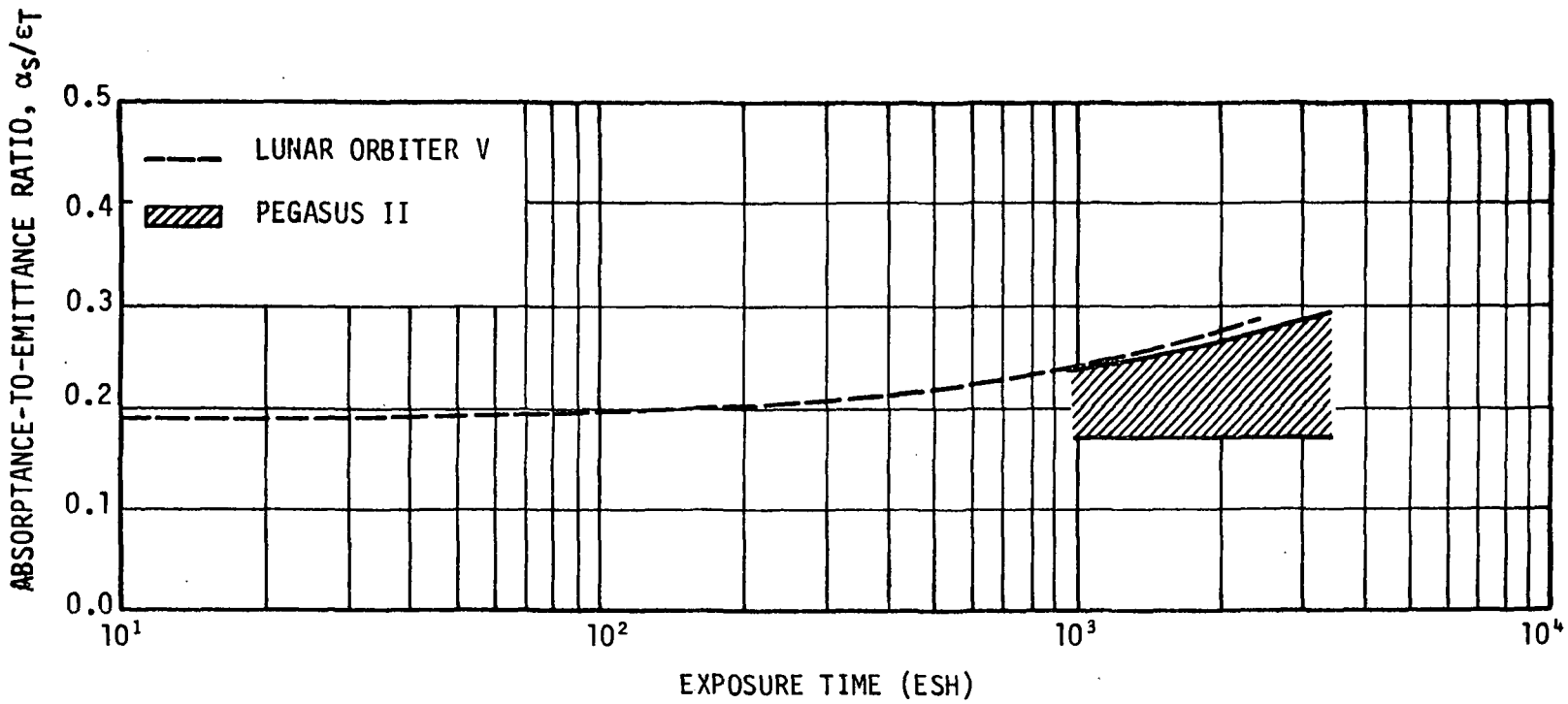

ANALYZED ABSORPTANCE-TO-EMITTANCE RATIO OF Z-93

ZIRCONIUM SILICATE WITH POTASSIUM SILICATE [LP 10 A]

Composition: Acid leached and calcined 1000 W grade "Ultrox" Zicronium Silicate of Metals and Thermit Corporation in potassium silicate binder. The pigment-to-binder ratio is 3.5:1 by weight.

Density: 4.0 g/cm^3

Recommended Thickness: 3.0 to 5.0 mils

Maximum Temperature: 495°K

Substrate: Aluminum alloy

Adhesion: Good. Base coat reacts with substrate and acts as primer.

Thermophysical Properties:

Initial Solar Absorptance, α_S = 0.240
Initial Hemispherical Emittance, ϵ_T = 0.870
Initial α_S/ϵ_T = 0.276
Solar Absorptance after 7000 ESH of UV = 0.530
Solar Absorptance after 10^{16} e/cm^2 = 0.260

Contamination Susceptibility: Very susceptible

Outgassing Characteristics: Weight loss in vacuum is less than 5%.

Refurbishment Capability: Not repairable; repainting required.

Source and Cost: The source is Lockheed Missile and Space Company. The cost is $740/gallon. Lockheed contact: Mr. L. Haslim, (415) 493-4411.

State of Development: Development to improve the UV stability is in progress. Parallel effort is continuing to replace this paint with a better one.

THERMATROL 2A-100 [TiO_2/METHYL SILICONE]

Composition: Calcined titanox RA-NC rutile TiO_2 of Titanium Pigment Corporation in DC 92007 methyl silicone binder. The pigment-to-binder ratio is 1:1 by weight. The paint is applied by spray technique and needs 24 hours of curing time.

Density: 1.5 g/cm^3

Recommended Thickness: Total dry film thickness of 3.5 to 5.0 mils including primer.

Maximum Temperature: 650°F

Substrate: Any clean substrate.

Adhesion: Good with Dow Corning A-4094 or equivalent primer, approximately 0.2-mil thick.

Thermophysical Properties:

Initial Solar Absorptance, α_S = 0.170
Initial Hemispherical Emittance, ϵ_T = 0.860
Initial α_S/ϵ_T = 0.197
Solar Absorptance after 500 ESH of UV = 0.310
Solar Absorptance after 6×10^4 EWH of protons = 0.590

Contamination Susceptibility: Quantitative data unknown. Requires protection against contamination.

Outgassing Characteristics: Low after coating has been fully cured.

Refurbishment Capability: Easy to repair; cleanable with detergent.

Source and Cost: The source is Lockheed Missile and Space Company, The cost is $60/gallon. Lockheed contact: Mr. L. Haslim, (415) 493-4411.

State of Development: No further development is going on at the present time.

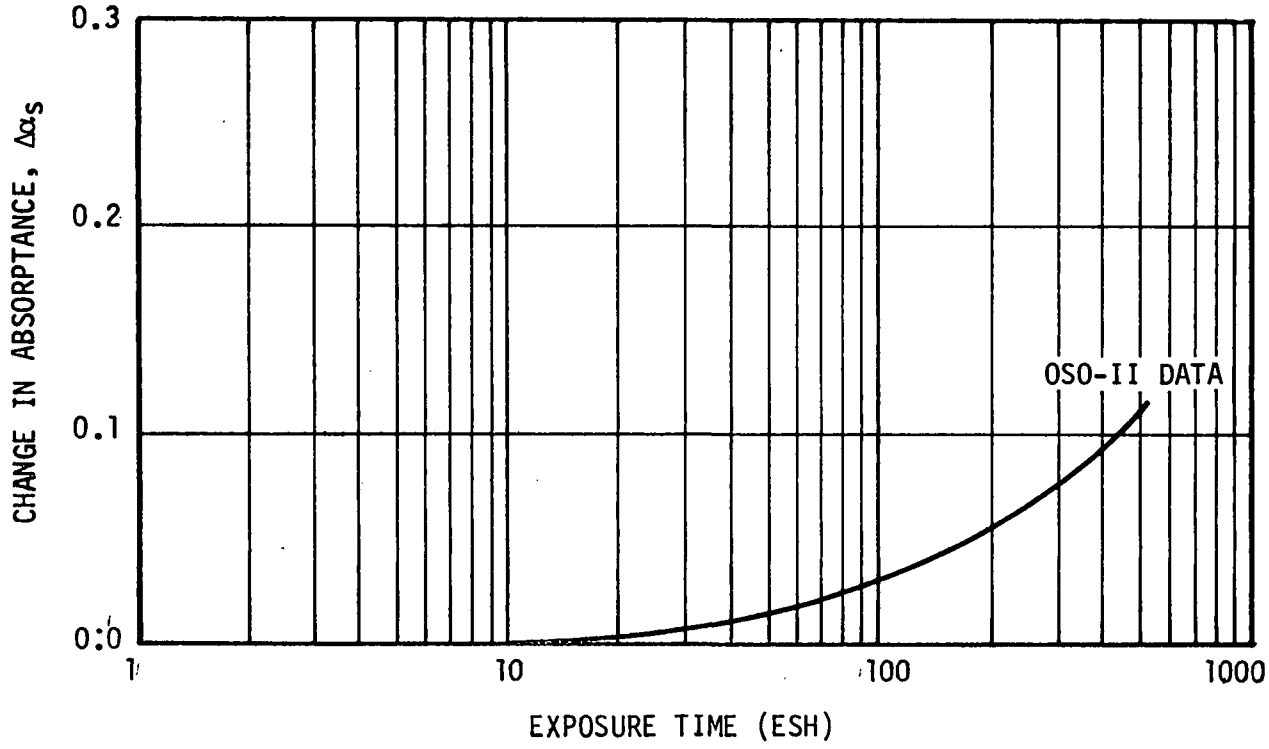

CHANGE IN NORMAL SOLAR ABSORPTANCE OF TiO_2/SILICONE COATING

TINTED WHITE KEMACRYL

Composition: TiO_2 pigmented acrylic flat paint. Only tinted white M49WC17 variety is approved for thermal control use.

Density: No data available.

Recommended Thickness: For external surfaces, the minimum thickness for opacity is 5.0 mils, and for internal applications, a minimum thickness of 1.0 mil should be maintained.

Maximum Temperature: Less than 450°F if alteration in surface finish and solar absorptance due to bubbling can be tolerated. If not, then the maximum temperature is less than 200°F.

Substrate: Any clean rigid substrate

Adhesion: Successfully survived 385 temperature cycles between 150°F and 70°F with a 12- to 15-minute cycling period in a vacuum of 10^{-5} millimeters of mercury. P415 primer required.

Thermophysical Properties:

Initial Solar Absorptance, α_S = 0.240
Initial Hemispherical Emittance, ϵ_T = 0.860
Initial α_S/ϵ_T = 0.279
Solar Absorptance after 485 ESH of UV = 0.360
Solar Absorptance after 10^{16} e/cm^2 = 0.300

Contamination Susceptibility: The surface is porous and requires protection against contamination.

Outgassing Characteristics: Requires a minimum of 14 days of room-temperature curing to remove volatile materials sufficiently.

Refurbishment Capability: No information available.

Source and Cost: The source is Sherwin-Williams Company, (216) 861-7000.

State of Development: No further development reported.

FULLER GLOSS WHITE

Composition: TiO_2 pigment in silicone-modified alkyd vehicle. Identification number S17-W-1.

Density: No data available.

Recommended Thickness: The minimum thickness for external use is 5.0 mils and that for internal use is 1.0 mil.

Maximum Temperature: 650°F

Substrate: Any clean rigid substrate capable of withstanding cure temperature of 465°F.

Adhesion: Cracking and loss of adhesion due to thermal cycling between -240°F and 70°F. Not recommended for use in locations reaching temperatures above 650°F.

Thermophysical Properties:

Initial Solar Absorptance, α_S = 0.290
Initial Hemispherical Emittance, ϵ_T = 0.900
Initial α_S/ϵ_T = 0.322
Solar Absorptance after 1000 ESH of UV = 0.380
Solar Absorptance after 10^{15} e/cm^2 = 0.300

Contamination Susceptibility: The surface must be protected from contamination. No quantitative data available.

Outgassing Characteristics: No data available.

Refurbishment Capability: No data available.

Source and Cost: W. P. Fuller Paint Company. Telephone number is unavailable.

State of Development: No further development of this particular coating is reported.

WHITE SKYSPAR

Composition: TiO_2-pigmented epoxy-base paint.

Density: No data available.

Recommended Thickness: For internal use, the minimum thickness is 1.0 mil and for external use it is 4.0 mils.

Maximum Temperature: 450°F

Substrate: Any rigid substrate

Adhesion: No data available.

Thermophysical Properties:

Initial Solar Absorptance, α_S = 0.250
Initial Hemispherical Emittance, ϵ_T = 0.910
Initial α_S/ϵ_T = 0.274
Solar Absorptance after 2000 ESH of UV = 0.600
Solar Absorptance after 2×10^6 EWH of protons = 0.370

Contamination Susceptibility: Must be protected from contamination. No qualitative or quantitative data available.

Outgassing Characteristics: No data available.

Refurbishment Capability: No data available.

Source and Cost: The source is Andrew Brown Company, Paint Number A423, Color 5A9185. Telephone number is unavailable.

ROKIDE A

Composition: Aluminum oxide flame-sprayed on substrate.

Density: No data available.

Recommended Thickness: No data available.

Maximum Temperature: No data available.

Substrate: Any metallic substrate.

Adhesion: Good

Thermophysical Properties:

Initial Solar Absorptance, α_S = 0.270
Initial Hemispherical Emittance, ϵ_T = 0.750
Initial α_S/ϵ_T = 0.360
Solar Absorptance after 1000 ESH of UV = 0.270

Contamination Susceptibility: No information available.

Outgassing Characteristics: Practically none.

Refurbishment Capability: No information available.

Source and Cost: Flame-sprayed on any metallic substrate by Norton Abrasive Company, (617) 853-1000.

State of Development: No further development is reported.

HUGHES INORGANIC WHITE H-2

Composition: Titanium dioxide in Sylvania PS-7 potassium silicate binder. Pigment-to-binder ratio is 4.4:1 by weight.

Density: No data available.

Recommended Thickness: 6.0 to 8.0 mils after curing

Substrate: Aluminum alloy

Adhesion: No data available.

Thermophysical Properties:

Initial Solar Absorptance, α_S = 0.180
Initial Hemispherical Emittance, ϵ_T = 0.880
Initial α_S/ϵ_T = 0.203
Solar Absorptance after 1300 ESH of UV = 0.320

Contamination Susceptibility: No information available.

Outgassing Characteristics: Weight loss of 0.02 percent when exposed to vacuum at 250° F. The weight loss is water vapor.

Refurbishment Capability: Extremely difficult to clean.

Source and Cost: The source is Hughes Aircraft Company, (213) 391-0711, Ext. 4428.

General Information: The coating is applied in three coats, each coat being baked for 1 hour at 225° F and the final coating baked for 1 hour at 260° F. An air brush is used for painting.

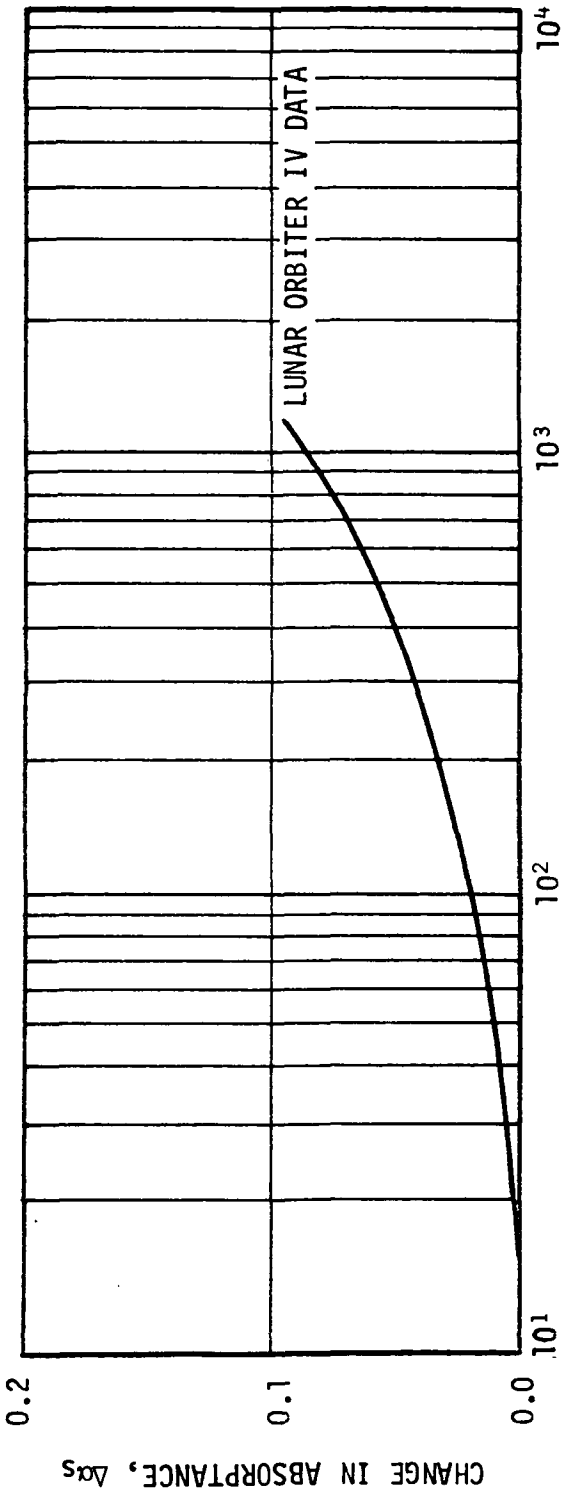

CHANGE IN NORMAL SOLAR ABSORPTANCE OF TiO_2/K_2SiO_3 COATING (HUGHES H-2)

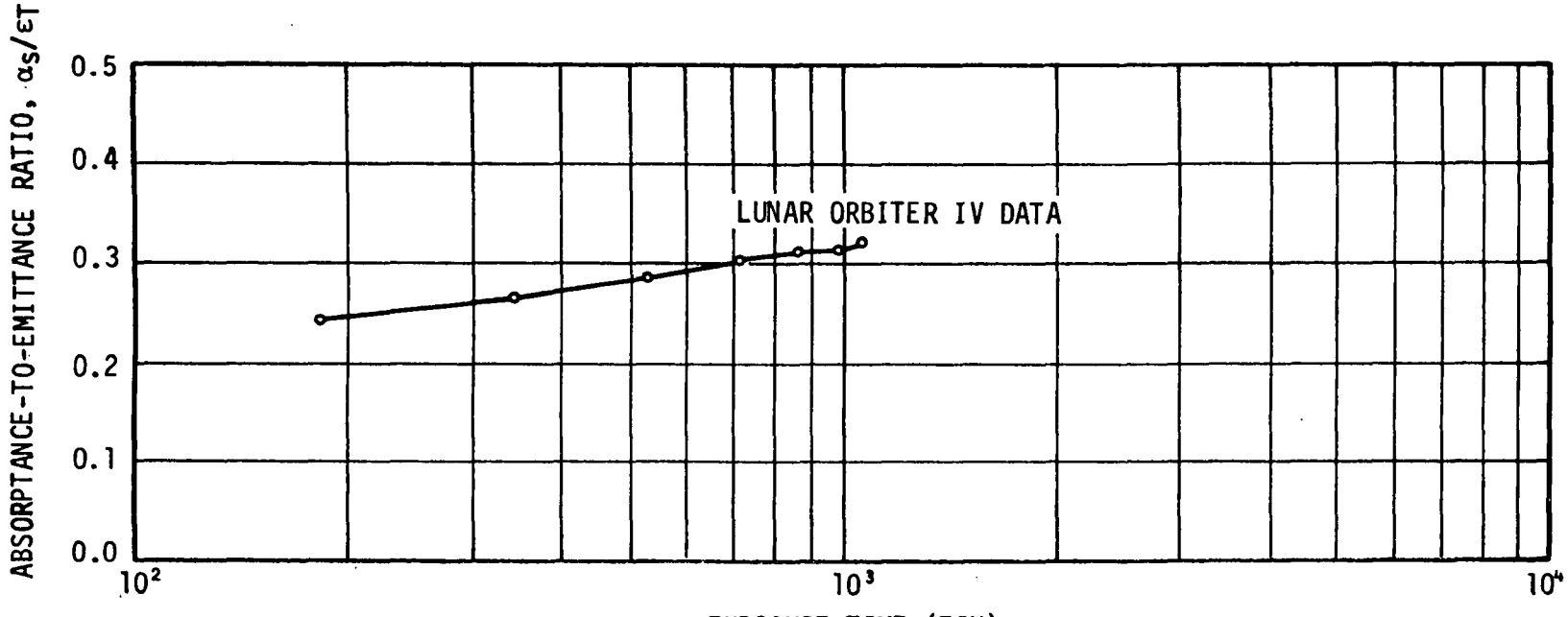

ABSORPTANCE-TO-EMITTANCE RATIO OF TiO_2/K_2SiO_3 COATING (HUGHES H-2)

ANODIZED ALUMINUM

Composition: 1199 aluminum alloy chemically brightened and electropolished in a solution of fluoboric acid. Anodized in a solution of ammonium tartrate.

Density: No data available.

Recommended Thickness: Film thickness proportional to voltage, 13.4 Å/V. Mostly films prepared at 300 volts were tested.

Maximum Temperature: Approximately 900°F

Substrate: 1199 aluminum alloy

Adhesion: Good

Thermophysical Properties:

Initial Solar Absorptance, α_S = 0.120
Initial Hemispherical Emittance, ϵ_T = 0.380 (at 300°K)
Initial α_S/ϵ_T = 0.316
Solar Absorptance after 1580 ESH = 0.120

Contamination Susceptibility: Contamination will degrade the coating.

Outgassing Characteristics: The steady-state weight loss is equal to or less than 0.04%/cm^2/hr.

Refurbishment Capability: No information available.

Source and Cost: The Boeing Company, (206) 656-2121.

State of Development: No further development is reported.

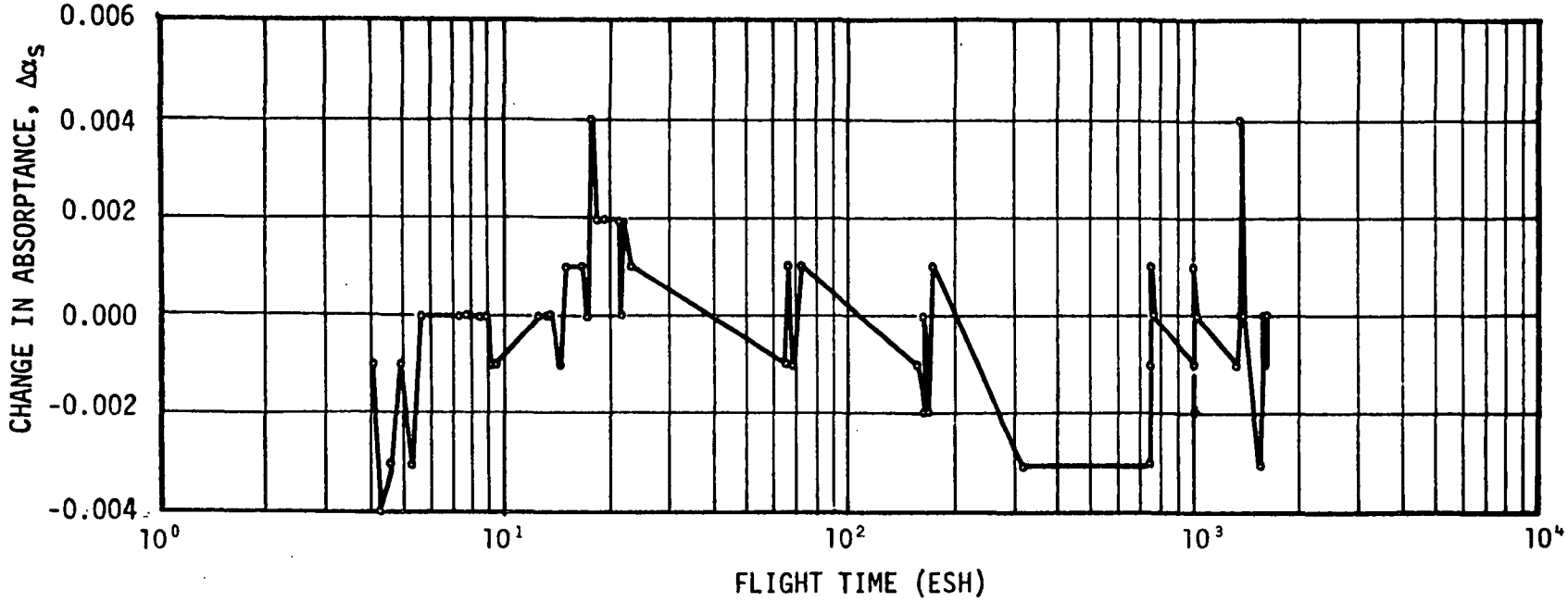

CHANGE IN NORMAL SOLAR ABSORPTANCE OF ANODIZED ALUMINUM

CAT-A-LAC BLACK

Composition: Carbon black pigment in epoxy vehicle.

Density: No data available.

Recommended Thickness: Minimum thickness for opacity is 1.0 mil.

Maximum Temperature: Approximately 250°F

Substrate: Aluminum alloy

Adhesion: Good

Thermophysical Properties:

Initial Solar Absorptance, α_S = 0.940
Initial Hemispherical Emittance, ϵ_T = 0.940
Initial α_S/ϵ_T = 1,000
Solar Absorptance after 2,400 flight hours = 0.910

Contamination Susceptibility: No data available.

Outgassing Characteristics: The rate of weight loss during temperature cycling from 25°C to 100°C is less than 0.2%/cm^2/hr when heated at a rate of 2°C/min in a vacuum of 10^{-6} torr. The steady-state weight loss at 100°C is less than 0.04%/cm^2/hr.

Refurbishment Capability: Repairable

Source and Cost: The source for this paint is Finch Paint and Chemical Company. Telephone number is unavailable.

State of Development: No further development of this paint is reported.

General Information: The paint takes 1 day to cure at room temperature and 48 hours at 150°F.

C2

BLACK KEMACRYL

Composition: Commerically available black acrylic flat paint.

Density: No data available.

Recommended Thickness: The minimum thickness is 1.5 mils for both external and internal applications.

Maximum Temperature: 450°F

Substrate: Any clean rigid substrate

Adhesion: Successfully survived 385 temperature cycles between -150°F and 70°F with cycling periods from 12 to 18 minutes in a vacuum of 10^{-5} millimeters of mercury.

Thermophysical Properties:

Initial Solar Absorptance, α_S = 0.930
Initial Hemispherical Emittance, ϵ_T = 0.880
Initial α_S/ϵ_T = 1.057
Solar Absorptance after 600 ESH of UV = 0.980

Contamination Susceptibility: The surface is porous and requires protection against contamination.

Outgassing Characteristics: Adhesive outgases and produces blisters on the paint surface at temperatures above 450°F.

Refurbishment Capability: No information available.

Source and Cost: This paint is a commercial product of Sherwin-Williams and is identified by the number M49BC12, (216) 861-7000.

State of Development: No further development of this paint is reported.

FULLER BLACK

Composition: Lamp black pigment in silicone vehicle. Identification Number 517-B-2.

Density: No data available.

Recommended Thickness: For both external and internal applications, the minimum thickness for opacity is 1.0 mil.

Maximum Temperature: 1,070°F

Substrate: Any rigid substrate capable of withstanding the cure cycle of 465°F.

Adhesion: Cracking and loss of adhesion after 170 cycles between 240 and 70°F.

Thermophysical Properties:

Initial Solar Absorptance, α_S = 0.890
Initial Hemispherical Emittance, ϵ_T = 0.880
Initial α_S/ϵ_T = 1.011
Solar Absorptance after 600 ESH of UV = 0.940

Contamination Susceptibility: No information available.

Outgassing Characteristics: No information available.

Refurbishment Capability: No information available.

Source and Cost: W. P. Fuller Paint Company. Telephone number is unavailable.

State of Development: No further development is reported.

ROKIDE C

Composition: Essentially chromic oxide (85% Cr_2O_3).

Density: No data available.

Recommended Thickness: No data available.

Maximum Temperature: 1,660°F

Substrate: René 41 with a 2.0-mil coating of nichrome

Adhesion: No coating failure resulted due to thermal shock for the René 41-nichrome-Rokide C system. To use Rokide C on other metallic substrate, however, thermal shock stability should always be checked. Since the bonding is mechanical, all substrates must be grit-blasted.

Thermophysical Properties:

Initial Solar Absorptance, α_S = 0.900
Initial Hemispherical Emittance, ϵ_T = 0.850
Initial α_S/ϵ_T = 1.059
Solar Absorptance after 1,000 ESH of UV = 0.900

Contamination Susceptibility: Surface contamination can be easily removed by sample cleaning. No data on the effect of contamination on the thermophysical properties are available.

Outgassing Characteristics: No data available.

Refurbishment Capability: Cleanable

Source and Cost: This coating is flame-sprayed by Norton Abrasive Company, (617) 853-1000.

State of Development: No further development is reported.

PLATINUM BLACK

Composition: This coating is essentially a deposit of finely divided platinum. It is deposited from a solution of chloroplatinic acid.

Density: 21 g/cm^3

Recommended Thickness: No data available.

Maximum Temperature: 1,200°F. Above 390°F some sintering of the platinum particles takes place.

Substrate: QMV beryllium

Adhesion: Good. No information on thermal cycling effects.

Thermophysical Properties:

Initial Solar Absorptance, α_S = 0.960
Initial Hemispherical Emittance, ϵ_T = 0.850
Initial α_S/ϵ_T = 1.106

Contamination Susceptibility: The surface is porous and must be carefully protected from contamination.

Outgassing Characteristics: None

Refurbishment Capability: No data available.

Source and Cost: Lockheed Missile and Space Company, (415) 493-4411.

State of Development: No further development is reported.

Bi_2S_3-DYED ANODIZED ALUMINUM

Composition: Anodized aluminum with repeated alternate dips of 3 to 5 minutes in solutions of bismuth nitrate and ammonium hydrosulfide. Anodizing was accomplished in about 60 minutes in a 15 percent sulfuric acid bath with a current density of 0.017 amp/cm^2 at room temperature.

Density: No data available.

Recommended Thickness: 26 micrometers

Maximum Temperature: No data available.

Substrate: 1100 (2-S) aluminum

Adhesion: After 10 cycles between 478°K and 80°K showed no peeling or spalling of the coating.

Thermophysical Properties:

Initial Solar Absorptance, α_S = 0.728
Initial Hemispherical Emittance, ϵ_T = 0.909
Initial α_S/ϵ_T = 0.801
Solar Absorptance after 3,540 ESH of UV + 10^{15} e/cm^2 = 0.760

Contamination Susceptibility: No information available.

Outgassing Characteristics: Practically none

Refurbishment Capability: No information available.

Source and Cost: Langley Research Center, Reference NASA TN D-4116, (703) 827-1110, Ext. 2986.

State of Development: No information available.

PbS-DYED ANODIZED ALUMINUM

Composition: This coating is prepared by repeated alternate dips of 5-minute anodized aluminum in solutions of lead acetate and then in ammonium hydrosulfide. Anodizing was accomplished in about 120 minutes in a solution of 15 percent sulfuric acid with a current density of 0.017 amp/cm^2 at room temperature.

Density: No data available.

Recommended Thickness: 17 micrometers

Maximum Temperature: No data available.

Substrate: 1100 (2-S) aluminum

Adhesion: Showed no peeling or spalling after 10 cycles between 478°K and 80°K.

Thermophysical Properties:

Initial Solar Absorptance, α_S = 0.861
Initial Hemispherical Emittance, ϵ_T = 0.912
Initial α_S/ϵ_T = 0.944
Solar Absorptance after 3,540 ESH of UV + 10^{15} e/cm^2 = 0.891

Contamination Susceptibility: No information available.

Outgassing Characteristics: No information available.

Refurbishment Capability: No information available.

Source and Cost: Langley Research Center, Reference NASA TN D-4116, (703) 827-1110, Ext. 2986.

State of Development: No information available.

NiS-DYED ANODIZED ALUMINUM

Composition: This coating is prepared by repeated alternate dips of 5 minutes each to anodized aluminum in solutions of nickel acetate and then in ammonium hydrosulfide. Anodizing was accomplished in about 120 minutes in a 15 percent sulfuric acid bath at room temperature with a current density of 0.017 amp/cm^2.

Density: No data available.

Recommended Thickness: 23 micrometers (thickness on which measurements are made).

Maximum Temperature: No data available.

Substrate: 1100 (2-S) aluminum

Adhesion: Showed no peeling or spalling after 10 cycles between 478°K to 80°K.

Thermophysical Properties:

Initial Solar Absorptance, α_S = 0.970
Initial Hemispherical Emittance, ϵ_T = 0.929
Initial α_S/ϵ_T = 1.044
Solar Absorptance after 3,540 ESH of UV + 10^{15} e/cm^2 = 0.972

Contamination Susceptibility: No data available.

Outgassing Characteristics: No data available.

Refurbishment Capability: No information available.

Source and Cost: Langley Research Center, Reference NASA TN D-4116, (703) 827-1110, Ext. 2986.

State of Development: No information available.

CoS-DYED ANODIZED ALUMINUM

Composition: This coating is prepared by dipping anodized aluminum for the first 15 minutes in Cobalt acetate and then in ammonium hydrosulfide for 5 to 15 minutes. Anodizing was accomplished in 120 minutes in a 15 percent sulphuric acid bath at room temperature with a current density of 0.017 amp/cm^2.

Density: No data available.

Recommended Thickness: 26 micrometers (thickness on which measurements are made).

Maximum Temperature: No data available.

Substrate: 1100 (2-S) aluminum

Adhesion: Showed no peeling or spalling after 10 cycles between 478°K and 80°K.

Thermophysical Properties:

Initial Solar Absorptance, α_S = 0.957
Initial Hemispherical Emittance, ϵ_T = 0.930
Initial α_S/ϵ_T = 1.029
Solar Absorptance after 3,760 ESH of UV + 10^{15} e/cm^2 = 0.963

Contamination Susceptibility: No information available.

Outgassing Characteristics: No information available.

Refurbishment Capability: No information available.

Source and Cost: Langley Research Center, Reference NASA TN D-4116, (703) 827-1110, Ext. 2986.

State of Development: No information available.

SANDOZ OA-DYED ANODIZED ALUMINUM

Composition: This coating is prepared by dipping anodized aluminum in Sandoz black OA for 30 minutes. Anodizing was accomplished in 60 minutes in a 15 percent sulfuric acid bath at room temperature with a current density of 0.017 amp/cm^2.

Density: No data available.

Recommended Thickness: 20 micrometers (thickness on which measurements were made).

Maximum Temperature: No data available.

Substrate: 1100 (2-S) aluminum

Adhesion: Showed no peeling or spalling after 10 cycles between 478°K and 80°K.

Thermophysical Properties:

Initial Solar Absorptance, α_S = 0.647
Initial Hemispherical Emittance, ϵ_T = 0.927
Initial α_S/ϵ_T = 0.698
Solar Absorptance after 3,540 ESH of UV + 10^{15} e/cm^2 = 0.684

Contamination Susceptibility: No information available.

Outgassing Characteristics: The steady-state weight loss at 100°C is less than or equal to 0.04%/cm^2/hr.

Refurbishment Capability: No information available.

Source and Cost: Langley Research Center, Reference NASA TN D-4116, (203) 827-1110, Ext. 2986. The dye is from Sandoz Chemical Works, Inc.

State of Development: No information available.

SANDOZ BK-DYED ANODIZED ALUMINUM

Composition: This coating is prepared by dipping anodized aluminum in Sandoz black BK for 30 minutes. Anodizing was accomplished in 60 minutes in a 15 percent sulfuric acid bath at room temperature with a current density of 0.017 amp/cm^2.

Density: No data available.

Recommended Thickness: 22 micrometers (thickness on which measurements were made).

Maximum Temperature: No data available.

Substrate: 1100 (2-S) aluminum

Adhesion: Showed no peeling or spalling after 10 cycles between 478°K and 80°K.

Thermophysical Properties:

Initial Solar Absorptance, α_S = 0.757
Initial Hemispherical Emittance, ϵ_T = 0.962
Initial α_S/ϵ_T = 0.817
Solar Absorptance after 3,540 ESH of UV + 10^{15} e/cm^2 = 0.786

Contamination Susceptibility: No data available.

Outgassing Characteristics: The steady-state weight loss at 100°C is equal to or less than 0.04%/cm^2/hr.

Refurbishment Capability: No information available.

Source and Cost: Langley Research Center, Reference NASA TN D-4116, (703) 827-1110, Ext. 2986. The dye is from Sandoz Chemical Works, Inc.

State of Development: No information on further development is available.

PYROMARK BLACK ON ALUMINUM

Composition: The exact composition of this paint is not available from the manufacturer.

Density: No data available.

Recommended Thickness: 32 micrometers (thickness on which measurements were made).

Maximum Temperature: No data available.

Substrate: 1100 (2-S) aluminum, grit-blasted

Adhesion: Showed no peeling or spalling after 10 cycles between 478°K and 80°K.

Thermophysical Properties:

Initial Solar Absorptance, α_S = 0.902
Initial Hemispherical Emittance, ϵ_T = 0.830
Initial α_S/ϵ_T = 1.086
Solar Absorptance after 3,440 ESH of UV + 10^{15} e/cm^2 = 0.903

Contamination Susceptibility: No information available.

Outgassing Characteristics: The steady-state weight loss of the silicone at 100°C is equal to or less than 0.04%/cm^2/hr.

Refurbishment Capability: No information available.

Source and Cost: The source is Tempil Corporation, (201) 757-8300.

General Information: This paint is applied on the clean-grit blasted aluminum substrate by standard paint-spraying technique. Each successive coat was first air-dried for 2 hours and then baked at 394°K for 2 hours. After the desired coating thickness was obtained, the baking temperature was gradually increased to 522°K and maintained for 1 hour.

State of Development: No information on further development is available.

PYROMARK BLACK ON INCONEL

Composition: The exact composition of this paint is not available from the manufacturer.

Density: No data available.

Recommended Thickness: 32 micrometers (thickness on which measurements were made).

Maximum Temperature: No data available.

Substrate: Inconel, grit-blasted

Adhesion: Showed no peeling or spalling after 10 cycles between 478°K and 80°K.

Thermophysical Properties:

Initial Solar Absorptance, α_S = 0.906
Initial Hemispherical Emittance, ϵ_T = 0.842
Initial α_S/ϵ_T = 1.076
Solar Absorption after 3,440 ESH of UV + 10^{15} e/cm^2 = 0.906

Contamination Susceptibility: No information available.

Outgassing Characteristics: The steady-state weight loss of the silicone at 100°C is equal to or less than 0.04%/cm^2/hr.

Refurbishment Capability: No information available.

Source and Cost: The source is Tempil Corporation, (201) 757-8300.

State of Development: No information available.

General Information: The paint is applied on the clear grit-blasted inconel substrate using standard spraying technique. Each successive coat is first air-dried for 2 hours and then baked at 394°K for 2 hours. After the desired coating thickness is reached, the baking temperature is gradually increased to 522°K and maintained for 1 hour.

SODIUM DICHROMATE BLACKENED INCONEL

Composition: Deposition of chromium oxide produced by chemical reaction between molten sodium dichromate and the substrate material.

Density: No data available.

Recommended Thickness: 9.6 micrometers (thickness on which measurements were made).

Maximum Temperature: No data available.

Substrate: Inconel, grit-blasted

Adhesion: Showed no peeling or spalling after 10 cycles between 478°K and 78°K.

Thermophysical Properties:

Initial Solar Absorptance, α_S = 0.951
Initial Hemispherical Emittance, ϵ_T = 0.840
Initial α_S/ϵ_T = 1.132
Solar Absorptance after 4,770 ESH of UV + 10^{15} e/cm^2 = 0.959

Contamination Susceptibility: No information available.

Outgassing Characteristics: No information available.

Refurbishment Capability: No information available.

Source and Cost: Langley Research Center, Reference NASA TN D-4116, (703) 827-1110, Ext. 2986.

General Information: Blackening procedure consists of covering the clean grit-blasted substrate surface with sodium dichromate crystals and reacting in a clean furnace at a temperature of 700°K for 30 minutes. Most uniform coatings can be obtained by repeating the procedure rather than doubling the reaction time in the furnace.

State of Development: No further development is reported.

BLACK NICKEL-PLATED ALUMINUM

Composition: Electrodeposited nickel on aluminum substrate.

Density: No data available.

Recommended Thickness: 2.8 micrometers (thickness on which measurements were made).

Maximum Temperature: No data available.

Substrate: 1100 (2-S) aluminum

Adhesion: Showed no peeling or spalling after 10 cycles between 478°K and 80°K.

Thermophysical Properties:

Initial Solar Absorptance, α_S = 0.959
Initial Hemispherical Emittance, ϵ_T = 0.686
Initial α_S/ϵ_T = 1.398
Solar Absorptance after 3,800 ESH of UV + 10^{15} e/cm^2 = 0.953

Contamination Susceptibility: No information available.

Outgassing Characteristics: No outgasing is expected.

Refurbishment Capability: No information available.

Source and Cost: Langley Research Center, Reference NASA TN D-4116, (703) 827-1110, Ext. 2986.

General Information: Black plating was achieved by placing clear and smooth substrate in a bath containing nickel sulphate (97.4 g/liter), sodium thiocyanate (74.9 g/liter), zinc sulfate (45.0 g/liter), and lead acetate (11.3 g/liter), and sending a current of density 10.76 to 21.53 amp/m^2 at 0.75 to 1.5 volts through the substrate and a nickel anode for 20 minutes. This paint suffered a loss of 12.9 percent in emittance due to simulated space environment.

State of Development: No further development is reported.

TABULATED SUMMARIES OF THERMAL CONTROL SURFACES

COATING	INITIAL THERMOPHYSICAL PROPERTIES			ULTRAVIOLET RADIATION DAMAGE			PROTON DAMAGE		ELECTRON DAMAGE		SYNERGISTIC DAMAGE $\Delta\alpha_s$
	α_s	ϵ_T	α_s/ϵ_T	$\Delta\alpha_s$ 1000 ESH	$\Delta\alpha_s$ 2000 ESH	$\Delta\alpha_s$ 3000 ESH	DOSE EWH	$\Delta\alpha_s$	DOSE e/cm^2	$\Delta\alpha_s$	
Optical Solar Reflector [Vapor-deposited silver on Corning 7940 fused silica overcoated with vapor deposited Inconel]	0.050	0.810	0.062	0.00			1,000	0.00	6×10^{14}	0.00	0.005 in 1580 ESH. Uncertainty of measured change in α_s is 0.5 α_s. Flight data OSO-III
Optical Solar Reflector [Vapor-deposited aluminum on Corning 7940 fused silica overcoated with vapor-deposited silicon monoxide]	0.100	0.810	0.123	0.00			1,000	0.00			
Silver coated FEP Teflon [Series-Emittance]											
2 mil silver TS-2	0.059	0.680	0.086				10,000	0.04			
5 mil silver TS-5	0.090	0.820	0.109				10,000	0.04			0.000 for 4600 ESH. Flight data OGO-VI
Aluminum coated FEP Teflon [Series-Emittance]											
2 mil Al, TA-2	0.130	0.670	0.194				10,000	0.06	10^{15}	Significant	
5 mil Al, TA-5	0.170	0.830	0.205				10,000	0.06	10^{16}	Significant	
10 mil Al, TA-10	0.210	0.890	0.235				10,000	0.05	10^{16}	Significant	
1 mil Al, TA-1	0.130	0.550	0.235								0.04 for 4000 ESH. Flight data Mariner V
Lanthanum Oxide in Potassium Silicate	0.083						200	0.007			0.160 for 270 ESH of UV + 5000 EWH of Proton

CONTAMINANT DEGRADATION AND EFFECTS	OUTGASSING PROPERTIES	ALLOWABLE TEMPERATURE LIMITS		APPLICATION AND ADHERENCE		COMMENTS
		°C	°F	SUBSTRATES USED	PROPERTIES	
Surface contamination does not cause permanent degradation. However these should be removed prior to launch	The adhesive used to bind the OSRs to the substrate will outgas. A minimum of 14 days curing is required to minimize outgassing during ascent. *The steady state weight* loss of RTV-615 at 100°C is greater than 0.04 percent/ cm^2/hr.	MAX. 260 MIN.	MAX. 500 MIN.	These mirrors are applied to the substrate with RTV-615 silicone, and has passed the sinusoidal and random-vibration tests.		Recommended standard mirror size approximately 1 × 1 × 0.008 inch thick. The OSRs are fragile. Coating thickness: 1000Å of silver plus 500Å Inconel *overcoat.*
	same as above	MAX. 260 MIN.	MAX. 500 MIN.	same as above		same as above
	No data available. Depends on the adhesive used. The steady state weight loss of Teflon 100°C is less than 0.04 percent/cm^2/hr.	MAX. MIN.	MAX. MIN.			
	same as above	MAX. MIN.	MAX. MIN.			
		MAX. 696 MIN. -190	MAX. 1284.8 MIN. -130	The formulation is applied by spray painting. The coating thickness is not known.		

COATING	INITIAL THERMOPHYSICAL PROPERTIES			ULTRAVIOLET RADIATION DAMAGE			PROTON DAMAGE		ELECTRON DAMAGE		SYNERGISTIC DAMAGE $\Delta\alpha_S$
	α_S	ϵ_T	α_S/ϵ_T	$\Delta\alpha_S$ 1000 ESH	$\Delta\alpha_S$ 2000 ESH	$\Delta\alpha_S$ 3000 ESH	DOSE EWH	$\Delta\alpha_S$	DOSE e/cm^2	$\Delta\alpha_S$	
Aluminum Oxide in Potassium Silicate	0.110	0.820			0.05				5.8×10^{15}	0.08	0.06 after 48-hour, Flight ATS-I
Cat-A-Lac white paint	0.120			0.09 after 2 hrs. of UV							
SiOx coated vapor-deposited aluminum	0.128	0.530 dependent on the thickness of SiOx film									The initial α_S/ϵ_T was 0.48 and changed to 0.66 after 2000 ESH. Flight data ATS-1. Explorer XXIII data over a 3 1/2 yr. period showed no significant degradation.
SiO_2 coated vapor-deposited aluminum	0.140	0.420 dependent on the thickness of SiO_2	0.334	0.03 for approx. 1μ thick film							0.06 after 1500 ESH. Flight data ATS-3
Al_2O_3 coated vapor-deposited aluminum	0.140	0.450 dependent on the thickness of Al_2O_3	0.311								0.075 after 200 ESH for a 1μ thick film of Al_2O_3. Flight data ATS-3

CONTAMINANT DEGRADATION AND EFFECTS	OUTGASSING PROPERTIES	ALLOWABLE TEMPERATURE LIMITS		APPLICATION AND ADHERENCE		COMMENTS
		°C	°F	SUBSTRATES USED	PROPERTIES	
		MAX. MIN.	MAX. MIN.			
	The steady state weight loss at 100°C is less than 0.04 percent/cm^2/hr.	MAX. MIN.	MAX. MIN.	1 day cure at room temperature		
	The steady state weight loss at 100°C is less than or equal to 0.04 percent/cm^2/hr.	MAX. 260 MIN.	MAX. 500 MIN.	Any clean rigid substrate. No curing needed.	No blistering. No failure after thermal cycling between 30 to 500°F.	Lowest solar absorptance requires polished metal or glass substrate.
		MAX. 260 MIN.	MAX. 500 MIN. 30 30	Any clean rigid substrate. No curing needed.	No blistering. No failure after thermal cycling between 30 to 500°F.	Lowest solar absorptance requires polished metal or glass substrate.
		MAX. 260 MIN.	MAX. 500 MIN. 30	Any clean rigid substrate. No curing needed.	No blistering. No failure after thermal cycling between 30 to 500°F.	Lowest solar absorptance requires polished metal or glass substrate

COATING	INITIAL THERMOPHYSICAL PROPERTIES			ULTRAVIOLET RADIATION DAMAGE			PROTON DAMAGE		ELECTRON DAMAGE		SYNERGISTIC DAMAGE
	α_S	ϵ_T	α_S/ϵ_T	$\Delta\alpha_S$ 1000 ESH	$\Delta\alpha_S$ 2000 ESH	$\Delta\alpha_S$ 3000 ESH	DOSE EWH	$\Delta\alpha_S$	DOSE EWH	$\Delta\alpha_S$	$\Delta\alpha_S$
Aluminized Mylar	0.130						10,000	0.00			
Hughes Organic H-10	0.150	0.860	0.174								$\Delta\alpha_S$ = 0.12 after 1000 ESH. Flight data Lunar Orbiter V.
Alzak	0.150	0.77	0.195								$\Delta\alpha_S$ = 0.09 after 2000 ESH. Flight data ATS-3
Lithafrax	0.150	0.870	0.172	0.06 (600 ESH)					10^{15}	0.09	
Synthetic Li/Al/SiO.	0.160	0.870	0.184	0.09 (485 ESH)					10^{15}	0.11	

CONTAMINANT DEGRADATION AND EFFECTS	OUTGASSING PROPERTIES	ALLOWABLE TEMPERATURE LIMITS		APPLICATION AND ADHERENCE		COMMENTS
		°C	°F	SUBSTRATES USED	PROPERTIES	
	The steady state weight loss at 100°C is less than 0.04 percent/cm^2/hr.	MAX. MIN.	MAX. MIN.			
		MAX. MIN.	MAX. MIN.			
The change in α_s due to RCS engine plume was between 2 to 70 percent depending on the position and time of exposure.		MAX. MIN.	MAX. MIN.			
		MAX. MIN.	MAX. MIN.		No failure at -240°F but failure at 70°F.	
		MAX. MIN.	MAX. MIN.		No failure at -260°F but failure at 70°F.	

COATING	INITIAL THERMOPHYSICAL PROPERTIES			ULTRAVIOLET RADIATION DAMAGE			PROTON DAMAGE		ELECTRON DAMAGE		SYNERGISTIC DAMAGE $\Delta\alpha_S$
	α_S	ϵ_T	α_S/ϵ_T	$\Delta\alpha_S$ 1000 ESH	$\Delta\alpha_S$ 2000 ESH	$\Delta\alpha_S$ 3000 ESH	DOSE EWH	$\Delta\alpha_S$	DOSE EWH	$\Delta\alpha_S$	
Thermatrol 2A-100	0.170	0.860		0.14 (500 ESH)			60,000	0.42	10^{16}	Severe	
Hughes Inorganic white H-2	0.178	0.876	0.203	0.14							$\Delta\alpha_S$ = 0.089 after 1000 ESH. Flight data Lunar Orbiter IV.
Z-93	0.184	0.880	0.209		Not measur-able		10,000	0.14			$\Delta\alpha_S$ = 0.066 after 2000 ESH. Flight data Lunar Orbiter V. $\Delta\alpha_S$ = 0.063 after 1000 ESH. Flight data Mariner IV. $\Delta\alpha_S$ = 0.150 after 6×10^4 mission hrs. Flight data SERT-II
Douglas White	0.184	0.880	0.209						10^{15}	0.11	$\Delta\alpha_S$ = 0.08 after 2000 ESH. Flight data Lunar Orbiter V.
S-13G	0.190	0.880	0.216	0.04			10,000	Severe			$\Delta\alpha_S$ = 0.128 after 1000 ESH. Flight data Lunar Orbiter IV. $\Delta\alpha_S$ = 0.14 after 1000 ESH. Flight data Mariner V.

CONTAMINANT DEGRADATION AND EFFECTS	OUTGASSING PROPERTIES	ALLOWABLE TEMPERATURE LIMITS		APPLICATION AND ADHERENCE		COMMENTS
		°C	°F	SUBSTRATES USED	PROPERTIES	
Requires protection against contamination.	For 3-day and 25-day room temperature curing, the outgassing is high beyond 140°F.	MAX. 343.33 MIN.	MAX. 650 MIN.	Any clean substrate. Primer required. Room temperature curing.		Surface is soft and rubbery. Material is electrostatic. 24 hr. cure at room temperature required. A minimum thickness of 35 to 50 mils required for external use and 1.0 mil for internal application.
		MAX. MIN.	MAX. MIN.			
The change in α_S due to RCS engine plume was between 50 to 80 percent depending on the position and time of exposures. Similarly, the change in ε_T was between 3 to 10 percent. $\Delta\alpha_S$ = 0.05 to 0.08, $\Delta\varepsilon_T$ = 0.00 Flight data Apollo 9.	The initial weight loss is 8×10^{-5} gm/cm^2, and the steady state loss is 5×10^{-11} gm/cm^2. The time to reach steady state is 20 hrs.	MAX. MIN.	MAX. MIN.	Aluminum or plastic substrates should be abraded and thoroughly cleaned. Applied by spraying, cured by air drying. Improved hardness by heat-curing at 745°R.	Hard, porous, brittle. Retains dirt and stains. Repairable.	4.5 to 6.0 mil coating thickness is required.
		MAX. MIN.	MAX. MIN.			
The change in α_S due to RCS engine plume was between 10 to 250 percent depending on the position and time of exposure.	The steady state weight loss at 100°C is equal to or less than 0.04 percent/cm^2/hr.	MAX. MIN.	MAX. MIN.	Any surface to which GE SS-4044 primer can be applied. Thorough cleaning of the surface is needed. Applied by spraying and air-cured.	Soft, rubbery. Thermal shock resistant if primer is not too thick. Cleanable, repairable.	5 to 8 mil thickness is recommended. 16 hrs. of air-curing is needed.

COATING	INITIAL THERMOPHYSICAL PROPERTIES			ULTRAVIOLET RADIATION DAMAGE			PROTON DAMAGE		ELECTRON DAMAGE		SYNERGISTIC DAMAGE $\Delta\alpha_S$
	α_S	ϵ_T	α_S/ϵ_T	$\Delta\alpha_S$ 1000 ESH	$\Delta\alpha_S$ 2000 ESH	$\Delta\alpha_S$ 3000 ESH	DOSE EWH	$\Delta\alpha_S$	DOSE EWH	$\Delta\alpha_S$	
B-1060	0.109	0.880	0.216	0.028 (125 ESH)					10^{14}	0.007	$\Delta\alpha_S$ = 0.091 after 1000 ESH. Flight data Lunar Orbiter IV.
Silicone (RTV-602) over Aluminum	0.200	0.800	0.250	0.012							$\Delta\alpha_S$ = 0.13 after 1500 ESH. Flight data Lunar Orbiter V.
Butvar over Aluminum	0.200	0.860	0.232	0.00 (250 ESH)							$\Delta\alpha_S$ = 0.25 after 70 ESH and 20,000 EWH of protons.
S-13	0.210	0.880	0.238		0.140		2×10^6	0.07			$\Delta\alpha_S$ = 0.120 after 1500 ESH. Flight data Pegasus I and OSO-II,-III $\Delta\alpha_S$ = 0.225 after 2000 ESH. Flight data Mariner V.
B-1056	0.210	0.880	0.238								$\Delta\alpha_S$ = 0.186 after 2000 ESH. Flight data Pegasus I. $\Delta\alpha_S$ = 0.155 after 1000 ESH. Flight data Lunar Orbiter I.

CONTAMINANT DEGRADATION AND EFFECTS	OUTGASSING PROPERTIES	ALLOWABLE TEMPERATURE LIMITS		APPLICATION AND ADHERENCE		COMMENTS
		°C	°F	SUBSTRATES USED	PROPERTIES	
		MAX. MIN.	MAX. MIN.			
		MAX. MIN.	MAX. MIN.			
		MAX. MIN.	MAX. MIN.			
	The initial weight loss is 1.2×10^{-2} gm/cm^2 and the steady state loss is 2.8×10^{-3} gm/cm^2. The time to reach steady state is 44 hrs.	MAX. MIN.	MAX. MIN.	Any surface to which GE SS-4044 primer can be applied. Standard cleaning of the surface needed. Spray-applied and air-cured.	Cleanable, repairable	3.5 to 5.5 mil coating thickness recommended. 16 hrs. of air-curing needed.
		MAX. MIN.	MAX. MIN.			

COATING	INITIAL THERMOPHYSICAL PROPERTIES			ULTRAVIOLET RADIATION DAMAGE			PROTON DAMAGE		ELECTRON DAMAGE		SYNERGISTIC DAMAGE
	α_S	ϵ_T	α_S/ϵ_T	$\Delta\alpha_S$ 1000 ESH	$\Delta\alpha_S$ 2000 ESH	$\Delta\alpha_S$ 3000 ESH	DOSE EMH	$\Delta\alpha_S$	DOSE e/cm^2	$\Delta\alpha_S$	$\Delta\alpha_S$
PV-100	0.220	0.870	0.253	0.170 (162 ESH)			3000	0.03			
Rutile TiO_2 in DC - R6-3488 Methyl Silicone	0.230	0.850	0.270								$\Delta\alpha_S$ = 0.18 after 1.3 years. Flight data Pegasus
Lockheed $ZrSiO_2/K_2SiO_3$ LP-10-A	0.240	0.870	0.276	0.040		0.290 (7000 ESH)			10^{16}	0.02	$\Delta\alpha_S$ = 0.044 after 500 ESH. Flight data OSO-II.
TiO_2 in Silicone	0.240	0.860	0.279								$\Delta\alpha_S$ = 0.16 after 73 hrs. Flight data Apollo 9.
Tinted White Kemacryl	0.240	0.860	0.279	0.120 (485 ESH)					10^{16}	0.06	$\Delta\alpha_S$ = 0.20 after 485 ESH of UV + 10^{15} e/cm^2

CONTAMINANT DEGRADATION AND EFFECTS	OUTGASSING PROPERTIES	ALLOWABLE TEMPERATURE LIMITS		APPLICATION AND ADHERENCE		COMMENTS
		°C	°F	SUBSTRATES USED	PROPERTIES	
		MAX. MIN.	MAX. MIN.			
	Appreciable outgassing beyond 130°F after room temperature cure.	MAX. MIN.	MAX. MIN.			
	Weight loss during vacuum is about 5.0 percent.	MAX. MIN.	MAX. 960°R MIN.	Standard spray gun technique is used. Base coat reacts with substrate and serves as primer. Room temperature cure is approx. 12 hrs.		The electron bombardment was not done in situ. 3.0 to 5.0 mil coating thickness required.
$\Delta\alpha_S$ due to launch was between 0.10 and 0.16 depending on location. Coating retrieved after 73 hrs. Similarly $\Delta\varepsilon_T$ was between 0.01 and 0.02. Flight data Apollo 9.		MAX. MIN.	MAX. MIN.			The samples were not brought back to Earth under vacuum.
Requires protection against contamination. No data available.	For a 2-day room temperature curing period, the outgassing is high for temperatures 150°F and above. For an 18-day cure at room temperature, the outgassing is low.	MAX. 232.2 MIN.	MAX. 450 MIN.	Any clean rigid surface. Primer required. Room temperature cured.	No failure after 385 thermal cycles between 150 to 70°F	A minimum of 5-mil dry film thickness required for external application. 14-day room temperature cure required to minimize blistering during ascent heating.

COATING	INITIAL THERMOPHYSICAL PROPERTIES			ULTRAVIOLET RADIATION DAMAGE			PROTON DAMAGE		ELECTRON DAMAGE		SYNERGISTIC DAMAGE
	α_S	ϵ_T	α_S/ϵ_T	$\Delta\alpha_S$ 1000 ESH	$\Delta\alpha_S$ 2000 ESH	$\Delta\alpha_S$ 3000 ESH	DOSE EWH	$\Delta\alpha_S$	DOSE e/cm^2	$\Delta\alpha_S$	$\Delta\alpha_S$
Leafing Aluminum in Silicone	0.250	0.260	0.961						8×10^{15}	0.00	$\Delta\alpha_S$ = 0.00 after 1.5 years. Flight data OSO-I $\Delta\alpha_S$ = 0.00 after 2.2 years. Flight data Mariner IV
White Skyspar in RTV-60 Silicone	0.250	0.910	0.274		0.350		2×10^6	0.12	10^{16}	0.07	$\Delta\alpha_S$ = 0.39 after 1000 ESH. Flight data OSO-II
R-960 TiO_2 in RTV-602 Silicone	0.270	0.760	0.355						10^{15}	Severe	$\Delta\alpha_S$ = 0.13 after 1.5 years. Flight data OSO-I
Rokide A	0.270	0.750	0.360	0.00							
Fuller Gloss White	0.290	0.900	0.322	0.09					10^{15}	0.01	$\Delta\alpha_S$ = 0.10 after 485 ESH of UV + 10^{15} e/cm^2

CONTAMINANT DEGRADATION AND EFFECTS	OUTGASSING PROPERTIES	ALLOWABLE TEMPERATURE LIMITS		APPLICATION AND ADHERENCE		COMMENTS
		°C	°F	SUBSTRATES USED	PROPERTIES	
$\Delta\alpha_s$ due to engine plume was between 0.07 and 0.42 depending on the position and time of exposure.		MAX. MIN.	MAX. MIN.			
		MAX. 232.2 MIN.	MAX. 450 MIN.	Any rigid substrate. Room temperature cured.		For internal application, 1.0 mil minimum thickness. For external application, 4.0 mil minimum.
	Appreciable outgassing beyond 130°F after room temperature cure	MAX. MIN.	MAX. MIN.			
		MAX. MIN.	MAX. MIN.	Any metallic substrate		
		MAX. 343.33 MIN.	MAX. 650 MIN.	Any clean rigid substrate capable of withstanding cure cycle. Cured by baking at 465°F.	Cracking and loss of adhesion after 170 cycles between -240 and 70°F.	A minimum of 5-mil dry film thickness required for external application and a minimum of 1.0 mil for internal application.

COATING	INITIAL THERMOPHYSICAL PROPERTIES			ULTRAVIOLET RADIATION DAMAGE			PROTON DAMAGE		ELECTRON DAMAGE		SYNERGISTIC DAMAGE
	α_S	ϵ_T	α_S/ϵ_T	$\Delta\alpha_S$ 1000 ESH	$\Delta\alpha_S$ 2000 ESH	$\Delta\alpha_S$ 3000 ESH	DOSE EWH	$\Delta\alpha_S$	DOSE e/cm^2	$\Delta\alpha_S$	$\Delta\alpha_S$
Kapton-H film on Aluminum	0.320	0.750	0.427		0.105				10^{16}	Severe	
Sandoz OA-Dyed anodized Aluminum	0.647	0.927	0.698								$\Delta\alpha_S$ = 0.037 after 3540 ESH of UV + 10^{15} e/cm^2
Chromic acid anodized Aluminum	0.700	0.730	0.959								$\Delta\alpha_S$ = 0.03 after 73 hrs. Flight data Apollo 9.
Bi_2S_3 Dyed anodized Aluminum	0.728	0.909	0.801								$\Delta\alpha_S$ = 0.032 after 3540 ESH of UV + 10^{15} e/cm^2
Sandoz BK-Dyed anodized Aluminum	0.757	0.926	0.817								$\Delta\alpha_S$ = 0.029 after 3540 ESH of UV + 10^{15} e/cm^2

CONTAMINANT DEGRADATION AND EFFECTS	OUTGASSING PROPERTIES	ALLOWABLE TEMPERATURE LIMITS		APPLICATION AND ADHERENCE		COMMENTS
		°C	°F	SUBSTRATES USED	PROPERTIES	
	The steady state weight loss at 100°C is equal to or less than 0.04 percent/cm²/hr.	MAX. MIN.	MAX. MIN.			
		MAX. MIN.	MAX. MIN.			
Contamination will degrade the α_s value.		MAX. MIN.	MAX. MIN.			
		MAX. MIN.	MAX. MIN.			
	The steady state weight loss at 100°C is equal to or less than 0.04 percent/cm²/hr.	MAX. MIN.	MAX. MIN.			

COATING	INITIAL THERMOPHYSICAL PROPERTIES			ULTRAVIOLET RADIATION DAMAGE			PROTON DAMAGE		ELECTRON DAMAGE		SYNERGISTIC DAMAGE
	α_S	ϵ_T	α_S/ϵ_T	$\Delta\alpha_S$ 1000 ESH	$\Delta\alpha_S$ 2000 ESH	$\Delta\alpha_S$ 3000 ESH	DOSE EWH	$\Delta\alpha_S$	DOSE e/cm^2	$\Delta\alpha_S$	$\Delta\alpha_S$
PbS-Dyed anodized aluminum	0.861	0.912	0.944								$\Delta\alpha_S$ = 0.030 after 3540 ESH of UV + 10^{15} e/cm^2
Fuller Black	0.890	0.880	1.011	0.05 (600 ESH)							
Rokide C	0.900	0.850	1.059	0.00							
Pyromark Black on aluminum	0.902	0.830	1.086								$\Delta\alpha_S$ = 0.001 after 3440 ESH of UV + 10^{15} e/cm^2
Pyromark Black on Inconel	0.906	0.842	1.076								$\Delta\alpha_S$ = 0.00 after 3440 ESH of UV + 10^{15} e/cm^2

CONTAMINANT DEGRADATION AND EFFECTS	OUTGASSING PROPERTIES	ALLOWABLE TEMPERATURE LIMITS		APPLICATION AND ADHERENCE		COMMENTS
		°C	°F	SUBSTRATES USED	PROPERTIES	
		MAX. MIN.	MAX. MIN.			
		MAX. 576.6 MIN.	MAX. 1070 MIN.	Any rigid substrate capable of withstanding cure cycle. Cured by baking at 465°F.	Cracking and loss of adhesion after 170 cycles between -240 and 70°F.	1-mil dry film thickness is minimum for both external and internal applications.
		MAX. 904.3 MIN.	MAX. 1660 MIN.	Rene' 41 with a 2-mil coating of Nichrome. Flame sprayed.	No failure after thermal cycling between 1600 to 70°F.	The bonding with substrate is mechanical and thermal shock can be a problem.
	The steady state weight loss of the silicone at 100°C is equal to or less than 0.04 percent/cm^2/hr.	MAX. MIN.	MAX. MIN.			
		MAX. MIN.	MAX. MIN.			

COATING	INITIAL THERMOPHYSICAL PROPERTIES			ULTRAVIOLET RADIATION DAMAGE			PROTON DAMAGE		ELECTRON DAMAGE		SYNERGISTIC DAMAGE
	α_S	ϵ_T	α_S/ϵ_T	$\Delta\alpha_S$ 1000 ESH	$\Delta\alpha_S$ 2000 ESH	$\Delta\alpha_S$ 3000 ESH	DOSE EMH	$\Delta\alpha_S$	DOSE e/cm^2	$\Delta\alpha_S$	$\Delta\alpha_S$
Black Kemacryl	0.930	0.880	1.057	0.05 (600 ESH)							
Pyromark Black	0.920	0.870	1.057								
Cat-A-Lac Black	0.940	0.940	1.00								-0.03 for 2400 flight hrs. Flight data Mariner V. This bleaching is unexplained.
Platinum Black on OMV Beryllium	0.940	0.850	1.106								
Sodium Dichromate Blackened Inconel	0.951	0.840	1.132								$\Delta\alpha_S$ = 0.008 after 4770 ESH of UV + 10^{15} e/cm^2

CONTAMINANT DEGRADATION AND EFFECTS	OUTGASSING PROPERTIES	ALLOWABLE TEMPERATURE LIMITS		APPLICATION AND ADHERENCE		COMMENTS
		°C	°F	SUBSTRATES USED	PROPERTIES	
Requires protection against contamination. No data available.		MAX. 232.2 MIN.	MAX. 450 MIN.	Any clean rigid substrate Primer required. Room temperature cured in a minimum of 14 days.	No failure after 385 thermal cycles between -150 and 70°F.	1.5 mil dry film thickness is minimum for both external and internal applications.
		MAX. MIN.	MAX. MIN.			
	The weight loss at 100°C is less than 0.04 percent/cm²/hr.	MAX. MIN.	MAX. MIN.	Any clear, rigid substrate.		
Must be carefully protected from contamination		MAX. 648.8 MIN.	MAX. 1200 MIN.	QMV Beryllium applied by spraying.	No information on thermal cycling effects.	
		MAX. MIN.	MAX. MIN.			

COATING	INITIAL THERMOPHYSICAL PROPERTIES			ULTRAVIOLET RADIATION DAMAGE			PROTON DAMAGE		ELECTRON DAMAGE		SYNERGISTIC DAMAGE
	α_S	ε_T	α_S/ε_T	$\Delta\alpha_S$ 1000 ESH	$\Delta\alpha_S$ 2000 ESH	$\Delta\alpha_S$ 3000 ESH	DOSE EWH	$\Delta\alpha_S$	DOSE e/cm^2	$\Delta\alpha_S$	$\Delta\alpha_S$
Du-Lite-3-D on type 304 SS	0.952	0.653	1.458								$\Delta\alpha_S$ = 0.007 after 3800 ESH of UV + 10^{15} e/cm^2
CoS Dyed anodized Aluminum	0.957	0.930	1.029								$\Delta\alpha_S$ = 0.006 after 3760 ESH of UV + 10^{15} e/cm^2
Black Ni-plated Aluminum	0.959	0.686	1.398								$\Delta\alpha_S$ = -0.006 after 3800 ESH of UV + 10^{15} e/cm^2
Sodium Dichromate Blackened Inconel	0.963	0.806	1.195								$\Delta\alpha_S$ = 0.003 after 2560 ESH of UV + 10^{15} e/cm^2
3M Black Velvet	0.968	0.923	1.048	0.00 (100 ESH)							

CONTAMINANT DEGRADATION AND EFFECTS	OUTGASSING PROPERTIES	ALLOWABLE TEMPERATURE LIMITS		APPLICATION AND ADHERENCE		COMMENTS
		°C	°F	SUBSTRATES USED	PROPERTIES	
		MAX. MIN.	MAX. MIN.			
		MAX. MIN.	MAX. MIN.			
		MAX. MIN.	MAX. MIN.			12.9 percent change in ϵ_T was observed.
		MAX. MIN.	MAX. MIN.			
	The steady state weight loss at 100°C is equal to or less than 0.04 percent/cm^2/hr.	MAX. MIN.	MAX. MIN.	1 hour cure at room temperature		

COATING	INITIAL THERMOPHYSICAL PROPERTIES			ULTRAVIOLET RADIATION DAMAGE			PROTON DAMAGE		ELECTRON DAMAGE		SYNERGISTIC DAMAGE
	α_S	ϵ_T	α_S/ϵ_T	$\Delta\alpha_S$ 1000 ESH	$\Delta\alpha_S$ 2000 ESH	$\Delta\alpha_S$ 3000 ESH	DOSE EWH	$\Delta\alpha_S$	DOSE e/cm^2	$\Delta\alpha_S$	$\Delta\alpha_S$
NiS-Dyed anodized aluminum	0.970	0.929	1.044								$\Delta\alpha_S$ = 0.002 after 3540 ESH of UV + 10^{15} e/cm^2

CONTAMINANT DEGRADATION AND EFFECTS	OUTGASSING PROPERTIES	ALLOWABLE TEMPERATURE LIMITS		APPLICATION AND ADHERENCE		COMMENTS
		°C	°F	SUBSTRATES USED	PROPERTIES	
		MAX. MIN.	MAX. MIN.			Slight change in ϵ_T is noted.
		MAX. MIN.	MAX. MIN.			
		MAX. MIN.	MAX. MIN.			
		MAX. MIN.	MAX. MIN.			
		MAX. MIN.	MAX. MIN.			

BIBLIOGRAPHY - PART II

1. "Results From the Thermal Control Coatings Experiment on OSO-III", Progress in Astronautics and Aeronautics, Vol. 21, Academic Press, New York, pp. 769-795, 1969

2. "Mariner V Temperature Control Reference Design, Test, and Performance", Presented at the AIAA 3rd. Thermophysics Conference, Los Angeles, California, June 24-26, 1968

3. "Preflight Testing of the ATS-1 Thermal Coatings Experiment", Progress in Astronautics and Aeronautics, Vol. 20, Academic Press, New York, pp. 491-505, 1967

4. "Ultraviolet Stability of Some White Thermal Control Coatings Characterized in Vacuum", Presented at the AIAA Thermophysics Specialist Conference, New Orleans, Louisiana, April 17-20, 1967

5. "Environmental Studies of Thermal Control Coatings for Lunar Orbiter", Progress in Astronautics and Aeronautics, Vol. 21, Academic Press, New York, pp. 797-817, 1969

6. "Thermal Control Experiments on the Lunar Orbiter Spacecraft", Progress in Astronautics and Aeronautics, Vol. 21, Academic Press, New York, pp. 819-852, 1969

7. "The Behavior of Several White Pigments as Determined by In Situ Reflectance Measurements of Irradiated Specimens", Technical Report, AFML-TR-68-198, August 1968

8. "In Situ Electron, Proton, and Ultraviolet Radiation Effects on Thermal Control Coatings", NASA, N69-23865

9. "Dependence of Thermal Control Coating Degradation Upon Electron Energy", NASA, N69-30549 and CFSTI

10. "Nuclear Environmental Effects on Spacecraft Thermal Control Coatings", NASA, SP-SS, ML-TDR-64-159, N65-26895

11. "Apollo 9 Thermal Control Coating Degradation", Manned Spacecraft Center, Houston, Texas, TRW Systems, Redondo Beach, California, May 1969

BIBLIOGRAPHY - Continued

12. "Effect of Electron Bombardment on the Optical Properties of Spacecraft Temperature Control Coatings", AIAA Journal 3, pp. 2318-2327, 1965

13. "Space Materials Handbook, Supplement 1 to the Second Edition of Space Materials Experience", NASA SP-3025, ML-TDR-64-40, Supplement 1, 1966

14. "In Situ Measurements of Spectral Reflectance of Thermal Control Coatings Irradiated in Vacuo", Progress in Astronautics and Aeronautics, Vol. 20, Academic Press, New York, pp. 281-296, 1967

15. "Some Fundamental Aspects of Nuclear Radiation Effects in Spacecraft Thermal Control Materials", NASA SP-55, ML-TDR-64-159, N65-26894, 1955

16. "Handbook of Optical Properties of Thermal Control Surfaces", Final Report, Vol. III, LMSC-A847882, June 25, 1967, NASA N67-34625

17. "The Effects of Ultraviolet Radiation on Low α/ϵ Surfaces", NASA-SP-55, 1965

18. "The Measurement of Solar Absorptance and Thermal Emittance", ESRO-TN-23, pp. 43, 1968

19. "Spectral Dependence of Ultraviolet - Induced Degradation of Coatings for Spacecraft Thermal Control", Progress in Astronautics and Aeronautics, Vol. 20, Academic Press, New York, pp. 265-280

20. "Development of a Barrier-Layer Anodic Coating for Reflective Aluminum in Space", Progress in Astronautics and Aeronautics, Vol. 20, Academic Press, New York, pp. 315-328, 1967

21. "Effects of the Ascent Environment on Spacecraft Thermal Control Surfaces", ASTM Special Tech. Pub. No. 453, October 1962

BIBLIOGRAPHY - Continued

22. "Pigmented Surface Coatings for Use in the Space Environment", ASD-TDR-52-840, Part II, February 1969

23. "The UV Degradation of Organic Coatings, III-Effect on Physical Properties", WADD TR60-703, December 1950

24. "Emissivity Coatings for Low-Temperature Space Radiators", NASA CR-1420 and CFSTI

25. "Preliminary Results from the Ames Emissivity Experiment on OSO-II", Progress in Astronautics and Aeronautics, Vol. 18, Academic Press, New York, pp. 459-472, 1966

26. "Radiation-Induced Absorption Bands in Spacecraft Thermal Control Coating Pigments", Progress in Astronautics and Aeronautics", Vol. 23, Academic Press, New York, pp. 189-218, 1970

27. "Exploratory Experimental Study on Neutral Charge Low Energy Particle Irradiation of Selected Thermal Control Coatings", NASA, N69-15965 and CFSTI

28. "Electron Energy Dependence for In-Vacuum Degradation and Recovery in Thermal Control Surfaces", Progress in Astronautics and Aeronautics, Vol. 23, Academic Press, New York, pp. 219-248, 1970

29. "Effects of Combined Electron - Ultraviolet Irradiation on Thermal Control Coatings in Vacuo at 77°K", Progress in Astronautics and Aeronautics, Vol. 21, Academic Press, New York, pp. 725-740, 1959

30. "Results from the ATS-3 Reflectometer Experiment", AIAA Papers No. 59-544

31. "Electron-Ultraviolet Radiation Effects on Thermal Control Coatings", Progress in Astronautics and Aeronautics, Vol. 21, Academic Press, New York, pp. 597-724, 1969

32. "Study of In-Situ Degradation of Thermal Control Surfaces", IITRI Report No. U6061-17, March 1969

BIBLIOGRAPHY - Continued

33. "Stable Temperature Control Surfaces for Spacecraft", JPL Report No. 32-340, November 1962

34. "Kapton Base Thermal Control Coatings", Paper presented at Symposium on Coatings in Space, Cosponsored by ASTM E-10 Sub VI on Space Radiation Effects and NASA, in cooperation with ASTME-21 on Space Simulation, Cincinnati, Ohio, December 11-12, 1969

35. "Solar Absorptivity and Thermal Emissivity of Aluminum Coated with Silicon Oxide Films Prepared by Evaporation of Silicon Monoxide", Applied Optics, Vol. 9, pp. 339-344, February 1970

36. "Recent Coating Developments and Exposer Parameters", presented at Thermal Control Working Group Meeting, Dayton, Ohio, August 16-17, 1967

37. "Effects of a Simulated Space Environment on Thermal Radiation Characteristics of Selected Black Coatings, NASA TND-4116

38. "Bright Anodized Coatings for Temperature Control of Space Vehicles", Plating, Vol. 51, pp. 1165-1172, December 1964

39. "Space Materials Handbook", N70-11113, AD692353, July 1968

40. "The Development of S-13G-type Thermal Control Coatings Based on Silicate-Treated Zinc Oxide", Progress in Astronautics and Aeronautics, Vol. 21, Academic Press, New York, pp. 741-766, 1969

41. "Series Emittance Thermal Control Coatings", presented at Thermal Control Working Group Meeting, Dayton, Ohio, August 16-17, 1967

42. "Effects of Combined Space Radiation on Some Materials of Low Solar Absorptance", DDC, AD666364

43. "Solar Radiation-Induced Damage to Optical Properties of ZnO-type Pigments", NASA, N69-13059 and CFSTI

BIBLIOGRAPHY - Continued

44. "An Experimental Study of the Combined Space Environmental Effects on a Zinc Oxide/Potassium Silicate Coating", Progress in Astronautics and Aeronautics, Vol. 20, Academic Press, New York, pp. 237-264, 1967

45. "Reflectance, Solar Absorptivity, and Thermal Emissivity of SiO_2 Coated Aluminum", Applied Optics, Vol. 8, pp. 275-281, February 1969

46. "High-Temperature Space-Stable Selective Solar Absorber Coating", Applied Optics, Vol. 4, pp. 917-925, August 1965

47. "Long-Duration Exposer of Spacecraft Thermal Coatings to Simulated Near-Earth Orbital Conditions", Progress in Astronautics and Aeronautics, Vol. 29, MIT Press, Mass., pp. 123-133, 1972

48. "Thermal Control Coating Degradation Data from the Pegasus Experiment Packages", Progress in Astronautics and Aeronautics, Vol. 20, Academic Press, New York, pp. 457-473, 1967

49. "Mariner-Mars Absorptance Experiment", Progress in Astronautics and Aeronautics, Vol. 18, Academic Press, New York, 1965, pp. 441-457, 1965

50. "Effects of Extreme Ultraviolet on the Optical Properties of Thermal Control Coatings", Progress in Astronautics and Aeronautics, Vol. 21, Academic Press, New York, pp. 667-695, 1969

51. "Properties of High Emittance Materials", NASA-CR-1278, 1969

52. "Preparation and Properties of Sputtered Bismuth Oxide Films", Brit. J. Appl. Phys. 18, 363, 1967

53. "Infrared Measurements of Cadmium Sulfide Thin Films Deposited on Aluminum", Phys. Status Solidi 32, 119, 1969

BIBLIOGRAPHY - Concluded

54. "Spectral and Total Emissivities of Rokide C on Motybdenum above 1800° F", J. Am. Ceram. Soc. 44, 374, 1961

55. "Anodized Aluminum Coatings for Temperature Control of Space Vehicles", AD 402381

56. "Nuclear and Space Radiation Effects on Materials", NASA SP-8053, June 1970

APPENDIX A. RAW DATA

ORGANIC COATINGS

COATING	INITIAL	$\Delta\alpha_S$ 100 ESH	$\Delta\alpha_S$ 1,000 ESH	$\Delta\alpha_S$ 2,000 ESH	SOURCE OF DATA	SPACE LOCATION	RADIATION ENCOUNTERED	BIBLIOGRAPHY REFERENCES
S-13 ZnO/RTV-602 (SP-500 in dimethyl silicone binder with GE SCR-05 catalyst IITRI	α_S = 0.21 ϵ_T = 0.88	 0.02 0.078 0.087 0.30 (α_S/ϵ_T)	0.14 0.096 0.196 0.186 0.45 (α_S/ϵ_T)	 0.225 0.56 (α_S/ϵ_T) 0.07 0.20	Pegasus I OSO-III Mariner V Mariner TCR ATS-1 Lab Mariner V	Near Earth Near Earth Venus Venus	UV (primarily) UV (primarily) Solar wind Solar wind 1.7×10^{18} p/cm^2 Combined	1 1 2 2 3
ZnO/RTV-602 Boeing B-1056	α_S = 0.21 ϵ_T = 0.88	0.050 0.033	 0.12 0.155	 0.186	Lab Pegasus I LO-I	 Near Earth Lunar	 Combined	4 4 6
S-13G K_2SiO_3 coated ZnO/RTV-602 IITRI (silicate treated ZnO in methyl silicone binder)	α_S = 0.19 ϵ_T = 0.88	 0.018 0.086 (400 (ESH)	0.03 0.05 0.128 0.34 (α_S/ϵ_T) 0.04 0.14	 Severe	Lab Lab Lunar Orbiter II Lunar Orbiter IV Lunar Orbiter IV OSO-III Mariner V Lab	 Lunar Lunar Lunar Near Earth	UV UV Combined Combined Combined UV (primarily) Combined 10^{16} p/cm^2	7 4 4 5 5 1 1 8
B-1060 (Modified S-13G made by Boeing) K_2SiO_3 coated ZnO/RTV-602 with 0.2% 1, 1, 3, 3 TMG	α_S = 0.19 ϵ_T = 0.88	0.028	 0.09 0.297 (α_S/ϵ_T)	 0.007	Lab Lab LO-IV LO-IV	 Lunar	UV 10^{14} 50 keV e/cm^2 Combined Combined	6 6 6 5
Titanox RA-NC/DC Q92009 silicone (Thermatrol 2A-100)	α_S = 0.17 ϵ_T = 0.86	0.14 (500 ESH)		 No change 0 to 42 Severe	Lab Lab Lab Lab		UV Nuclear 5×10^{16} 10 keV p/cm^2 10^{16} 80 keV e/cm^2	9 10
TiO_2/silicone (R-960 in RTV-602) (Thermatrol)	α_S = 0.27 ϵ_T = 0.76			Severe 0.13 (1.5 years)	Lab OSO-I		10^{16} 80 keV e/cm^2 UV	9
Rutile TiO_2/methyl silicone (DC XR6-3488) (Thermatrol)	α_S = 0.23 ϵ_T = 0.85			0.18 (1.3 years)	Pegasus	Near Earth	UV (primarily)	
TiO_2/silicone white paint	α_S = 0.24 ϵ_T = 0.86	0.16 (73 ESH)			Apollo 9	Lunar	Combined	11

ORGANIC COATINGS (Concluded)

COATING	INITIAL	$\Delta\alpha_S$ 100 ESH	$\Delta\alpha_S$ 1,000 ESH	$\Delta\alpha_S$ 2,000 ESH	SOURCE OF DATA	SPACE LOCATION	RADIATION ENCOUNTERED	BIBLIOGRAPHY REFERENCES
Calcined china clay/ silicone (plasma clay/ RTV-602) Hughes Organic H-10	α_S = 0.15 ε_T = 0.86	0.19 (α_S/ε_T)	0.120 0.315 (α_S/ε_T)		LO-V LO-V	Lunar Lunar	Combined Combined	6 5
Leafing aluminum/ phenylated silicone	α_S = 0.25 ε_T = 0.26			No change 0.00 (1.5 years) 0.00 (2.2 years)	Lab OSO-I Mariner IV		8×10^{14}, 50 keV e/cm^2 Combined	9
Silicone over aluminum (RTV-602 over 1199 aluminum)	α_S = 0.20 ε_T = 0.80	0.256 (α_S/ε_T)	0.344 (α_S/ε_T) 0.01	0.13 (1,500 ESH)	LO-V LO-V	Lunar Lunar	Combined Combined	5 6
Fuller glass white (TiO_2/silicone-modified alkyd) white silicone paint 517-W-1	α_S = 0.29 ε_T = 0.90	0.02	0.10 (485 ESH) (60°F) 0.09 0.01 (300°F) 0.06 (485 ESH) (60°F)	No change	Lab Lab Lab Lab Lab		10^{16}e/cm^2 UV 10^8 rads (C) UV 10^{15} e/cm^2 UV	12 13 10 12 12
PV-100 (TiO_2/silicone alkyd vehicle) made by Vita-Var Paint Company	α_S = 0.22 ε_T = 0.87	0.17			Lab Lab		10^{16} 3 keV p/cm^2 10^{16} 145 keV e/cm^2	14 14 15
Tinted white kemacryl (Sherwin-Williams M49WC17) TiO_2/acrylic	α_S = 0.24 ε_T = 0.86	0.03 0.02 (60°F)	0.12 (485 ESH) 0.00 (300°F) 0.20 (485 ESH) (60°F)	0.04 0.06 0.04 (-180°F)	Lab Lab Lab Lab Lab		5 x 10^7 rads (C) UV 10^{16} e/cm^2 10^{15} e/cm^2 UV + 10^{15} e/cm^2	10 12 12 12 12
White skyspar epoxy coating (TiO_2/epoxy)	α_S = 0.25 ε_T = 0.91		0.39	0.35 ± 0.06 0.12 0.24 (485 ESH) 0.07 (60°F)	Lab OSO-II Lab Lab		UV UV (primarily) 2 x 10^8 rads (C) UV + 2 x 10^{16} e/cm^2 10^{16} e/cm^2	16 17 10 12 12
Cat-A-Lac black (carbon/epoxy)	α_S = 0.94 ε_T = 0.94							12 18

INORGANIC SILICATE

COATING	INITIAL	$\Delta\alpha_S$ 100 ESH	$\Delta\alpha_S$ 1,000 ESH	$\Delta\alpha_S$ 2,000 ESH	SOURCE OF DATA	SPACE LOCATION	RADIATION ENCOUNTERED	BIBLIOGRAPHY REFERENCES
Z-93 (Zno in potassium silicate binder)	α_S = 0.18 ϵ_T = 0.88			Not measurable	Lab			1
				Not measurable	OSO-II	Near Earth	UV (primarily)	1
			0.005 (1,580 ESH)	Not measurable	OSO-III	Near Earth	UV (primarily)	1
				Not measurable	Pegasus-II			19
			0.063		Mariner IV	Inter-planetary	Solar wind	1
			0.049		Lunar V	Inter-planetary	Solar wind	1
			0.05 to 0.08	7.3 hours in space	Apollo 9		Solar wind	11
				0.14	Lab		10^{16} p/cm^2	20
		0.005	0.056	0.066	LO-V		Solar wind	15, 21, 22 23, 41, 42
Douglas white (Z-93 type)	α_S = 0.184 ϵ_T = 0.880		0.049 α_S/ϵ_T = .0.240	0.08 α_S/ϵ_T = 0.275	LO-V LO-V	Lunar Lunar	Combined Combined	6 6
Lockheed zirconium silicate/potassium silicate ($ZnO_2 \cdot SiO_2$ + K_2SiO_3) LP 10A	α_S = 0.24 ϵ_T = 0.87	0.240		0.29 (7,000 ESH)	Lab		UV	9
				0.02	Lab		10^{15} e/cm^2	24
		0.018	0.045 (500 (ESH)		OSO-II	Near Earth	UV (primarily)	25
			0.04 (485 ESH) (60°F)		Lab		UV	12
			0.06 (485 ESH) (60°F)		Lab	Measurement not done in situ	UV + 10^{16} e/cm^2	12
Lockheed synthetic Li/Al/SiO_4 + sodium silicate	α_S = 0.16 ϵ_T = 0.87	0.16 (-180°F)	0.16 (60°F)	0.09	Lab		10^{14} n/cm^2	12
			0.09 (485 ESH)	0.11 (300°F)	Lab		10^{15} e/cm^2	12
					Lab		UV	12
Lithafrax 2123 (lithium aluminum silicate + sodium silicate)	α_S = 0.15 ϵ_T = 0.87		0.06	0.085	Lab		UV	12
				0.14	Lab		2 x 10^8 rad	10
		0.15 (60°F)	0.09 (300°F)	0.06 (-180°F)	Lab		10^{15} e/cm^2	12
			0.06 (485 ESH		Lab		UV	12
				0.10 (485 ESH) (60°F)	Lab		UV + 10^{16} e/cm^2	12
Hughes inorganic white (H-2) (TiO_2/ K_2SiO_3) Sylvania PS-7	α_S = 0.178 ϵ_T = 0.876		0.14		Lab		UV	5, 6
			0.089		LO-IV	Lunar	Combined	5, 6
Lanthanum oxide in potassium silicate	α_S = 0.083			0.014	Lab		10^{17} p/cm^2	26, 27
Aluminum oxide + potassium silicate (Al_2O_3 + K_2SiO_3)	α_S = 0.11 ϵ_T = 0.82	0.13 (162 ESH)			Lab		UV	9
					Lab		UV	27
					ATS-I			3
			α_S/ϵ_T = 0.21	48 hours after flight	ATS-I			3
			0.08		Lab		5.8 x 10^{15} e/cm^2	28
			0.05 (2,100 (ESH)				UV	29
			0.13 (2,800 (ESH)				5.8 x 10^{15} e/cm^2	29

OXIDE

COATING	INITIAL	$\Delta\alpha_S$ 100 ESH	$\Delta\alpha_S$ 1,000 ESH	$\Delta\alpha_S$ 2,000 ESH	SOURCE OF DATA	SPACE LOCATION	RADIATION ENCOUNTERED	BIBLIOGRAPHY REFERENCES
Rokide C chromic oxide	$\alpha_S = 0.90$ $\varepsilon_T = 0.85$			0.00	Lab		UV	16
Chromic acid anodized aluminum	$\alpha_S = 0.70$ $\varepsilon_T = 0.73$			0.03 (7.3 hours) (degradation caused by contamination)	Apollo 9 (Lunar)		Combined	11
Alzak anodic oxidation of aluminum	$\alpha_S = 0.15$ $\varepsilon_T = 0.77$		0.001 0.06	0.09	OSO-III ATS-3 AOA		UV UV (primarily)	30 31 1 32 32

COMPOSITE COATINGS (SECOND SURFACE MIRRORS)

COATING	INITIAL	$\Delta\alpha_S$ 100 ESH	$\Delta\alpha_S$ 1,000 ESH	$\Delta\alpha_S$ 2,000 ESH	SOURCE OF DATA	SPACE LOCATION	RADIATION ENCOUNTERED	BIBLIOGRAPHY REFERENCES
Silver-coated Teflon (series-emittance)	α_S = 0.059 ε_T = 0.68 α_S = 0.090 ε_T = 0.82	0.00 (180 ESH) + p		0.04 (TS-2) 0.04 (TS-5) 0.03 (TS-10) 0.00	Lab Lab Lab OGO-VI	 400 to 1,000 polar orbit	1.8×10^{16} p/cm^2 1.8×10^{16} p/cm^2 1.8×10^{16} p/cm^2	33 33 33 33
Aluminum-coated Teflon (series-emittance)	α_S = 0.13 ε_T = 0.67 α_S = 0.17 ε_T = 0.83 α_S = 0.21 ε_T = 0.89 α_S = 0.13 ε_T = 0.55	0.07 (51 ESH) 0.017 0.002	 0.016 0.021 0.021	0.06 (TA-6) 0.06 (TA-5) 0.05 (TA-10) 0.026 (TA-1) 0.022 0.031	Lab Lab Lab Mariner V		1.8×10^{16} p/cm^2 1.8×10^{16} p/cm^2 1.8×10^{16} p/cm^2 Combined	33 33 33 2 34 35
Polyimide/aluminum Kapton-H film on aluminum (series-emittance)	α_S = 0.32 ε_T = 0.75			0.105 (20,000 hours) Severe	Lab Lab		UV 10^{16} e/cm^2	36 9
SiO_x-coated vacuum deposited on aluminum	α_S = 0.128 ε_T = 0.53	0.50 (α_S/ε_T)	0.61 (α_S/ε_T)	0.66 (α_S/ε_T) 0.00	ATS-1 Explorer XXIII			3 37
Al_2O_3-coated vapor deposited on aluminum	α_S = 0.14 ε_T = 0.28	0.60 (α_S/ε_T)	0.64 (α_S/ε_T) 0.055	0.67 (α_S/ε_T) Negligible 0.075	ATS-1 Lab ATS-3		 10^{16}, 80 keV e/cm^2	3 9 32
Butvar over aluminum (series-emittance)	α_S = 0.20 ε_T = 0.86	Thermophysical properties dependent on thickness of Butvar	0.25 (70 ESH)				UV + 2.1×10^{16} p/cm^2	12
Silver on fused silica overcoated with inconel (optical solar reflector) (Corning 7940 fused silica)	α_S = 0.05 ε_T = 0.76		 0.005 (1,580 ESH)	0.00 0.00 0.00 0.00	 OSO-III		UV Solar wind Protons Electrons	38 16 1 1
Aluminum on silica overcoated with silicon oxide (optical solar reflector) (Corning 7940 fused silica)	α_S = 0.10 ε_T = 0.81			0.00 0.00 0.00 0.00			UV Solar wind Protons Electrons	38 16 1

MISCELLANEOUS COATINGS

COATING	INITIAL	$\Delta\alpha_S$ 100 ESH	$\Delta\alpha_S$ 1,000 ESH	$\Delta\alpha_S$ 2,000 ESH	SOURCE OF DATA	SPACE LOCATION	RADIATION ENCOUNTERED	BIBLIOGRAPHY REFERENCES
Sodium dichromate blackened inconel	α_S = 0.951 ϵ_T = 0.840			0.959 (4,770 ESH)	Lab		UV + 10^{15} e/cm^2	39
Sodium dichromate blackened inconel X	α_S = 0.963 ϵ_T = 0.806			Negligible 0.960 (2,560 ESH)	Lab		UV + 10^{15} e/cm^2	39
Bi_2S_3-dyed anodized aluminum [1100(2-5) Al]	α_S = 0.728 ϵ_T = 0.909			0.760 (3,540 ESH)	Lab		UV + 10^{15} e/cm^2	39
CoS-dyed anodized aluminum [1100(2-5) Al]	α_S = 0.957 ϵ_T = 0.930			0.963 (3,760 ESH)	Lab		UV + 10^{15} e/cm^2	39
NiS-dyed anodized aluminum [1100(2-5) Al]	α_S = 0.970 ϵ_T = 0.929			0.972 (3,540 ESH)	Lab		UV + 10^{15} e/cm^2	39
PbS-dyed anodized aluminum [1100(2-5) Al]	α_S = 0.861 ϵ_T = 0.912			0.891 (3,540 ESH)	Lab		UV + 10^{15} e/cm^2	39
Sandoz BK-dyed anodized aluminum [1100(2-5)Al]	α_S = 0.757 ϵ_T = 0.926			0.786 (3,540 ESH)	Lab		UV + 10^{15} e/cm^2	39
Sandoz AO-dyed anodized aluminum [1100(2-5)Al]	α_S = 0.647 ϵ_T = 0.927			0.684 (3,540 ESH)	Lab		UV + 10^{15} e/cm^2	39
Black Ni-plated aluminum [1100(2-5) Al]	α_S = 0.959 ϵ_T = 0.686			Negligible 0.953 (3,800 ESH)	Lab		UV + 10^{15} e/cm^2	39
Pyromark black on aluminum [1100(2-5) Al] (high-temperature black paint on aluminum)	α_S = 0.902 ϵ_T = 0.830			Unaffected 0.903 (3,440 ESH)	Lab		UV + 10^{15} e/cm^2	39
Pyromark black on inconel (high-temperature black paint on aluminum)	α_S = 0.906 ϵ_T = 0.842			Unaffected 0.906 (3,440 ESH)	Lab		UV + 10^{15} e/cm^2	39
Du-Lite-3-D on type 304SS	α_S = 0.952 ϵ_T = 0.653			Stable 0.945 (3,900 ESH)	Lab		UV + 10^{15} e/cm^2	39
Aluminized Mylar	α_S = 0.13 ϵ_T = 0.024		0.00	Unaffected			10^{16} p/cm^2	14

APPENDIX B. CONVERSION FACTORS

CONVERSION FACTORS

	METRIC	ENGLISH	ENGLISH	METRIC
DISTANCE	1 km 1 cm 1μ (10^{-4}cm) 1A (10^{-8}cm)	0.62137 mi 0.3937 in. 0.3937 mil 3.937×10^{-9} in.	1 mi 1 in. 1 mil	1.60935 km 2.54001 cm 25.4001 μ
AREA	1 m^2 1 cm^2	10.7639 ft^2 0.1550 $in.^2$	1 ft^2 1 $in.^2$	0.09290 m^2 6.4516 cm^2
VOLUME	1 m^3 1 cm^3	35.3144 ft^3 0.061023 $in.^3$	1 ft^3 1 $in.^3$	0.028317 m^3 16.3872 cm^3
WEIGHT	1 g	0.0022046 lb av.	1 lb av.	453.592 g

WORK AND ENERGY

1 g-cal (mean) = 0.0011628 watt-hr = 4.186 joules (abs)
= 0.0039685 Btu (mean)

1 Btu (mean) = 251.98 g-cal (mean) = 1054.8 joules (abs)
= 0.2930 watt-hr

1 joule (abs) = 10^7 ergs = 0.23889 g-cal (mean) = 2.778×10^{-4} watt-hr
= 9.4805×10^{-4} Btu (mean)

POWER

1 watt = 0.001341 horse power = 14.33 g-cal/min
= 1 joule/sec = 0.056896 Btu (mean)/min

TEMPERATURE

Degrees Kelvin (°K) = 1.8°R = °C + 273.16 = (°F + 459.69)/1.8
Degrees Centigrade (°C) = °K - 273.16 = °R/1.8 - 273.16 = (°F - 32)/1.8
Degrees Rankin (°R) = °F + 459.69 = 1.8 °K = 1.8 °C + 491.69
Degrees Fahrenheit (°F) = °R - 459.69 = 1.8°K - 459.69 = 1.8°C + 32

APPROXIMATE SOLAR CONSTANT

1350 watts/m^2
125 watts/ft^2
2 g-cal/cm^2-min
0.12 Btu/ft^2-sec

WAVELENGTH-ENERGY

1 micron (10^4A) = 1.24 eV = 10,000 cm^{-1}
wavelength λ (A) = 1.24×10^4/eV